



# **INVESTIGATING THE RHEOLOGICAL BEHAVIOR OF WITBANK COAL WATER MIXTURES**

**PRINCE OWUSU GYEBI**

Dissertation submitted in fulfilment of the requirements for the degree of

**Master of Science in Engineering**

Department of Chemical Engineering

February 2016

The copyright of this thesis vests in the author. No quotation from it or information derived from it is to be published without full acknowledgement of the source. The thesis is to be used for private study or non-commercial research purposes only.

Published by the University of Cape Town (UCT) in terms of the non-exclusive license granted to UCT by the author.

## DECLARATION

I hereby declare that the work on which this thesis is based is my original work (except where acknowledgements indicate otherwise) and that neither the whole work nor any part of it has been, is being, or is to be submitted for another degree in this or any other university. I authorize the University to reproduce for the purpose of research either the whole or any portion of the contents in any manner whatsoever.

Name: Prince Owusu Gyebi

Signature

Signed by candidate

## **ACKNOWLEDGEMENTS**

My extreme gratitude goes to the Lord God Almighty for His attention, backup and guidance and remarkable grace throughout this work.

My sincere appreciation goes to Professor Jean-Paul Franzidis for his advice and invaluable inputs towards the completion of this subject, and to Professor David Deglon for making time to endorse me to bring my task to completion.

I like to convey my earnest gratitude to the staff of the Centre for Minerals Research (CMR) Laboratory, University of Cape Town, especially Mrs Shireen Govender, the lab manager, Kenneth Maseko, Monde Bekaphi, Loraine Nkemba, Aisha and Ruben van Schalkwyk for assisting me throughout the pragmatic work of this task.

I owe my late mother, Mrs Elizabeth Owusu Manu a lot of gratitude for her beloved.

Ultimately, the financial support from the South African Mineral to Metals Research Institute (SAMMRI) and the South African National Research Foundation (NRF) is thankfully recognized.

## ABSTRACT

South Africa has large low-grade coal reserves. With the prospect of expanding its coal demands for exports and power generation, it is important that the beneficiation and transport of coal in the country are economical. The current mode of transporting coal has some drawbacks, which include inefficient rail infrastructure, long distances, and several environmental concerns related to air pollution, water pollution, and traffic risks. It is, therefore, important to investigate efficient means of coal transportation, which will also reduce environmental impacts. The transport of highly concentrated coal-water slurries through pipelines has attracted the attention of many researchers as an efficient and economical means of fine coal utilization. The primary objectives of this study are to investigate the importance of surface charge, solids concentration and particle size on the stability and rheological behaviour of Witbank coal. This work was carried out to arrive at a sounder discernment of the function of dispersion addition on coal-water mixtures rheology and stability.

The zeta potential measurement of coal samples was performed with an electrophoresis instrument (Malvern zetasizer). The study was initially focused on the effect of electrolyte addition (KCl) on the surface properties of Witbank coal and its demineralised derivatives at varying pH conditions. The zeta potential determined in demineralised water and 1 M KCl solutions obtained an absolute zeta potential value of -38.68 mV and -23.68 mV at the natural pH (i.e. 8) of coal respectively. Dispersants addition to both solutions at the same pH (i.e. 8) strongly affected the surface charge of the coal surface. Dispersants increased the surface charge towards more negative values, thus increasing surface electrostatic repulsion. The most important change in zeta potential was observed for Norilose 8058 at -63.06 mV with demineralised solution at 0.3 wt. % dosage.

The rheological test indicates that CWM were strongly non-Newtonian and showed shear thinning (pseudoplastic) behavior as coal concentration increases above 51 with. %. The empirical non-Newtonian model (Herschel-Bulkley) fitted showed a reasonable approximation of the experimental data tested. Moreover, rheological tests on solids concentration indicate that an increase in solids concentration resulted in a rise in high yield stresses and increased viscosity due to an increase in the number of particles per unit volume. On the other hand, rheological tests on particle size indicate that yield stress and apparent viscosity increased with a decrease in particle size. In the case of dispersion addition on rheology, results indicate that dispersants improved repulsion on the coal surface. With an initial apparent viscosity of 0.13

Pa.s at a coal concentration of 54 wt.%, by adding dispersants on coal surface, the apparent viscosity was decreased to 0.02 Pa.s with Norilose 8058 at 0.3 wt.% dispersion dosage.

The influence of stability for the storage component of the coal water slurry was investigated using the static stability test. Static stability employed using dispersants strongly affected the surface charge of coal. Results showed that CWM prepared without dispersants showed poor stability after 48 hours with penetration ratio of 35 %. By adding dispersants to CWM, stability was improved after 120 hours with penetration ratio of more than 75 %, thus improving electrostatic repulsion between particles.

# TABLE OF CONTENTS

<b>DECLARATION</b> .....	i
<b>ACKNOWLEDGEMENTS</b> .....	ii
<b>ABSTRACT</b> .....	iii
<b>TABLE OF CONTENTS</b> .....	v
<b>LIST OF FIGURES</b> .....	viii
<b>LIST OF TABLES</b> .....	xi
<b>ABBREVIATIONS</b> .....	xii
<b>CHAPTER ONE: INTRODUCTION</b> .....	1
<b>1.1 PROBLEM STATEMENT</b> .....	2
<b>1.2 OBJECTIVES</b> .....	3
<b>1.3 KEY QUESTIONS</b> .....	3
<b>1.4 SCOPE OF THIS STUDY</b> .....	3
<b>1.5 THESIS LAYOUT</b> .....	4
<b>CHAPTER TWO: LITERATURE REVIEW</b> .....	5
<b>2.1 PARTICLE SURFACE CHARGE</b> .....	5
2.1.1 Surface charge .....	5
2.1.2 Zeta potential .....	6
2.1.3 DLVO theory .....	7
<b>2.2 RHEOLOGY</b> .....	8
2.2.1 Rheology of fluids .....	9
2.2.2 Viscosity and yield stress .....	10
2.2.3 Rheological models .....	12
2.2.4 Rheological measurements .....	13
2.2.5 Factors affecting rheology of suspension .....	16
<b>2.3 COAL WATER MIXTURES (CWMs)</b> .....	22
2.3.1 Industrial applications.....	24

2.3.2 Advantages of CWMs .....	25
2.3.3 Factors affecting CWMs.....	26
<b>2.4 CHAPTER SUMMARY .....</b>	<b>37</b>
<b>CHAPTER THREE: EXPERIMENTAL METHODOLOGY .....</b>	<b>39</b>
<b>3.1 MATERIALS.....</b>	<b>39</b>
3.1.1 Coal sample .....	39
3.1.2 Dispersants.....	43
<b>3.2 METHODS .....</b>	<b>44</b>
3.2.1 Zeta potential .....	44
3.2.2 Rheology.....	44
3.2.3 Static stability .....	45
<b>3.3 PROGRAMME .....</b>	<b>46</b>
3.3.1 Zeta potential .....	47
3.3.2 Rheology.....	47
3.3.3 Static stability .....	48
<b>3.4 EXPERIMENTAL ERROR.....</b>	<b>48</b>
<b>CHAPTER FOUR: RESULTS AND DISCUSSION .....</b>	<b>50</b>
<b>4.1 SURFACE CHARGE .....</b>	<b>50</b>
4.1.1 Effect of pH .....	50
4.1.2 Effect of dispersants .....	52
<b>4.2 RHEOLOGY .....</b>	<b>54</b>
4.2.2 Rheological models .....	57
4.2.3 Effect of solids concentration .....	59
4.2.5 Effect of pH .....	64
4.2.6 Effect of dispersants .....	67
<b>4.3 STATIC STABILITY .....</b>	<b>69</b>
4.3.1 Effect of particle size.....	69

4.3.2 Effects of dispersants .....	70
<b>CHAPTER FIVE: CONCLUSION AND RECOMMENDATION.....</b>	<b>72</b>
<b>5.1 CONCLUSIONS .....</b>	<b>72</b>
<b>5.2 RECOMMENDATIONS .....</b>	<b>73</b>
<b>CHAPTER SIX: REFERENCES .....</b>	<b>75</b>
<b>CHAPTER SEVEN: APPENDICES .....</b>	<b>83</b>

## LIST OF FIGURES

Figure 2-1: A schematic representation of electrical double layer at the mineral-water interface (Adapted from (Nguyen and Schulze, 2004) .....	6
Figure 2-2: Schematic diagram of DLVO interaction with interaction energy (W) showing how interactions change with distance (adapted from Israelachvili, 1992).....	8
Figure 2-3: Graph showing the various types of fluid behaviour (Adapted from He <i>et al.</i> , 2004) .....	9
Figure 2-4: Viscosity gradient of a fluid in a pipe .....	11
Figure 2-5: Schematic diagram of a single-gap (a) and double-gap (b) concentric cylinders showing actual sample filling (TA Instrument, 2010) .....	15
Figure 2-6: Schematic diagram of a cone and plate (c) and parallel plate (d) measuring systems showing actual sample filling (TA Instrument, 2010) .....	16
Figure 2-7: Schematic diagram showing the effect of coal loading on the apparent viscosity of CWS at $128 \text{ s}^{-1}$ (Adapted from Tiwari <i>et al.</i> , 2003).....	17
Figure 2-8: Schematic diagram showing the effect of particle size on the apparent viscosity of CWS with 60% coal loading (Adapted from Buranasrisak and Narasingha, 2012).....	19
Figure 2-9: Schematic diagram showing variation of apparent viscosity of CWM with mixing ratio of coal particles of mean different sizes (Adapted from Roh <i>et al.</i> , 1995) .....	19
Figure 2-10: Schematic diagram showing dependence of viscosity as a function of volume percent concentration for different particle sizes (Adapted from Barnes <i>et al.</i> , 1989).....	21
Figure 2-11: Illustration of particle suspension showing the dependence of the volume of sediment on particle aggregation at a given solids content (Atlas <i>et al.</i> , 1985, Laskowski and Parfitt, 1989) .....	22
Figure 2-12: Schematic flow sheet for upgrading process (Usui <i>et al.</i> , 1999) .....	28
Figure 2-13: Schematic diagram of a microwave pre-treatment process (Meikap <i>et al.</i> , 2005) .....	29
Figure 2-14: The effect of increasing coal concentration on the apparent viscosity of a CWM at 30 Pa shear stress (adapted from Shukla <i>et al.</i> , 2008) .....	30
Figure 2-15: Schematic representation of monosized and polysized particle packing (adapted from Yavuz and Küçükbayrak, 1998).....	31
Figure 2-16: The effect of dispersant concentration on the zeta potential of coal surface (Adapted from Dincer <i>et al.</i> , 2003).....	33

Figure 2-17: The effect of dispersant type and concentration on the zeta potential measurements of coal samples (Atesok <i>et al.</i> , 2002).....	34
Figure 2-18: Adsorption of dispersant additives on coal particles surface (Adapted from Zhu <i>et al.</i> , 2014).....	36
Figure 2-19: The effect of dispersant type and concentration on coal concentration (Atesok <i>et al.</i> , 2003).....	37
Figure 3-1: Cumulative particle size distribution .....	40
Figure 3-2: Diagram showing SEM images of the different particles sizes and portion selected for EDS .....	42
Figure 3-3: The chemical structure of carboxymethyl cellulose .....	43
Figure 3-4: Diagram showing the separation of coal water slurry in cylinder after several days of storage.....	45
Figure 3-5: Static stability measuring cylinders with measuring rod .....	46
Figure 3-6: Schematic diagram showing experimental programme .....	47
Figure 4-1: Graph of zeta potential (mV) versus pH of demineralised water and 1 M KCl ..	50
Figure 4-2: Graph of zeta potential at pH 8 in demineralised water with the addition of dispersants.....	52
Figure 4-3: Graph of zeta potential of coal at natural pH 8 in 1 M KCl with the addition of dispersants in solution.....	53
Figure 4-4: Graph showing shear stress as a function of shear rate.....	55
Figure 4-5: Graph showing shear stress as a function of shear rate.....	55
Figure 4-6: Graph showing viscosity versus shear rate for the shear thinning system.....	56
Figure 4-7: Graph showing the comparison of the predicted model fit with coal at 54 wt. %	57
Figure 4-8: Graph of Herschel-Bulkley yields stress versus solids concentration for $-75 \mu\text{m}$ particle size .....	60
Figure 4-9: Graph of $-75 \mu\text{m}$ particle size showing the relationship between the apparent viscosity and solids coal concentration with 0 % dispersant at a shear rate of $200 \text{ s}^{-1}$ .....	61
Figure 4-10: Graph of yield stress versus particle size on CWM at 54 wt.% coal concentration .....	62
Figure 4-11: Graph showing the effect of particle size $D_{50}$ on the apparent viscosity of CWS with 54 wt.% at shear rate of $200 \text{ s}^{-1}$ .....	63
Figure 4-12: Graph showing yield stress as a function of pH at a shear rate of $200 \text{ s}^{-1}$ .....	65

Figure 4-13: Graph showing the effect of pH on the apparent viscosity of CWM ( $d_{50}= 27.97 \mu\text{m}$ ).....	66
Figure 4-14: Graph showing Bingham yield stress as a function of dispersant concentration at 54 wt.% .....	67
Figure 4-15: Graph showing apparent viscosity of CWMs at $200 \text{ s}^{-1}$ with a varying dispersing dosage at solid concentration 54 wt.%.....	68
Figure 4-16: Graph showing stability of a coal sample prepared using different particle size	69
Figure 4-17: Graph showing the stability of a coal sample prepared using at 0.2 % wt. dosages of Sendep 30F, Sendep 30D and Norilose 8058 (coal content: at 54 wt.%)......	70

## LIST OF TABLES

Table 3-1: D <sub>50</sub> values of coal particles as determined by Malvern Mastersizer size analysis .	40
Table 3-2: Proximate and ultimate analysis of coal samples on dry basis.....	41
Table 3-3: Elemental composition spectrums for Witbank coal.....	42
Table 3-4: Physical properties of dispersants used for viscosity and stability experiments ....	43
Table 3-5: Summary of zeta potential test .....	47
Table 3-6: Summary of rheological tests .....	48
Table 3-7: Summary of stability tests .....	48
Table 3-8: Showing coefficient of variation of measured variables .....	49
Table 4-1: Rheological model with -75- $\mu$ m particle size with different coal concentration ...	58
Table A-1: Zeta potential of coal in demineralised water.....	83
Table A-2: Zeta potential of coal in KCl ( $1 \cdot 10^{-1}$ mol/dm <sup>-3</sup> ).....	83
Table A-3: Zeta potential with Sendep 30D at natural pH of 8 in KCl ( $1 \cdot 10^{-1}$ mol dm <sup>-3</sup> ).....	84
Table A-4: Zeta potential with Sendep 30F at natural pH in KCl ( $1 \cdot 10^{-1}$ mol dm <sup>-3</sup> ).....	84
Table A-5: Zeta potential with Norilose 8058 at natural pH in KCl ( $1 \cdot 10^{-1}$ mol dm <sup>-3</sup> ).....	85
Table A-6: Zeta potential with Sendep 30D at natural pH in demineralised water.....	85
Table A-7: Zeta potential with Sendep 30F at natural pH in demineralised water.....	86
Table A-8: Zeta potential with Norilose 8058 at natural pH in demineralised water.....	86
Table B-1: CWM formulation formulas .....	87
Table B-2: Witbank coal mixture preparation for viscosity tests without dispersant agents...	87
Table B-3: Variation of coal and water with dispersants at 56 wt.% (PSD: -75 $\mu$ m, d <sub>50</sub> - 27.97 $\mu$ m).....	88
Table B-4: Variation of coal and water with dispersants at 58 % (PSD: -75 $\mu$ m, d <sub>50</sub> - 27.97 $\mu$ m) .....	88
Table B- 5: Variation of coal and water with dispersants at 60 wt.% (PSD: -75 $\mu$ m, d <sub>50</sub> - 27.97 $\mu$ m).....	89
Table B-6: Yield stress with 54 wt.% solids concentration on different particle sizes .....	89
Table B-7: Rheological model rheograms at 54 wt.% without chemical agents.....	90

## ABBREVIATIONS

ASTM	American Society for Testing and Materials
CMC	Carboxymethyl Cellulose
CWM	Coal Water Mixtures
CWS	Coal Water Slurries
CWF	Coal Water Fuels
DLVO	Derjaguin-Landua-Verwey-Overbeek
EDL	Electrical Double Layer
EDS	Energy Dispersive Spectroscopy
HLCWS	Highly Loaded Coal Water Slurries
NSF	Naphthalene Sulfonic Formaldehyde
PSD	Particle-size Distribution
PSS	Polystyrene Sulfonic Acid
PMA	Poly Methyl Acrylate
SEM	Scanning Electron Microscopy
S-194	Rhansam Gum
S-60	Gellan Gum
UBCWM	Upgraded Brown Coal Water Mixture
VDL	Van der Waals
Wt. %	Weight Percent

## CHAPTER ONE: INTRODUCTION

The South Africa's energy economy depends heavily on coal: it accounts for about 70% of the primary energy consumption, 93% of electricity generation, and 30% of liquid petroleum fuels (Eberhard, 2011). A current problem in the South African coal industry is the transportation of coal to export markets and power generation stations, which has become difficult due to ageing and inefficient rail infrastructure. The trouble is intensified by the long distance of coal haulage, delays in the time needed to load and unload wagons, and environmental challenges related to air contamination, water contamination, traffic hazards, and noise from haulage trucks. Due to the increasing usage of coal, there is a need to get an alternative source of fine coal utilization with less environmental contamination as well as economic benefits (Thompson and Aude, 1981)

The conveyance of highly concentrated coal water mixtures through pipelines has attracted considerable attention as an efficient and economical way of fine coal utilization. This manner of transporting coal mixtures is reliable, environmentally friendly and has been employed to transport heavy masses of clean coal with low ash content. The fine, suspension of coal in water is required to contain 60-75% coal, 25-40% water and nearly 1% dispersing additives (Atesok *et al.*, 2005; Dincer *et al.*, 2003).

However, the preparation of CWM is affected by the physical properties of the coal (moisture, ash, and sulfur), solids concentration, dispersing additives, and particle size (Atesok, 2000; Laskowski, 2001). A major challenge faced in highly suspended CWM is the viscosity. A typical CWM is required to have a low viscosity that can be pumped with low power requirements as well as good stability suitable for its transport and storage. However, transportation of highly loaded coal suspensions is problematic due to quick settling and high viscosity (Atesok *et al.*, 2002). Previous studies suggest that it is possible to minimize high viscosity at a given solids concentration by the addition of dispersing additives (Dincer *et al.*, 2003; Ongsirimongkol and Narasingha, 2012; Umar *et al.*, 2009).

The functional mechanism of these additives on coal surface is a combination of steric or electrostatic repulsion forces (Pawlic, 2007). Polymers such as carboxymethyl celluloses (CMCs) are used as rheological modifiers. Most celluloses are strongly hydrophilic, soluble, and chemically reactive due to the presence of polar carboxyl groups (Wang *et al.*, 2011). Recently published papers on the effect of polymers on rheological behavior in aqueous

suspensions report that CMCs are strongly dominated by their molar mass and degree of substitution (Barba *et al.*, 2002; Kulicke *et al.*, 1996). Atesok *et al.* (2005) observed that the significance of these polymers could be predicted by measuring the zeta potential on the coal surfaces. Aktas (2000) established that high negative values of zeta potential obtained led to minimum viscosity and good dispersion.

Also, prevention of sedimentation in highly concentrated suspensions is of great importance in most rheological studies. Boylu *et al.* (2005) examined the effect of CMCs on the stability of coal-water slurries and observed that the polymeric anionic dispersing additive had a significant influence on the stability of coal-water slurries and recommended the use of CMCs for the improvement of rheological properties. Nevertheless, the stability of CWMs depends on various parameters such as the coal concentration, particle size, the suspending liquid, pH, storage time, dispersion type, and dosage (Aktas *et al.*, 2000; Dincer *et al.*, 2003).

Particle size and distribution is one of the most important rheological properties, and many authors (Buranasrisak and Narasingha, 2012; Roh *et al.*, 1995) have put its significance forward. Roh *et al.* (1995) concluded that CWSs with the best rheological properties are obtained with a bimodal distribution to give maximum packing density and low apparent viscosities. Lagos and Nguyen, (1996) proposed that when the particle size range increases, viscosity levels decrease. Nevertheless, depending on the bulk density, a reduction in the viscosity may be observed at high shear rate.

In the scope of this study, possible use of Witbank coal for CWMs with dispersants was investigated. The presence of dispersants has been proven to cause a substantial effect on the surface properties of minerals in suspensions. The aim of this thesis is to examine the factors governing the surface charge interactions, rheology, and stability of Witbank coal in solution.

## **1.1 PROBLEM STATEMENT**

There have been no studies on the effect of solids concentration, particle size, and pH on the rheological behaviour of bituminous coal from South Africa. The fundamental reason for the rheological and stability behaviour of bituminous coal from South Africa as it relates to zeta potential analysis is also not well understood. Hence, the effect of dispersing agents on the aforementioned properties and the reasoning behind are not clearly understood due to the heterogeneous composition of coal varying from one source to another.

## **1.2 OBJECTIVES**

The study was conducted to find out whether a CWM with a high concentration of coal, low viscosity, and good stability could be developed with the following objectives:

1. To determine zeta potential as a function of pH, electrolyte concentration and dispersing agent additions.
2. To determine the rheological behavior as a function of solids concentration, particle size, pH and dispersing agent addition.
3. To determine the stability behavior as a function of particle size and dispersing agent addition.

## **1.3 KEY QUESTIONS**

The following key issues were addressed to meet the objectives of this work:

- What effect does the variation in pH, electrolyte concentration and dispersant addition have on the zeta potential?
- What effect does the change in solids concentration, particle size and dispersant addition have on the rheological behavior?
- What effect does the variation in particle size and dispersant addition have on the stability?

## **1.4 SCOPE OF THIS STUDY**

- The study was limited to a bituminous coal from Witbank and did not extend to any other coal in South Africa.
- Electrophoretic zeta potential measurements were applied to read the surface interaction of the coal before investigating the rheological behaviour of the coal particles. The findings of this research were restricted to the pH range of 2 to 10. However, most experiments were investigated at the natural pH of coal samples (pH of 8).
- The three different dispersing agents (Sendep 30D, Sendep 30F, and Norilose 8058) for this study were selected based on their variation in molecular weight and degree of substitution.

- The effect of particle size on rheology was limited to four different particle sizes with diameters passing -63  $\mu\text{m}$ , -75  $\mu\text{m}$ , -106  $\mu\text{m}$ , and -150  $\mu\text{m}$ . These particle sizes were selected based on the restrictions placed on the range of coal particle sizes that can be tested in the rheometer used in this study. A particle size with a  $D_{50}$  of -75  $\mu\text{m}$  was used in most of the experiments. Where another particle size was used, this will be highlighted in the relevant section.
- In keeping with the scope of this study, the solids concentration was varied between 10-60 wt. %, while keeping all other variables such as pH, temperature and particle size constant to minimize their impact. The maximum solids concentration of 42 vol.% (i.e. 54 wt.%) was obtained with a particle size  $D_{50}$  of 27.97  $\mu\text{m}$ . This represents the maximum solids concentration obtained for this particle size without chemical additives.
- The rod penetration approach was used to investigate the static stability of Witbank coal water mixtures.

## **1.5 THESIS LAYOUT**

This thesis consists of five chapters with appendices. Chapter 1 provides an outline of the approach taken to fulfil the main objectives, critical questions, and scope of this investigation. Chapter 2 provides a literature review of relevant findings from previous publications that are needed to assist the researcher with knowledge on the subject of CWMs expanding more on the effect of particle surface charge, solids concentration, particle shape and dispersing additives. Chapter 3 discusses the materials, experimental methods and the overall experimental program used in this research. Based on the techniques used experimental errors associated with the tests were outlined. Chapter 4 presents the results on zeta potential as a function of pH, ionic electrolyte concentration, and dispersing agent addition. Moreover, the rheological behavior of the suspension as a function of solids concentration, particle size, pH, and a chemical additive is discussed. In Chapter 5, the conclusions are drawn from the research, and the recommendations for further studies were outlined. Finally, the list of references cited and the Appendix obtained from experimental analysis follow at the end of the report.

## CHAPTER TWO: LITERATURE REVIEW

This chapter presents an overview of the available relevant literature on coal water mixtures (CWMs). The review begins with a brief description of the fundamental concepts of particle surface charge. This is followed by a short overview on the rheology of suspensions. Finally, previous studies on coal water mixtures are reviewed in relevance to South Africa's economy.

### 2.1 PARTICLE SURFACE CHARGE

#### 2.1.1 Surface charge

Surface chemistry interactions are very important for the interfacial reaction that occurs between solid-liquid and solid-gas (Prutton, 1994). Particles immersed in aqueous suspensions eventually develop surface charge via some mechanisms such as isomorphous substitution, ionization, differential dissolution, and surface adsorption. The process of acquiring surface charge eventually makes a suspension stable or unstable through some processes such as sedimentation, flocculation, and coalescence.

Two primary mechanisms contribute significantly to the surface charge of particles. Firstly, the association of inorganic groups such as carboxylic, phenolic and hydroxyl functional groups. In the presence of inorganic groups, surface charge developed mostly depends on the pH of the aqueous phase due to the presence of  $H^+$  and  $OH^-$  as the potential determining ions. Secondly, the surface charge can be determined by the adsorption of specific ions in the aqueous phase such as a dispersant and polymeric electrolyte.

In suspension rheology, when the surface charge is high, particles are dispersed, which likely results in low sedimentation stability and decreased viscosity. However, when the surface charge is low, particle aggregates and the viscosity increases. According to Pawlic (2005), anionic polymers affect the surface charge of minerals by adsorbing onto the mineral surfaces. These polymers decrease the surface charge towards more negative values, thus increasing electrostatic repulsion. However, the strength and magnitude of an average charge are dependent on the pH and ionic strength of the surrounding medium. According to Liu *et al.* (2000), polysaccharides adsorption is mostly dependent on the ionic radii, the coordination number of metal ions on the mineral surface and the valence state.

### 2.1.2 Zeta potential

The theories governing the electrical double layer surrounding particles have been well documented (Nguyen and Schulze, 2004). When particles are placed in an aqueous medium, irrespective of the means of charge acquisition negatively charged particles (anions) will attract positively charged particles (cations) due to electrostatic attraction. This eventually leads to the formation of a diffuse layer around the particle. Two regions are developed, a stern layer ( $\delta$ ) where the ions are strongly bound and a diffuse layer where the ions are less firmly associated. Within the diffuse boundary, the particles behave as a single entity at an imaginary boundary. The potential at this boundary is called the zeta potential.

The combination of the charged surface and the unequal distribution of co-ions and counter-ions near the surface of a particle are termed an electrical double layer. A schematic representation of the electrical double layer at the mineral-water interface is shown in Figure 2-1. In aqueous solutions, the formation of a double layer is crucial for the stability of the colloid. However, the electrical double layer structure is sensitive to electrolytes concentration and temperature (Laskowski, 2001).

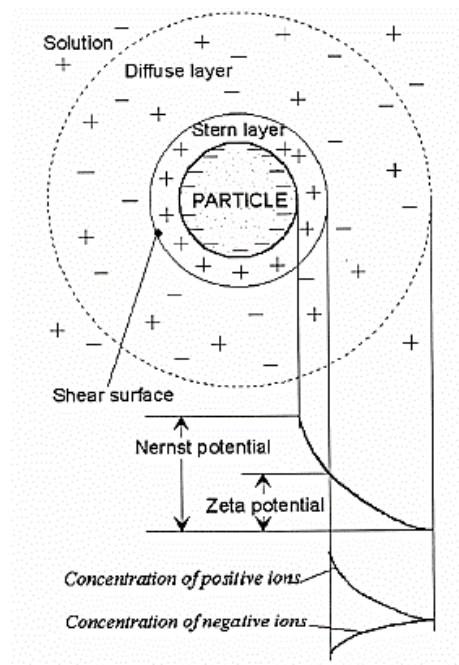


**Figure 2-1:** A schematic representation of electrical double layer at the mineral-water interface (Adapted from (Nguyen and Schulze, 2004))

### 2.1.3 DLVO theory

DLVO theory has a significant contribution to the electrostatic force and colloidal stability. According to the DLVO theory (Derjaguin and Landua, 1941, Verwey, and Overbeek, 1948), the magnitude of a stabilizing energy barrier can be calculated from the electrostatic repulsion ( $V_R$ ) and the Van der Waals attraction ( $V_A$ ) forces. According to Hamaker's method (Hamaker, 1937), the Van der Waals attractive and electrostatic repulsive forces can be represented as shown in Equation (2.1) and (2.2) respectively:

$$V_A = -A / (12\pi D^2) \quad (2.1)$$

$$V_R = 2\pi\epsilon a \zeta^2 \exp(-kD) \quad (2.2)$$

Where  $a$  is the particle radius,  $\pi$  is the permeability of the solvent,  $k$  is the function of the ionic composition,  $\zeta$  is the zeta potential,  $A$  is the Hamaker constant (Joules), and  $D$  is the distance between particles.

Van der Waals forces arise from dipole-dipole interactions and are always attractive forces. On the other hand, repulsive electrical layer, double effects results from the electrical double overlap of similarly charged particles in an aqueous medium when near each other. In a typically concentrated suspension, attraction forces tend to destabilize the mineral suspension, whereas repulsive forces impart stability. According to Leong (2005), the effect of intermolecular forces, stability and rheology of suspension systems can be described regarding the Van der Waals attractive and repulsive electrical double layer forces surrounding the particles. The illustration shown in Figure 2-2 by Israelachvilli, (1992) can be used to summarize the DLVO theory as follows: (a) Colloidal particles remain stable; (b) Colloidal particles remain 'kinetically' stable at the secondary minimum; (c) Colloidal particles coagulate, surface come into secondary minimum; (d) Colloids coagulation occurs rapidly; (e) Coalescence between surface and colloids increases.

High stability is achieved between two particles of identical double-layer charge if the potential energy due to the attraction is less than the potential energy due to repulsion. Also, it has been anticipated that aggregation occurs at the primary minimum, whereas the likelihood of weak aggregation can be attained in the secondary minimum (Kaji *et al.*, 1987).

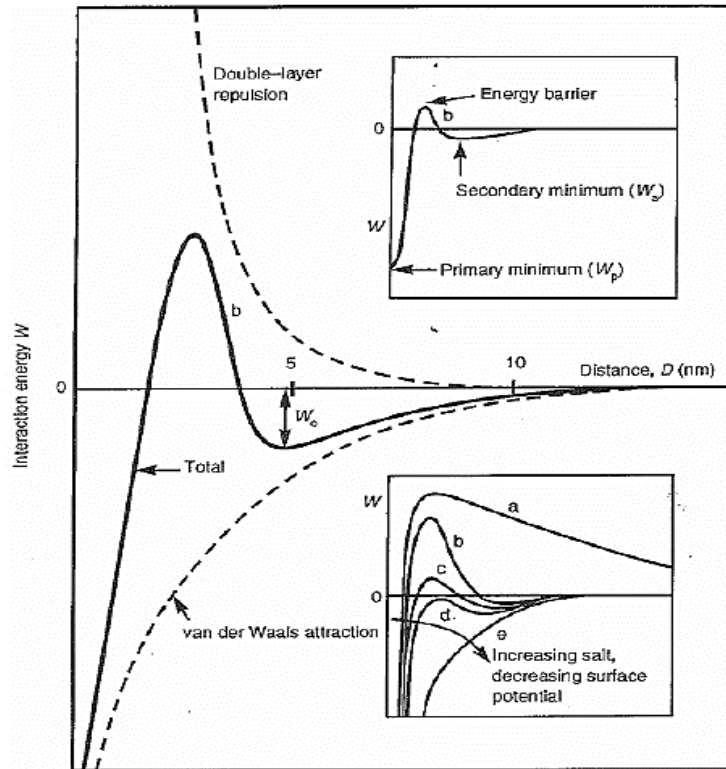


**Figure 2-2:** Schematic diagram of DLVO interaction with interaction energy ( $W$ ) showing how interactions change with distance (adapted from Israelachvili, 1992)

## 2.2 RHEOLOGY

Rheology is the science of deformation of flow. The term ‘rheology’ originates from the Greek word ‘rheos’ which means ‘flowing’ and has been defined as the science of flow by Mezger, 2006. This concept applies to substances that have complex molecular structures, whose flow cannot be characterized by a single value of viscosity (Chhabra and Richardson, 2011). Researchers such as Daniel Bernoulli, Lagrange, and Euler discovered the initial theories of rheology during the 18<sup>th</sup> century. However, the first test relating to rheology in the laboratory was conducted by Truesdell and Noll (1992). Rheology measures the properties of flow, and the study of rheology has wide application in most industries, especially in the chemical, mechanical, pharmaceutical, food processing industries, etc. Rheological studies focus on controlling the flow properties of industrial products, end-use performance, and how these materials behave under stress. Some useful applications of rheology are listed below:

1. To analyse the effect of frictional pressure drop of a slurry through a pipeline
2. To determine the effect of surrounding temperatures on the flow behavior of slurries
3. To understand the behavior of high-loaded paste slurries through a pipeline.

4. In most industrial application, the choice of an appropriate pump for the transfer of materials through pipelines is dependent on the information of the rheological properties of the material.

### 2.2.1 Rheology of fluids

Several kinds of fluids have different flow behaviors that can be predicted by rheological models. There are two main categories of fluids: Newtonian and non-Newtonian fluids. These include; pseudoplastic (shear thinning), plastic, thixotropic, rheopectic and dilatant fluids (shear thickening). A graphical representation of different fluid behaviors is shown in Figure 2-3.

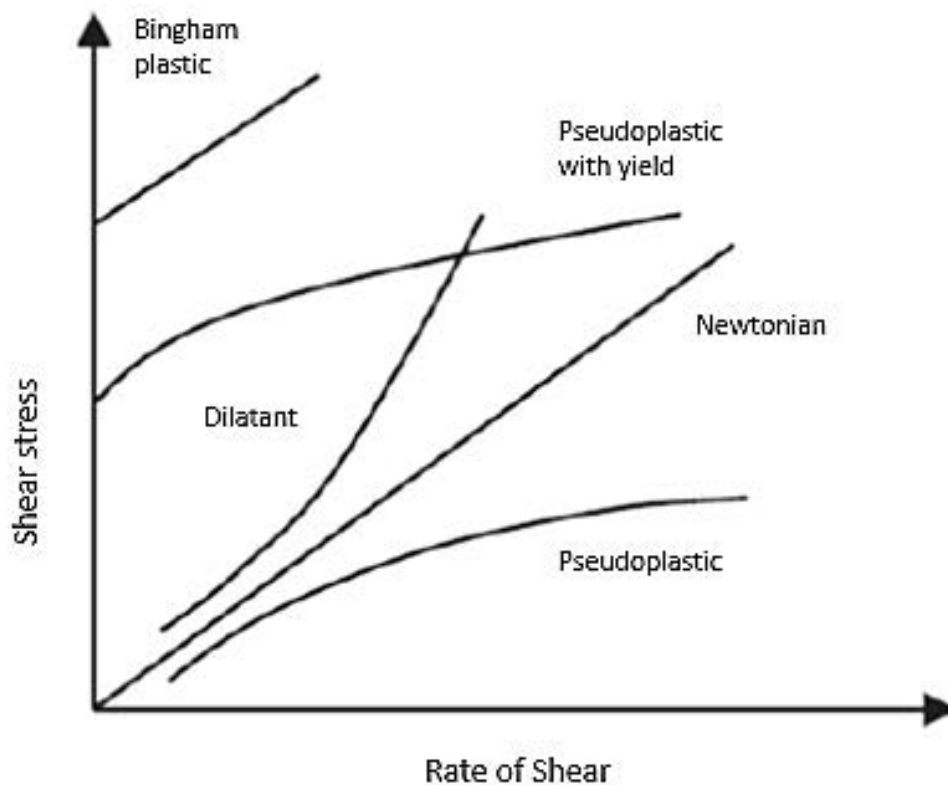


**Figure 2-3:** Graph showing the various types of fluid behaviour (Adapted from He *et al.*, 2004)

#### Newtonian Fluids

Newtonian fluids follow Newton's law of flow. In a Newtonian system, the relationship between shear stress and rate of shear is linear. This implies that the viscosity is constant at a given temperature or density, irrespective of how much force is applied. Water and oil are good examples of Newtonian fluids.

## Non-Newtonian fluids

A non-Newtonian fluid does not follow Newton's law of flow. In a non-Newtonian systems, the relationship between shear stress and shear rate is non-linear. This implies that the viscosity is not constant and changes with shear rate. They are influenced by the experimental procedures such as shaking, agitation, speed of rotating spindles, etc. The measured viscosity is normally termed as apparent viscosity. The three most important non-Newtonian fluids, mostly related to rheological applications are discussed below.

### *Bingham Plastic fluids*

Plastic rheology is commonly described as a system in which no flow occurs until shear stress reaches its critical transition point. This point is usually termed 'yield value'. After exceeding the yield value, the fluids exhibit a linear function between the shear stress and shear rate. In most plastic flow systems when the applied stress is below the expected yield value, the fluid will behave as a solid. However, after exceeding the yield value, the relationship between the shear stress and rate of shear usually acts as a Newtonian fluid. Toothpaste and tomato ketchup are good examples of this type of fluid.

### *Dilatant fluids*

Dilatant fluids' (shear thickening) are liquids or solutions whose viscosity increases with increasing shear stress. In most dilatant fluids, the system increases in volume (dilate) once an external force is exerted. Corn starch is an example.

### *Pseudoplastic fluids*

Pseudoplastic fluids (shear thinning) on the other hand have a decreased viscosity with increasing shear rate (Laskowski, 2011). They become thinner with increasing shear rate or agitation. This is probably due to the breakdown of internal fragments structure or network in a fluid as the shear rate increases. Mineral slurries are good examples of this type of fluid.

## **2.2.2 Viscosity and yield stress**

Viscosity is the proportionality constant between the applied shear stress and the resulting shear rate. As previously explained in Section 2.2.1, when a fluid is Newtonian the viscosity is constant, whereas the viscosity of non-Newtonian fluid changes with shear rate referred to as apparent viscosity. Highly viscous fluids have more resistance to flow; the more viscous the

fluid, the more power will be required to pump it. Low viscous fluids have less resistance to flow and, therefore, will require less force. The viscosity of every system can be defined by its coefficient of viscosity  $\mu$  ( $\mu$ , units = Poise). Hence, for a material requiring a shear stress of one dyne per square centimetre (dynes/cm<sup>2</sup>) to produce a shear rate of one reciprocal second has a viscosity of 1 poise or 100 centipoises. Figure 2-4 shows the velocity gradient of a fluid moving at a constant velocity ( $u$ ) through a pipe. The proportionality constant termed  $\mu$  is the viscosity of the fluid. Newton's equation relates the shear stress of the fluid to its viscosity as shown in Equation (2.3).

$$\tau = \mu \frac{\partial u}{\partial y} \quad (2.3)$$

Where  $\tau$ ,  $u$ , and  $\mu$  are the shear stress, velocity distance, and coefficient of viscosity respectively, where  $(\partial u/\partial y)$  is the velocity gradient at which shearing occurs.

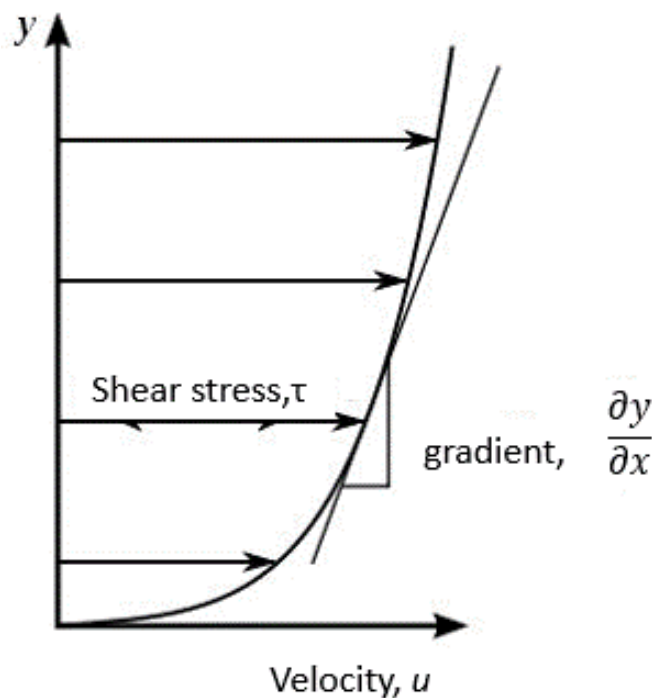


**Figure 2-4:** Viscosity gradient of a fluid in a pipe

It is worth mentioning that 'viscosity' forms an integral position as an essential fluid property from the industry perspective. Another controversial fluid property is 'yield stresses'. As previously emphasized in Section 2.2.1, the initial concept of yield stress ( $\tau_y$ ) (Pa) was discovered by Bingham and Greene (1920) and has since been a valuable property in the prediction of non-Newtonian fluids. Materials and fluids have yield values, which can be

defined as the minimum force required to initiate flow. According to Barnes, (1999), it is very difficult to describe yielding due to the variety of yield/strain curves shown by rare materials.

However, yield stress has shown to be useful in most engineering applications. In material design, the yield value can be defined as the point at which a material starts deforming plastically and does not return to its original value when the stress is removed. In most plastic deformation processes, once the yield value is exceeded, the shape change of deformation can be self-reversing after the force is removed. Moreover, knowledge of yield stress is crucial for the control of many process techniques in structural engineering such as forging and pressing.

The studies of yielding have been a major challenge in suspension rheology due to problems of aggregation, flocculation, and rapid settling. Addai-Mensah and Ralston, 2005 proposed that the fundamental understanding of these fluid properties is very necessary for most rheological studies. Although the relationship between suspension viscosity and yield stress seems to be complex, they each provide basic knowledge of intermolecular interactions and surface chemistry that can be useful in understanding rheological suspension behavior (He *et al.*, 2009).

### **2.2.3 Rheological models**

Several models have been proposed to describe the relationship between shear stress and the shear rate of non-Newtonian fluids. These models are applied to predict fluid behavior as Newtonian, pseudoplastic, dilatant, and Bingham plastic depending on the choice of fluid adjustable parameters such as consistency (K) or fluid behavior index ( $\eta$ ). The most frequently used models in the rheological properties of slurry flows are discussed.

#### **2.2.3.1 Bingham Plastic model**

The Bingham Plastic model is the simplest of among the rheological models. The Bingham plastic model is expressed as follows (Bingham, 1922):

$$\tau = \tau_0 + \mu_p \dot{\gamma} \eta \quad (2.4)$$

Where  $\tau_0$  is the yield stress,  $\eta$  is the fluid behavior index, and  $\mu_p$  is the plastic viscosity independent of shear rate.

### 2.2.3.2 Power Law model

The Power Law model uses a non-linear expression to describe the relationship between shear stress and shear rate, which corresponds better to the actual behaviour of most rheological suspension. The Power law measures the deviation from the Bingham Plastic fluid behaviour i.e. Bingham fluids have  $\eta$  value equal to 1, but Power law predictions show that the fluid can be expressed as pseudoplastic (shear thinning) if  $\eta$  is less than 1 and dilatant fluid (shear thickening) if the  $\eta$  is greater than 1. The Power law is expressed as (Reiner, 1926):

$$\tau = K\gamma^\eta \quad (2.5)$$

Where  $\tau$  is the shear stress,  $\gamma$  is the shear rate, K termed as the consistency index, which also serves as the viscosity index of the system. The shear rate is raised to the  $\eta^{\text{th}}$  power and is termed the flow behavior index.

### 2.2.3.3 Herschel-Bulkley model

The Herschel-Bulkley model, often termed the upgraded Power law model, uses a non-linear expression to describe the relationship between shear stress and the shear rate of fluid behaviour (Herschel-Bulkley, 1926). In contrast to the Bingham and Power-law models, this model corrects the deficiencies in the Bingham model by replacing the plastic viscosity with the Power law expression (K), i.e. making this a three-parameter model. The Herschel-Bulkley model is expressed as:

$$\tau = \tau_0 + K\gamma^\eta \quad (2.6)$$

An exponent  $\eta$  can express the non-linearity Herschel-Bulkley model. The fluid behaviour can be expressed as pseudoplastic (shear thinning) if  $\eta$  is less than one, dilatant (shear thickening) if  $\eta$  is greater than 1 and Newtonian fluid if  $\eta$  equals to 1.

## 2.2.4 Rheological measurements

The rate at which materials deform under an applied stress can be measured with a device known as a rheometer. A rheometer measures the rheology of a fluid. Two significant variables measured by a rheometer are stress ( $\tau$ ) and strain rate ( $\gamma$ ).

In general, rheometers consist of measuring systems and these are related to the components of the rheometer that are in direct contact with the measuring sample. The measuring systems are of two parts: (a) a fixed member or stator (e.g. Peltier plate); (b) a geometry (rotor) which is usually attached to the rheometer spindle. The geometry of the rheometer consists of four main types of measuring systems (TA Instrument, 2010):

- Cone and plate
- Parallel plate
- Concentric-Cylinders (single or double)

#### **2.2.4.1 Concentric-Cylinders Geometries**

Concentric cylinders are used to measure the unique rheological behaviour of fluids. It uses a vane or bob rotating spindles to measure a fluid resistance to flow and determine its viscosity resistance in a simple shear flow field. Rheograms are used to determine the relationship between shear stress and shear rate. Two most common types of concentric cylinders are the single gap and double gap concentric cylinders.

Figure 2-5 (a) shows a single-gap cylinder, although the single-gap looks similar like double-gap cylinder, it has only one gap. From the diagram, the sample in the rheometer can be represented as the blue filling region as located in the annulus gap between the two coaxial cylinders. A rotor (e.g. bob attachment) represents the rotating spindle. The outer portion is consisting of a cup known as the stator.

Figure 2-5 (b) illustrates a double-gap concentric-cylinder, the rotor of the double-gap is uncapped, hollow and comprises of an inner and outer wall with two annulus gaps. Low shear stress is obtained in double-gap rheometers as compared to single-gap rheometer.

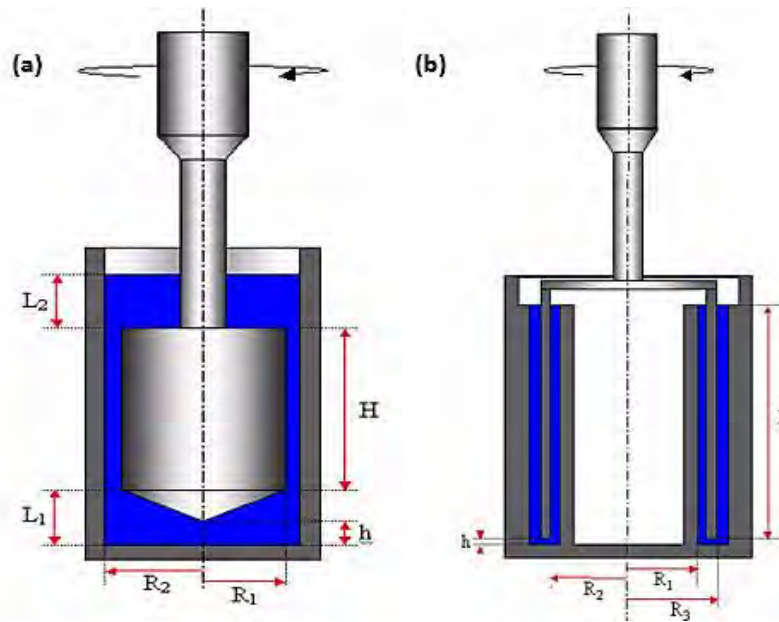


**Figure 2-5:** Schematic diagram of a single-gap (a) and double-gap (b) concentric cylinders showing actual sample filling (TA Instrument, 2010)

#### 2.2.4.2 Cone and Parallel Plates Geometries

The principle of operation behind the parallel plate rheometer is similar to the cone-plate rheometer. Similarly, both cone and parallel plates measuring instruments have Peltier plate, Upper Heated Plates (UHP), Environmental Test Chamber (ETC), Electrically Heated Plates and Temperature Systems (TA instrument, 2010). Figure 2-6 (c) shows a cone plate measuring system. It consists of a flat stator and an inverted cone with a conical angle. More importantly to avoid damage to the cone and plate, the distance between the two plates is controlled by a set gap. The gap is usually placed at the truncated distance  $T$  as shown in the diagram. The angle of the cone and the plate is estimated from one to two degrees depending on the type of experiment to run.

Figure 2-6 (d) illustrates a parallel plate measuring cylinder. The parallel plate consists of a circular flat plate rotor and a flat plate stator. The angle between both plates is arranged to be parallel. The gap between both plates is estimated not less than 1 % of the plate's diameter. The sample in rheometer can be represented as the blue filling region shown in both images.

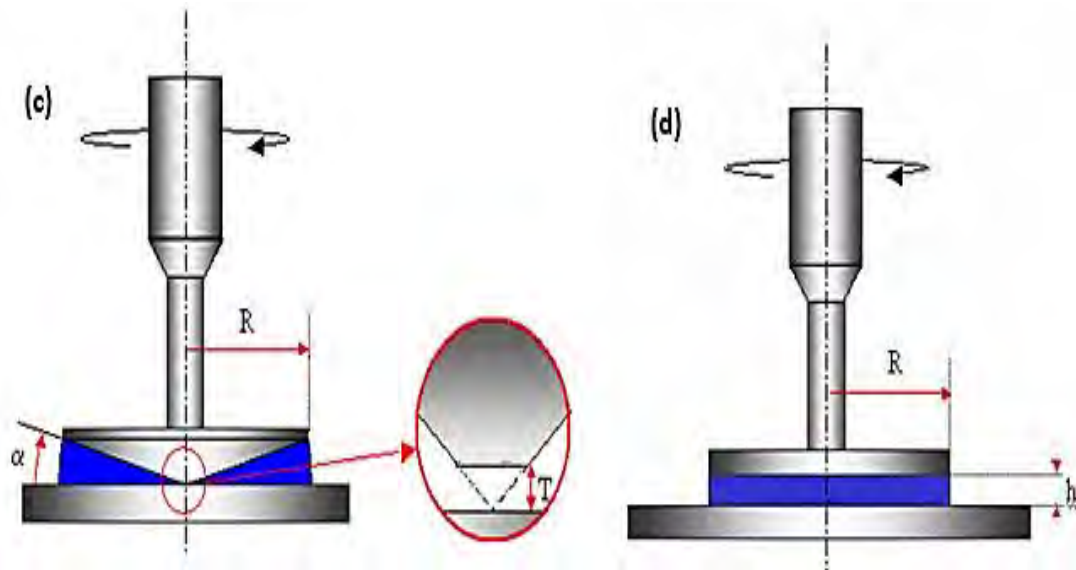


**Figure 2-6:** Schematic diagram of a cone and plate (c) and parallel plate (d) measuring systems showing actual sample filling (TA Instrument, 2010)

## 2.2.5 Factors affecting rheology of suspension

### 2.2.5.1 Solids concentration

In suspension rheology, the primary objective is to achieve the highest possible solids concentration at an acceptable viscosity during the processing. Maximizing solids concentration is directly related to increasing the number of particles in the suspension. The more particles are closely compacted, the greater inter-particle interaction in the slurry, and the amount of free water between the particles decreases accordingly. Figure 2-7 illustrates the effect of increasing the coal loading on the apparent viscosity at a shear rate of  $128 \text{ s}^{-1}$ . Coal loading was varied between a minimum of 56 wt.% to a maximum of 70 wt.%. It can be seen that the apparent viscosities increased from 187 to 1263 mPa s with a rise in coal loading from 56 to 70 wt.%.

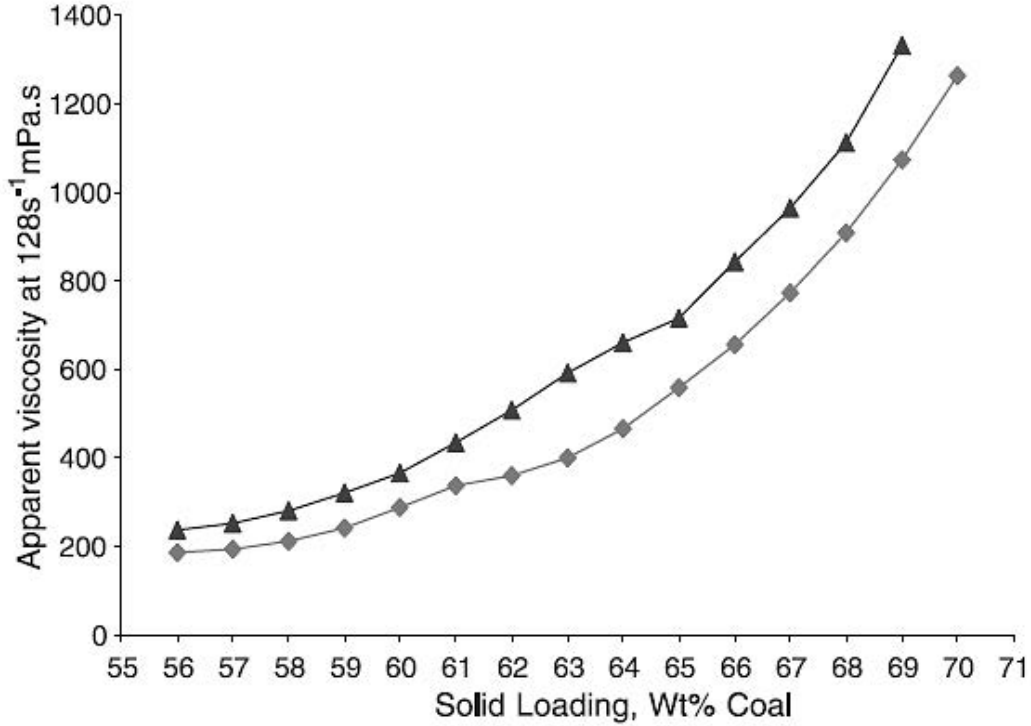


**Figure 2-7:** Schematic diagram showing the effect of coal loading on the apparent viscosity of CWS at 128 s<sup>-1</sup> (Adapted from Tiwari *et al.*, 2003)

The term solids concentration is equivalent to the term solids loading and solids volume fraction. The volume fraction ( $\phi$ ) is calculated depending on the nature of the coal. The volume fraction ( $\phi$ ) of high-rank coals can be calculated using the Equation (2.7) below (Goudoulas *et al.*, 2003):

$$\phi = \frac{\frac{m_{coal}}{\rho_{coal}}}{\frac{m_{H2O}}{\rho_{H2O}} + \frac{m_{coal}}{\rho_{coal}}} \quad (2.7)$$

Where  $m_{coal}$  is the mass of coal,  $\rho_{coal}$  is the density of coal,  $m_{H2O}$  is the weight of water, and  $\rho_{H2O}$  is the density of water.

According to Goudoulas *et al.*, 2003, the volume fraction ( $\phi$ ) of a low-rank coal can be calculated from the Equation (2.6) below by taking into account the moisture content of the coal.

$$\phi = \frac{1 + a_{hum} \frac{m_{coal}}{\rho_{coal}}}{1 + \left(\frac{m_{H2O}}{\rho_{H2O}}\right) + \left(\frac{m_{coal}}{\rho_{coal}}\right)} \quad (2.6)$$

Where  $m_{coal}$  is the mass of coal,  $\rho_{coal}$  is the density of coal,  $m_{H_2O}$  is the weight of water,  $\rho_{H_2O}$  is the density of water and  $a_{hum}$  is the moisture content of coal.

### **2.2.5.2 Particle size**

Particle size and distribution is one of the most important rheological properties, and many authors (Buranasrisak and Narasingha, 2012; Roh *et al.*, 1995) have put its significance forward. Particle size occupies a particular volume and the volume occupied is directly related to the size and shape distribution of the dispersed phase. Smaller particles will occupy a greater number of particles per unit volume in comparison to a similar suspension containing larger particles for the same solids concentration. Moreover, as the particle size decreases, the attractions between smaller particles get stronger. Figure 2-8 demonstrates the effect of particle size on the apparent viscosity. At a constant solids concentration of 60 wt.% reported for all tests, it can be seen that there were some differences observed with the viscosities of the coal suspension. The smaller particle size range showed a higher apparent viscosity than those of the larger ones. The fluid behavior can be described as non-Newtonian pseudoplastic fluid.

Nevertheless, the issue of particle size on coal-water slurries viscosity can be improved by mixing different ratios of fine and coarse coal at various ratios. The illustration in Figure 2-9, by Roh *et al.*, 1995 demonstrates the effect of blending different proportions of fine coal and coarse coal versus apparent viscosity. It can be observed that the viscosity was low at fine to a coarse blending ratio of 35±5: 65±5 irrespective of the mean size ratio.

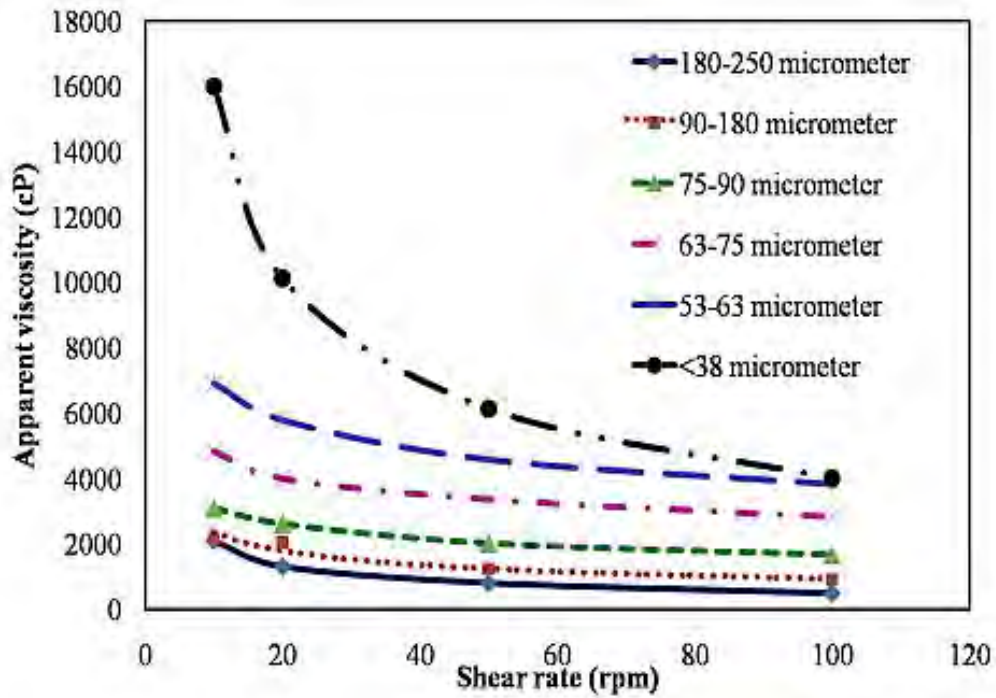


**Figure 2-8:** Schematic diagram showing the effect of particle size on the apparent viscosity of CWS with 60% coal loading (Adapted from Buranasrisak and Narasingha, 2012)

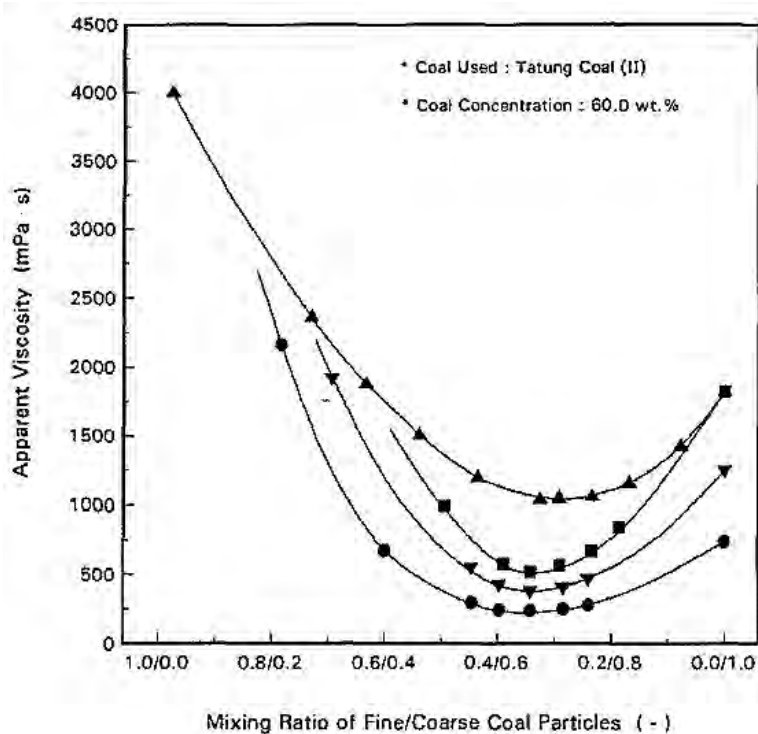


**Figure 2-9:** Schematic diagram showing variation of apparent viscosity of CWM with mixing ratio of coal particles of mean different sizes ( $d_{f,m}/d_{c,m}$ ) ( $\mu\text{m}$ ):  $\blacktriangle$ , 25/48;  $\blacksquare$ , 12/48;  $\blacktriangledown$ , 12/75;  $\bullet$ , 12/114 (Adapted from Roh *et al.*, 1995)

### 2.2.5.3 Particle shape

The particle shape in slurries varies depending on the nature of the material and it has been identified as having a massive effect on suspensions. Common shapes obtained after pulverization varies from regular cubes to rods, spheres, grains, and plates depending on the material. Early studies by Barnes *et al.*, 1989, present critical summaries of the relationships between particle shape and viscosity. The illustration in Figure 2-10 demonstrates how different particle shape, ranging from spherical to rod-like shapes will affect viscosity. A rod-like particle with high aspect ratio (length versus width) will increase viscosity in the presence of neighbouring particle with the same shape because the particle cannot interact and rotate smoothly.

In addition to these rheological effects, particle shape affects physical parameters such as drag force, solids concentration, and agglomeration. More importantly, particle shape affects the motion of a particle in a suspending fluid. For example, the drag forces within a moving fluid depend on the shape of the particle in relation to the direction of fluid flow. Therefore, it is expected that fluids containing flat-like particle shapes will align parallel to the direction of flow, and less drag force will be observed in comparison to the similar particles arranged perpendicular to the direction of flow.

The determination of a surface charge also depends on the shape of the particle. Agglomeration is likely to occur in a suspension containing long fibrous particle shapes. Moreover, large volumes are obtained from a moving fluid due the presence of longer shaped particle sizes.

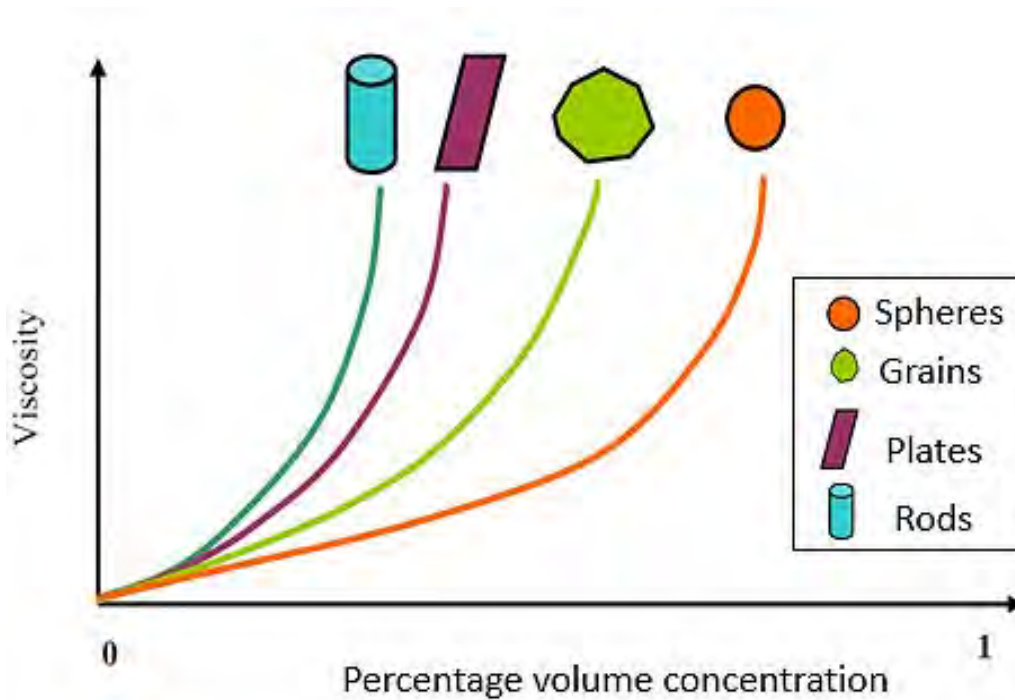


**Figure 2-10:** Schematic diagram showing dependence of viscosity as a function of volume percent concentration for different particle sizes (Adapted from Barnes *et al.*, 1989)

#### 2.2.5.4 Surface charge

As previously explained in Section 2.1.3, particle interactions in a colloidal suspension may be predicted from the Van der Waals attraction and electrical double layer repulsive forces (DLVO theory). However, in mineral slurries, high stability is required during the storage and transportation periods to prevent fast sedimentation. Stability of suspensions can be categorised into three broad categories: (a) sedimentation (static) stability; (b) aggregation stability and (c) mechanical (dynamic) stability. Sedimentation (static) stability prevents particles settling out into a solid cake by gravity. Unlike the colloidal systems minerals suspensions settle rapidly under gravity, leaving a clear water. Good sedimentation translates into the gentle mixing of slurry suspension, and the opposite is valid for poor sedimentation, which may require high-intensity agitation before pumping.

Sedimentation stability exists because of aggregate stability. Aggregation stability is a function of inter-particle forces. The high attraction between particles eventually increases the desired particle size by aggregation, which is unwanted and can jam fuel injectors during the

atomization stage. The pumping and pipeline transportation is mostly related to dynamic stability (Turian *et al.*, 2002)

The illustration in Figure 2-11 summarizes the relationship between surface charge and stability. When the surface charge is zero, particles agglomerate, causing particles to form large aggregates leading to the formation of high viscosity, high yield stress, and low solids content. The opposite is valid when the surface charge is high. A well-dispersed system is obtained, with low viscosity as well as increased maximum solids content. Nevertheless, the stability of CWSs depends on several elements such as the effect of particle shape, coal concentration (percent solids), pH, dispersant type and dosage and the effect of storage time (Boylu *et al.*, 2004).

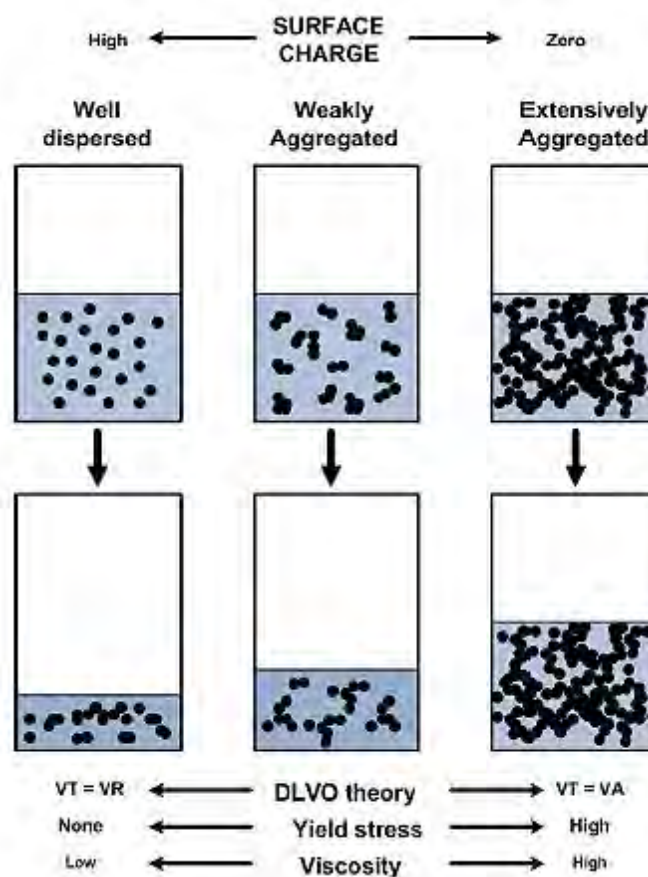


**Figure 2-11:** Illustration of particle suspension showing the dependence of the volume of sediment on particle aggregation at a given solids content (Atlas *et al.*, 1985, Laskowski and Parfitt, 1989)

### 2.3 COAL WATER MIXTURES (CWMs)

Coal water mixtures consist of finely ground coal suspended in a liquid, such as oil or water, together with small amounts of dispersing additives to improve stability and homogeneity. The

primary purpose of coal water mixtures is to make solid coal behave as an essential liquid fuel that can be transported and stored. The suspensions developed include (Horsfall, 1990):

- Coal-oil mixture (COM), a mixture of coal and fuel oil that may contain up to 10 percent water
- Coal-oil-water mixture (COW), COM with more than 10 percent water
- Coal-methanol mixture (Methanol)
- Coal-methanol-water mixture (CMW)
- Coal-water mixtures (CWMs), a mixture of coal and water

The utilization of coal water mixtures has been investigated and practised since the 1950's. The world oil crises in the 1970s accelerated the development of CWMs as an alternative fuel. The focus of the initial preparations was mainly on bituminous coals (medium rank) and anthracite (high rank). However, the recent introduction of the coal upgrading process and chemical additives has made the utilization of sub-bituminous (low-rank) coals possible and feasible (Usui *et al.*, 1999).

The first operational pipeline slurry transport system was commissioned in 1957 by the railroad coal cooperation in the United States. The long-distance coal pipeline system for Ohio's consolidation coal was about 172 km long and carried approximately 1.3 metric tonnes of coal per year. After six years of operations, the advantage of the slurry pipeline technology proved to be a cheaper and more viable alternative bulk transport system for coal. Further tests of coal water mixtures (CWMs) were conducted in the United States, Germany, and the Soviet Union (Russia) in the 1960s.

In 1962, President Kennedy supported the idea of coal slurry transportation and suggested it might symbolize a means of transporting coal economically and improve the depressed conditions in the coal industry. The Black Mesa coal slurry pipeline was constructed in 1964, commissioned in 1970, and operated from then until it was shut down in 2005 due to problems regarding environmental pressure on water utilization and its subsequent effect on the local communities. The Black Mesa pipeline operated successfully, carrying coal from Arizona Mines to the Mahara generating station in Southern Nevada over a length of 273 miles. The 18-inch pipeline transported approximately 4.8 million metric tons of coal per year. Coming after the commissioning of the Black Mesa pipeline slurry, several pipeline slurries have been

commissioned. Today CWMs pipelines are the favourite method of coal transportation in rural areas such as India, Russia, China, Canada, Germany, Japan, Sweden, and Italy.

### **2.3.1 Industrial applications**

The surge among different continents to develop new coal water mixture technologies to substitute the conventional road and railroad transportation is increasing and significant improvements of the CWMs have been realized. A variety of end-users for CWMs have been identified, including heat and power generation, diesel-engine fuel, the iron and steelmaking industry, coal gasification, non-ferrous furnaces and fluidised bed gasification. Some more important projects are listed below.

#### **2.3.1.1 United States**

In the United States, the first commercial CWMs plant was established in 1980. In 1985, the Babcock and Wilcox (B&W) company operated a CWM production plant with a design capacity of 18 000-200 000 tonnes per year. The US Fluid Carbon Inc. operated a CWM production plant capacity of 250 000 tonnes per year. The plant supplied CWM to Carolina Electric and Gas Utilities Division for power generation in the 75 MW coal ignition boilers (Warchol and Vecci, 1985).

#### **2.3.1.2 Russia**

In Russia, the design and construction of a 5 metric tonnes plant were constructed at Ugleprovod in Belovo. The prepared CWM was pumped through a 260 km-long pipeline via a 500 mm pipe to a combustion facility in the Novosibirsk power station. On the CWM preparation stage, less than 1 % plasticizer – sulphate salts of naphthalene formaldehyde were used with water being the dispersed medium (37 %). The concentration of the coal obtained was approximately 62 wt.%. (Osborn and Fonseca, 1992).

#### **2.3.1.3 China**

In China, several CWMs research programmes have been established since the 1980s. The enquiry and development increased rapidly due to the increased fuel costs. However, during most operations it was established that the stability of most coal slurries was poor (Liu and Li, 2000). The largest CWM constructed had a capacitance of 7 MW per annum and was built in the Shaanxi coal area. The prepared CWMs with a capacity of approximately 5.6 MT per year

is pumped through a 333 km-long course to reach Xincheng and continues to Dagang, which is about 853 km-long away (Yuvuz and Kububayrak, 1998).

### **2.3.2 Advantages of CWMs**

#### **2.3.2.1 NO<sub>x</sub> and SO<sub>x</sub> emissions**

Coal is formed from the accumulations of organic matter from the remnants of natural plants and animals, which eventually decay to form hard sedimentary coal rocks. The presence of the many carbon-formed materials contributes to the source of environmental contaminations. With 93% of Eskom's electricity generated from coal-fired stations, indeed, this implies a significant environmental challenge (Eberhard, 2011). The combustion of coal from coal-fired plants results mainly in the emissions of oxides of sulphur (SO<sub>x</sub>), nitrogen (NO<sub>x</sub>) and carbon dioxide's (CO<sub>2</sub>).

The combustion of coal slurries in incinerators produces fewer emissions of NO<sub>x</sub> and SO<sub>x</sub> compared to dry pulverized coal burning. This is explicated by the low flame temperatures obtained due to the presence of moisture in the fuel. According to Warchol *et al.* 1986, nitrous oxide (NO<sub>x</sub>) emissions with steam atomization are lower than with air atomization. This is because the exothermic conversion of carbon-to-carbon monoxide is increased in air atomization rather than steam atomization.

#### **2.3.2.2 Power generation and Export markets**

The coal mines in South Africa generates over 10 million tonnes of ultra-fines coal (< 150µm) per year, which is approximately 4% of the annual coal production. Various methods of converting these coal fines into useful product proposed include (Reddick et al., 2007):

- Beneficiation, dewatering and exporting the ultra-fines
- Production of coal water mixtures slurries from the ultra-fines
- Production of solid fuel (Dewater, and sell the ultra-fines).

Dewatering these high-quality, ultra-fines have several advantages from the environmental, economic, and social perspective. However, a more cost-effective beneficiation should be considered. This is because, with all the expensive dewatering equipment installed on these

coal-ultra fine deposits, such as thermal dewatering units, pressure filters and solar panels, the product is still unacceptable and alternative markets have to be sourced.

According to Laskowski (2011), flotation remains the best option for beneficiating ultra-fine coals. The huge monetary value associated with drying and dewatering will significantly reduce when CWM technology is employed after flotation. The flotation product can be pumped to the power generation stations and export markets through slurry pipelines. Likewise, the upgrading of CWM preparation facilities in existing wash plant, tailing dams, existing flotation concentrates will further cut the high investment cost due to the use of existing infrastructure.

### **2.3.2.3 Dust emissions**

The significant reason for the involvement of most countries like Japan, United States, China, and Russia, is to reduce the large emission of dust during pulverised coal storage and shipping. Air pollution caused by coal rail transport and stockpiles in open carriages contributes to a substantial source of dust emissions in South Africa. These harmful emissions could be reduced by using CWM fuel. The pulverised coal mixed with chemical additives and some quantity of water has proven to be the best option to reduce dust emissions. Although the heating value is significantly reduced, coal dust emissions into the atmosphere during transport and storage are drastically reduced.

### **2.3.3 Factors affecting CWMs**

A suitable CWM consists of a high pulp density, low viscosity, good stability, and low ash content. Increasing coal concentration eventually affects slurry viscosity due to less free water available in the suspension. In this instance, for a maximum efficiency of coal CWM, the coal concentration should be high while maintaining its viscosity at a minimum level for easy storage and transport via pipelines. These essential operating conditions can be maintained by considering the entire system parameters, which comprises interactions between coal properties, particle size, particle shape, ambient temperature, and chemical additives.

Several process stages for the production of coal-water slurries have been described in the technical literature. These include formulation, transportation, storage, atomization, and combustion. The behaviour of coal-water mixture at low, medium, and high shear rate essentially determines its behaviour during transportation, pumping and atomization. At each process stage, the suspension is required to have certain characteristics to be commercially feasible. These are referred as the primary factors and are related to the rheology and stability

of the mixture. Although these major factors determine the suitability of the suspension, they are defined by a set of secondary factors (i.e. particle size and chemical additives) related to the ease of slurry preparation. Factors affecting the preparation of CWMs are outlined in Section 2.3.3.1 to 2.3.3.5.

### 2.3.3.1 Coal type

The physical and chemical properties of coal play a key influence on the stability and fluidity of CWM. These include (Tiwari *et al.*, 2003):

- ash contents of coal and inherent moisture
- oxygen-containing functional groups, e.g. hydroxyl oxygen ( $\text{O}_{\text{OH}}$ ) and carboxyl oxygen ( $\text{O}_{\text{COOH}}$ )
- organic factors such as oxygen/carbon ratio (O/C)

The moisture and ash content in most coals decreases with increasing coal rank. It has been anticipated that mineral compounds contained in the ash, such as calcium and magnesium can dissolve to form metallic cations, which can decrease the anionic potential on the surface of coal particles by reducing the electrostatic repulsion forces. Moreover, the presence of clay minerals can also determine the ash content and as well display higher swelling properties with water. In addition, the hydrophilic characteristics of coal are influenced by the presence of moisture content and oxygen-containing functional groups (hydroxyl oxygen ( $\text{O}_{\text{OH}}$ ) and carboxyl oxygen ( $\text{O}_{\text{COOH}}$ )).

High hydrophobicity depicting the presence of low oxygen-containing groups on the surface of the coal will enhance the formation of highly loaded coal water mixtures (Tiwari *et al.*, 2003). However, the surface nature of many low-rank coals is hydrophilic with moisture content as high as 40%. Based on these disparities, several upgrading processes have been developed to upgrade the surface properties of low-rank coals to facilitate the preparation of coal water mixtures. (Meikap *et al.*, 2005; Usui *et al.*, (1999)).

Usui *et al.* (1999) developed a technology in which low-rank coal is first subjected to vacuum drying. Rheological studies identified that the process was economically viable with the quality of low-rank coal comparable with bituminous coals. They found that the upgraded coal reduced

the high cost associated with the utilization of low-rank coals. An upgrading process is schematically shown in Figure 2-12.

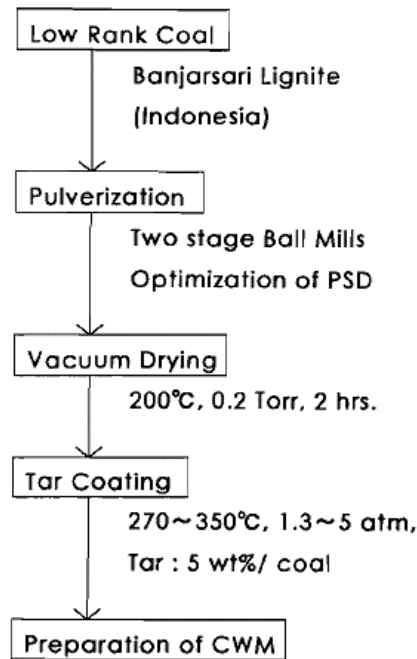


**Figure 2-12:** Schematic flow sheet for upgrading process (Usui *et al.*, 1999)

Meikap *et al.* (2005) investigated the rheological behaviour of high ash Indian coal using a microwave pre-treatment process. They found that shear stress for high-ash coal was higher than that of microwave pre-treated coal. This was attributed to the changes taking place on the surface appearances of the coal after the microwave treatment. The microwaved-treated coal caused a decrease in the apparent viscosity of the suspensions. The slurries exhibited pseudoplastic characteristics. Figure 2-13 shows the schematic diagram of the microwave pre-treatment set-up.

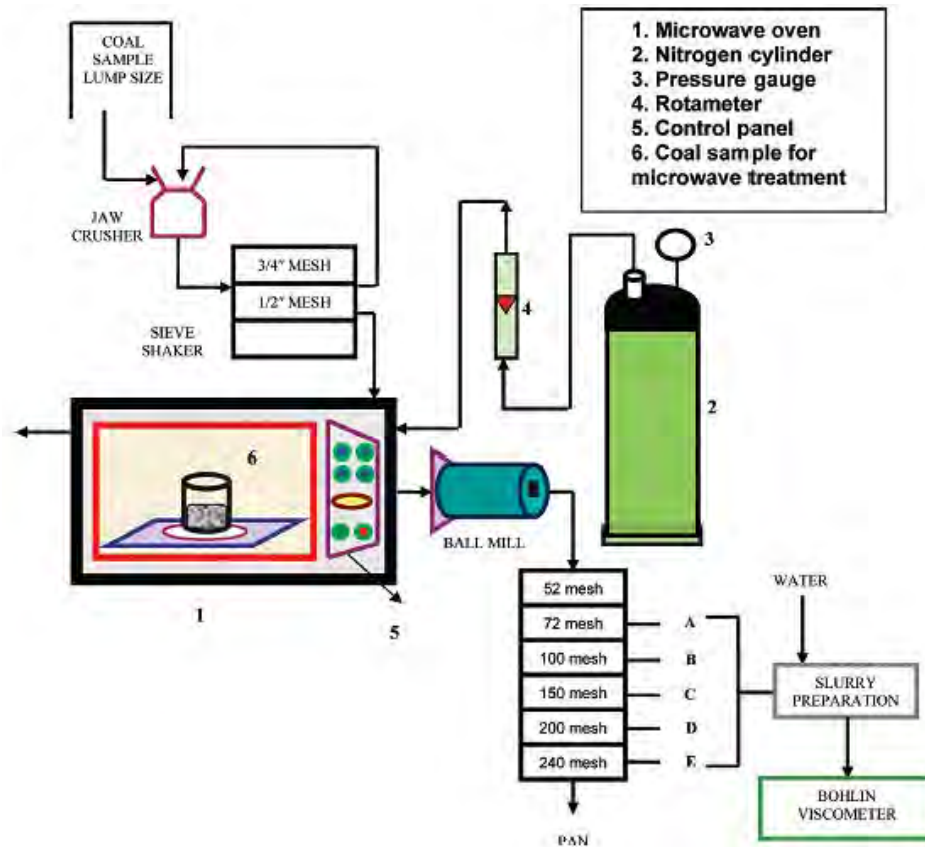


**Figure 2-13:** Schematic diagram of a microwave pre-treatment process (Meikap *et al.*, 2005)

It is noteworthy that Usui *et al.*, (1997) and Meikap *et al.*, (2005) noted that pre-treatment process makes in a significant influence on coal-slurry beneficiation. In fact, the tar coating process heated the low-rank coal up to a temperature of 200°C using hot water drying. Under these high temperature and pressure conditions, most oxygen groups are removed, exposing the coal surface to condensed volatilized oil and hydrocarbons. In this case, the volatilized oil and hydrocarbons exposed on the surface of coal forms a tar-like coating preventing the re-absorption of water molecules. The upgrading process changes the surface chemistry of the coal, increasing the hydrophobicity and promoting the characteristics of a high rank bituminous coal.

### 2.3.3.2 Solids concentration

Solids concentration is one of the most important parameters in the preparation of coal-water mixtures. The idea of achieving a highly loaded concentration is affected by various parameters of which the following is important: (a) the particle size distribution and particle shape; (b) the properties of the coal; (c) the inter-particle attractions in the presence of aqueous medium; (d) the pH, presence of electrolyte and chemical additives. However, the primary aims of

CWMs to obtain the highest solids concentration possible at an acceptable viscosity. Increasing solids concentration has a significant influence on rheological properties. For example: (1) the resistance to flow increases with increasing solids concentration; (2) the viscosity also increases accordingly; (3) the rheological behaviour deviates from a Newtonian fluid to a high viscosity non-Newtonian fluid. Figure 2-14 by Shukla *et al.*, (2008), demonstrates the effect of increasing solids concentration on suspension apparent viscosity. For all coal the stocks, it can be determined that it was prepared with or without water droplets. As the concentration stock increases, the particle-particle interactions increases, contributing to the establishment of a more viscous mixture with high concentration as it reaches above 35 with.%. At a coal concentration of 40 wt.%, it approaches its maximum limit known as the critical solids concentration. At the critical solids concentration, the viscosity of the suspension rises steeply indicating more collision and maximum inter-particle attraction.

Therefore, to obtain CWMs with a minimum viscosity and as well achieve a high absorption, two important factors need to be improved: (a) the particle shape and size distribution; (b) the addition of suitable chemical additives and stabilisers.

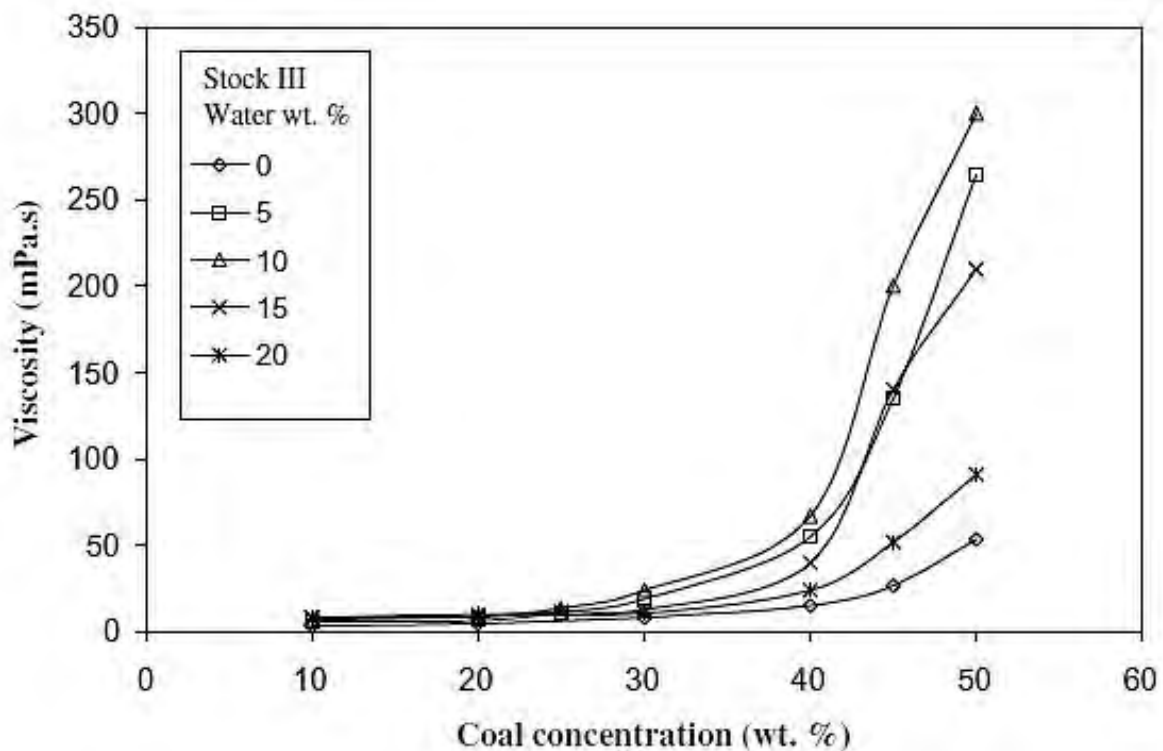


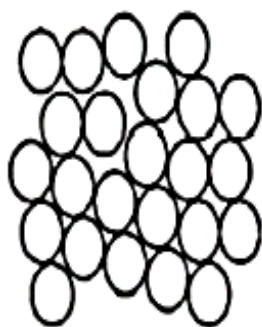
**Figure 2-14:** The effect of increasing coal concentration on the apparent viscosity of a CWM at 30 Pa shear stress (adapted from Shukla *et al.*, 2008)

### 2.3.3.3 Particle size

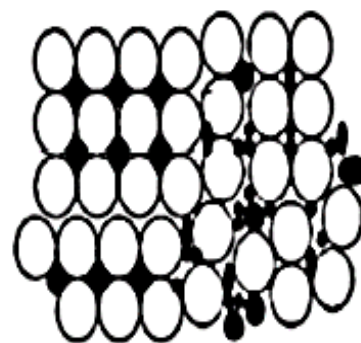
In coal-water slurries, particle size plays a vital role in the operating variables such as sedimentation behaviour, aggregation stability, and rheology. Minimum viscosities can be achieved in CWSs by optimizing its particle size fraction. According to Sadler and Sim (1991), a critical determinant in achieving maximum solids content with low viscosity also depends on the particle size, particle shape and particle size distribution.

Laskowski, (2001) suggested that, in a typical CWM preparation, particle size diameter should be at an uttermost of 300  $\mu\text{m}$  and with 70-80 % of the particle diameter below 75  $\mu\text{m}$ . With these limits in mind, Farries (1968) proposed that the particle-size in a loaded coal slurry could be optimised with the theory of packing. Hence, a bi-modal and uni-modal particle-size distribution was proposed. However, the processing of a bi-modal size distribution will usually require two grinding mills, one for coarser fractions and one of the fine fractions, but the grinding cost limits the size and yield of the fine fractions produced.

According to Lagos and Nguyen, (1996), studying the effect of particle size on the Australian coals, optimum mixing of fines to coarser ratios was attained at 40:60 with ideal coarse (208 - 279  $\mu\text{m}$ ) and fines (-45  $\mu\text{m}$ ). Furthermore, Barnes *et al.*, (1986) observed that by mixing different ratios of fines and coarser coal particles as  $35\pm 5:65\pm 5$ , coal slurries with optimum viscosities can be prepared. The presentation of fines as shown in Figure 2-15 will reduce the volume of water required as fluidising medium, therefore increasing the slurries maximum packaging efficiency.



**Monosized particles**



**Polysized particles**

**Figure 2-15:** Schematic representation of monosized and polysized particle packing (adapted from Yavuz and Küçükbayrak, 1998)

#### 2.3.3.4 Coal surface charge

Coal particles in aqueous medium acquire surface charge through mechanisms such as adsorption. These surface charges acquired leads to the formation of hydration, hydrophobic and steric forces. According to Johnson *et al.*, (2000), hydration forces usually play repulsive forces, whereas hydrophobic attraction forces tend to attract particles in an aqueous phase.

The scientific approach to determining the interactions of the nature of coal surface chemistry and particle interactions is mostly predicted by electrophoretic measurements. When estimating using electrophoretic measurements, the level at which the zeta potential passes through the zero line is termed the isoelectric point (i.e.p). The isoelectric point is the level at which suspension is less stable. In aqueous coal suspension, the isoelectric point is largely affected by impurities such as silicates. Sun and Campbell (1996) projected that the presence of petrographic composition such as ash, pyrite, calcium, and magnesium could also affect the coal surface charges. Mishra and Kanungo (2000) proposed that the presence of oxides/hydroxides such as clays or ferric oxide ( $\text{Fe}_2\text{O}_3$ ) and the presence of sulphide minerals, mostly iron disulphide ( $\text{FeS}_2$ ) and iron sulphide ( $\text{FeS}$ ) also affect the coal electrokinetic behaviour. Nevertheless, coal surface charges are mostly dependent on suspension pH, electrolyte concentration and the presence of dispersing additives (Johnson *et al.*, 2000). Some relevant studies are outlined as follows.

Dincer *et al.* (2003) used three dispersing agents, viz. polyisoprene sulphonic acid soda (Dynaflow-K), AC 1320 and naphthalene sulfonate-formaldehyde condensate, together with a stabilizing agent sodium salt of carboxymethyl cellulose (CMC-Na) to investigate the effect of dispersant addition on coal surface. They establish that the zeta potential of the bituminous coal at natural pH was attained at -20 mV, but was changed towards more negative values as the quantity of reagent increased. The negatively charged surfaces of the coal resulted in mutual repulsion hence flocculation was prevented, and the dispersion was achieved. Figure 2-16 shows the effect of dispersants addition on coal surface using zeta potential measurements.

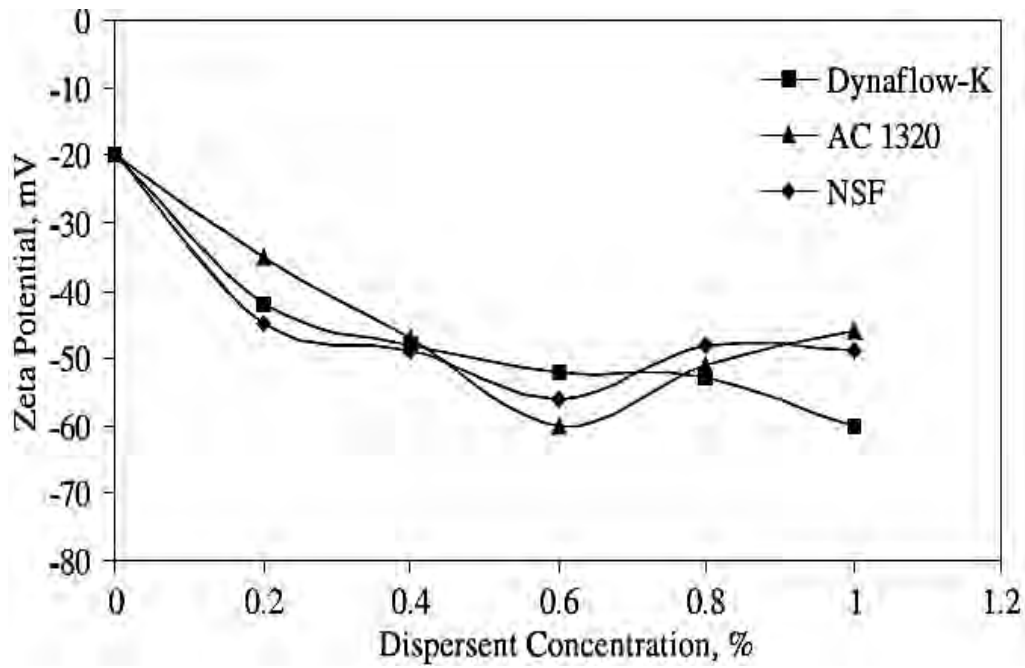


**Figure 2-16:** The effect of dispersant concentration on the zeta potential of coal surface (Adapted from Dincer *et al.*, 2003)

Atesok *et al.* (2002) also noted similar effects on three different Turkish coals. The increase of chemical additives (dispersant and stabilizer) drastically reduced the zeta potential of the coal samples. The slurry acquired an acceptable zeta potential of -60 mV at pH 10 in the presence of chemical additives. The effect of zeta potential taken on coal samples containing different concentrations of dispersing agents is shown in Figure 2-17

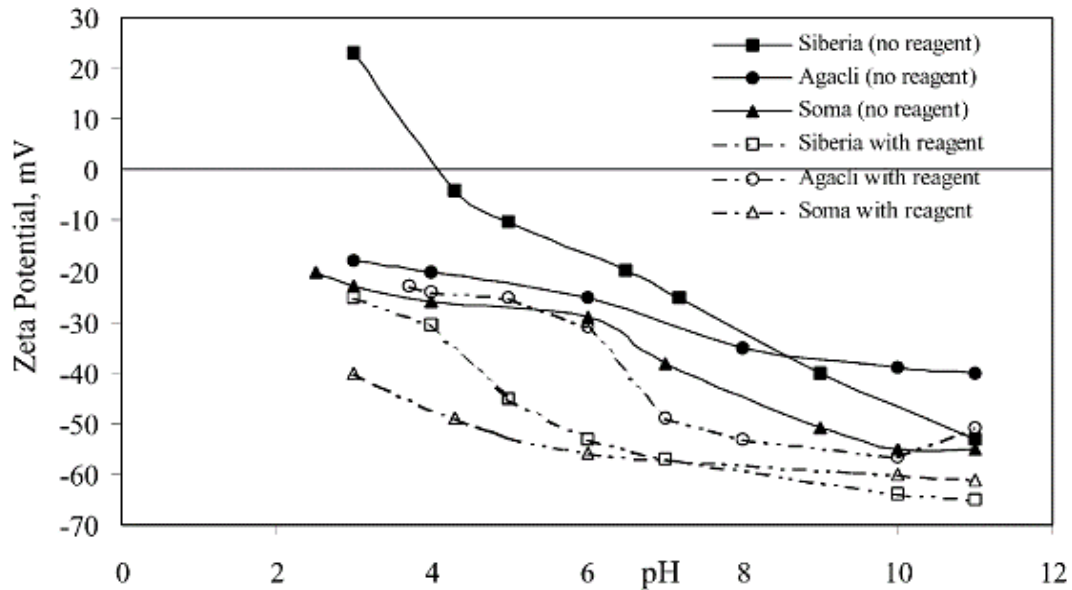


**Figure 2-17:** The effect of dispersant type and concentration on the zeta potential measurements of coal samples (Atesok *et al.*, 2002)

### 2.3.3.5 Chemical additives

The rheological behaviour of coal-water slurries depends strongly on the surface characteristics of the coal. However, at high solids loadings, the mixture is unlikely to be acceptable due to high viscosity and poor stability. Chemical additives may improve these characteristics by the following:

- Modify zeta potential.
- Improve stability of the particles by preventing particles settling into hard-packed agglomerates under gravity.
- Improves coal-water slurries fluidity through the reduction of surface hydrophobicity.

Chemical additives may be categorised according to their specific functions as follows.

#### *Stabilizers*

As summarized in Section 2.2.5.4 (Figure 2-11) by Atlas *et al.*, (1989), coal particles tend to settle under gravity in suspension when the surface charge is zero. Hence, such a system is stabilized against settling. Stabilisers are added to make up a three-dimensional structure between coal particles in suspension, which hinders settling and, thus, increases slurry stability. In most cases, the network structure set up by stabilizers is broken up as soon as the slurry

begins to flow. However, an overdose of stabilizing agent will increase the rigidity of the mixture, which in turn will increase the viscosity. A proper balance should, therefore, exist between stabiliser dosage and CWM preparation.

### *Dispersants*

Coal surfaces are naturally hydrophobic (Laskowski, 2011). However, the surface hydrophobicity characteristics of coal particles in aqueous suspension can be improved by the addition of dispersants. Dispersants usually prevent aggregation or flocculation by giving a net charge on the surface of particles by electrostatic and steric repulsion (Pawlik, 2005).

In Figure 2-18, the dispersion mechanism of dispersants on coal particles in water is summarised. When dispersing agents surround coal particles, its surface becomes more hydrophilic and forces solids particles to be dispersed in aqueous suspensions through the adsorption of the dispersants on the coal surface. Dispersants consist of polar heads (strongly hydrophilic) and non-polar tail (hydrophobic). The non-polar tail is adsorbed onto the hydrophobic coal surface, leaving the polar heads protruding. This allows the coal particle to be surrounded by a thin layer of water molecules, which prevent particles coming in contact with each other, therefore allowing easily fluidity of coal suspension.

The efficiency of a dispersing agent is affected by elements such as polymer concentration, molar volume, degree of substitution and molecular weight (Barba *et al.*, 2002; Kulicke *et al.*, 1996). Some important studies are outlined as follows.

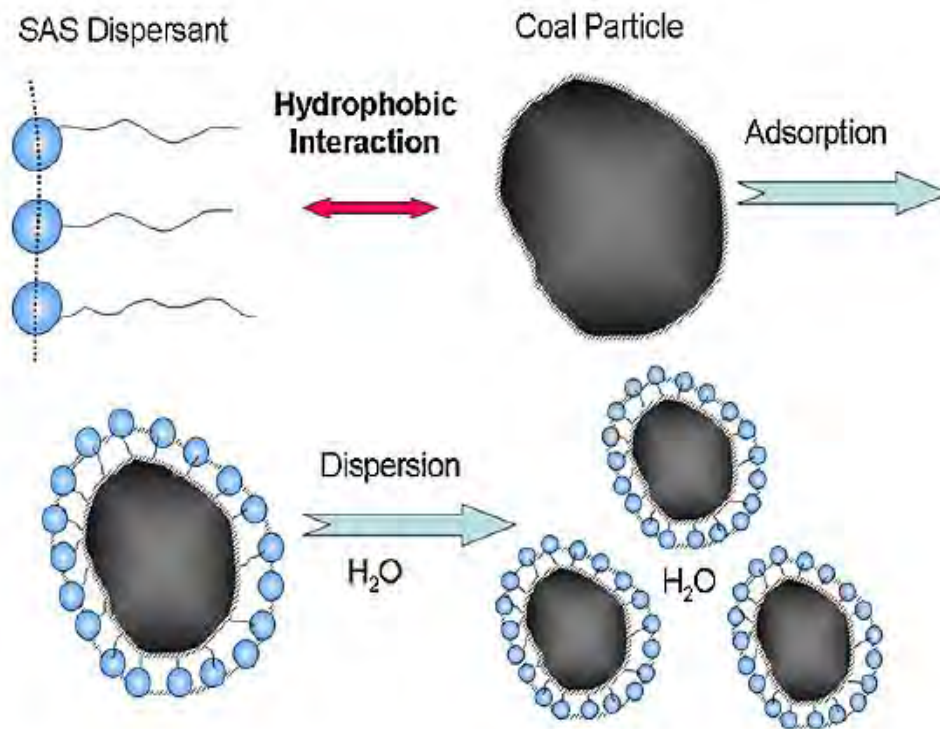


**Figure 2-18:** Adsorption of dispersant additives on coal particles surface  
(Adapted from Zhu *et al.*, 2014)

Aktas and Woodburn (2000) studied Triton X-405 as a non-ionic surfactant and concluded that to produce pumpable slurries with more than 60 % solids; it would be necessary first to achieve a significant level of demineralisation, and to use high levels of reagent addition.

Atesok *et al.* (2003) observed that the addition of chemical additives (dispersant and stabilizer) will drastically reduce the viscosity of coal suspension. Figure 2-19 demonstrates the effect of dispersant additives obtained at a solids concentration of 63 % wt. The slurry acquired an initial viscosity of 2050 cP in the absence of dispersing agents. However, the viscosity reduced rapidly in the presence of the dispersing agent, and the viscosity was found to be 500 cP at a dispersant dosage of 0.4 %.

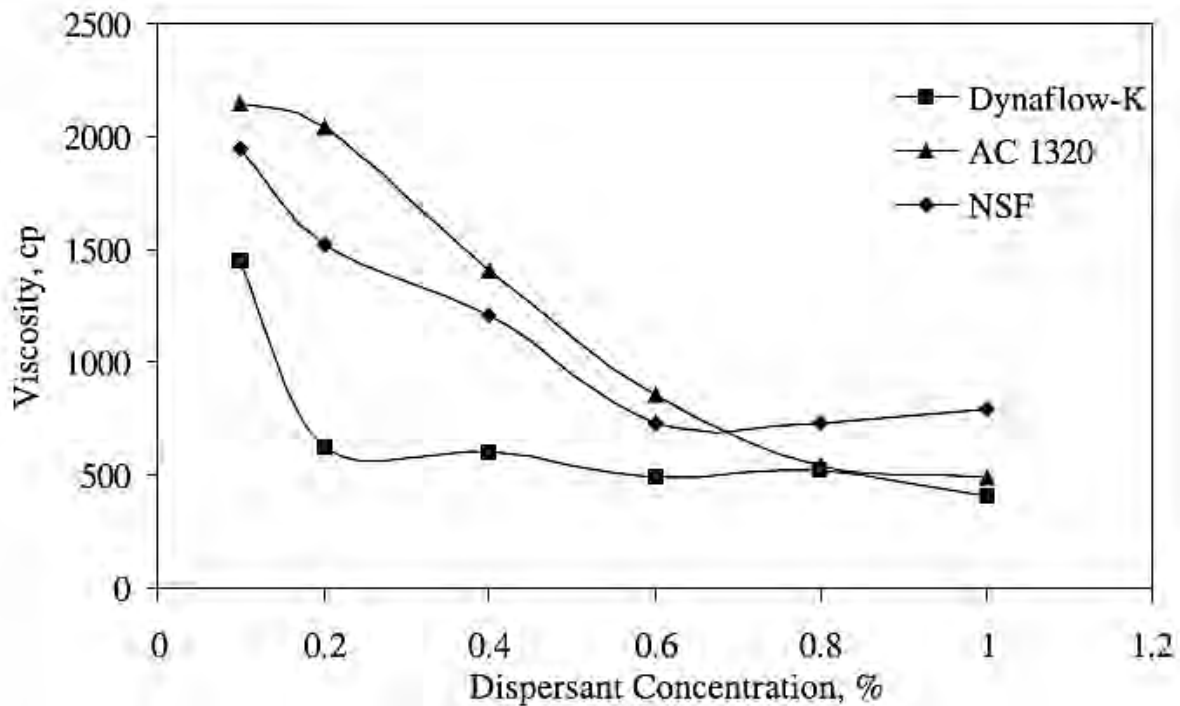


**Figure 2-19:** The effect of dispersant type and concentration on coal concentration  
(Atesok *et al.*, 2003)

## 2.4 CHAPTER SUMMARY

From the preceding sections, the basic concept of different factors affecting the suitability of CWMs relevant to this study has been reviewed. The review has mostly been on the brief descriptions of the fundamental concepts of particle surface charge and suspension rheology concerning how it affects the suitability of coal-water slurries.

The literature reviewed on the surface charge has established that different theories exist on fundamental topics such as repulsive electrical double layer and Van der Waals attractive forces (DLVO theory). All these hypotheses are significant and should be considered when analysing particle surface properties. Therefore, to acquire a fuller apprehension of the interactions occurring at the mineral surface, an electrophoretic analysis (e.g. Zeta potential measurements) was carried out in this research to investigate the mineral-surface charge interactions.

The review comprehensively discussed the different elements that influence on the rheology of CWMs such as the effect of solids concentration, particle size, coal properties, and chemical additives. An extensive work has been done on coal solids concentration, and this has been within the context of attaining the highest solids concentration possible with low viscosity.

Comparatively, few works have been done on particle size and coal properties on rheology. A fundamental understanding of Witbank coal rheology within the context of solids concentration, particle size, and chemical additives is necessary. The response of the rheological properties will be evaluated regarding apparent viscosity and yield stress.

The basic fundamental findings that are associated with the preparation of CWMs has been outlined, to date no work has been performed on the rheological and the stability behaviour of Witbank coal water mixtures. Since the chemical composition of coal samples contributes to their rheological behaviour and stability, the results reviewed by other researchers are not directly transferable. Therefore, the need to interpret the underlying concepts of Witbank coal suspension will be beneficial in future for the different cell types we have in South Africa.

## **CHAPTER THREE: EXPERIMENTAL METHODOLOGY**

This chapter describes the materials and methods applied to accomplish the aims of this work. The materials and coal analysis measured to obtain the feed sample is outlined in section 3.1. This is followed by Section 3.2, which describes the experimental methods applied to investigate the particle surface charge, rheological and stability techniques. A summary of the experimental programme relating to surface charge, rheology, and stability methods is given in Section 3.3. Finally, reproducibility of experimental analysis obtained is outlined in Section 3.4.

### **3.1 MATERIALS**

#### **3.1.1 Coal sample**

40 kg run of mine ore was obtained from the Anglo Coal Company (Witbank Coal-fields, South Africa). Before experimental test work, several tests, such as Malvern analysis of particle size, proximate analysis, ultimate analysis, scanning electron microscopy (SEM) was carried out on the coal sample.

The bulk sample for the study was received moist and was air-dried for 72 hours. For this reason, maximum control of water and reagent addition on the coal surfaces was attained. The addition of reagents was applied on a dry coal basis. Hence, dry grinding was employed in the laboratory experiments. The large coal particles above 5 mm were crushed below 2.8 mm using the laboratory cone-crusher. The -2.8 mm size fractions were riffled into bags of 1 kilogram. To obtain a product of different particle sizes, the 1kg coal sample was dry ground at 256 rotations per min (RPM) in the research lab-type rod mill with a milling time of 15 minutes. The milled sample was separated into several size fractions by screening.

##### **3.1.1.1 Particle size**

The particle sizes as indicated in Figure 3-1 shows the distribution of the fine ground coal with diameters passing -63  $\mu\text{m}$ , -75  $\mu\text{m}$  and -106  $\mu\text{m}$  respectively. Table 3-1 shows the  $D_{50}$  values of the particle size used. These particle sizes were chosen specifically for this study due to the restrictions on the particular particle size that can be employed in the rheometer for this study.

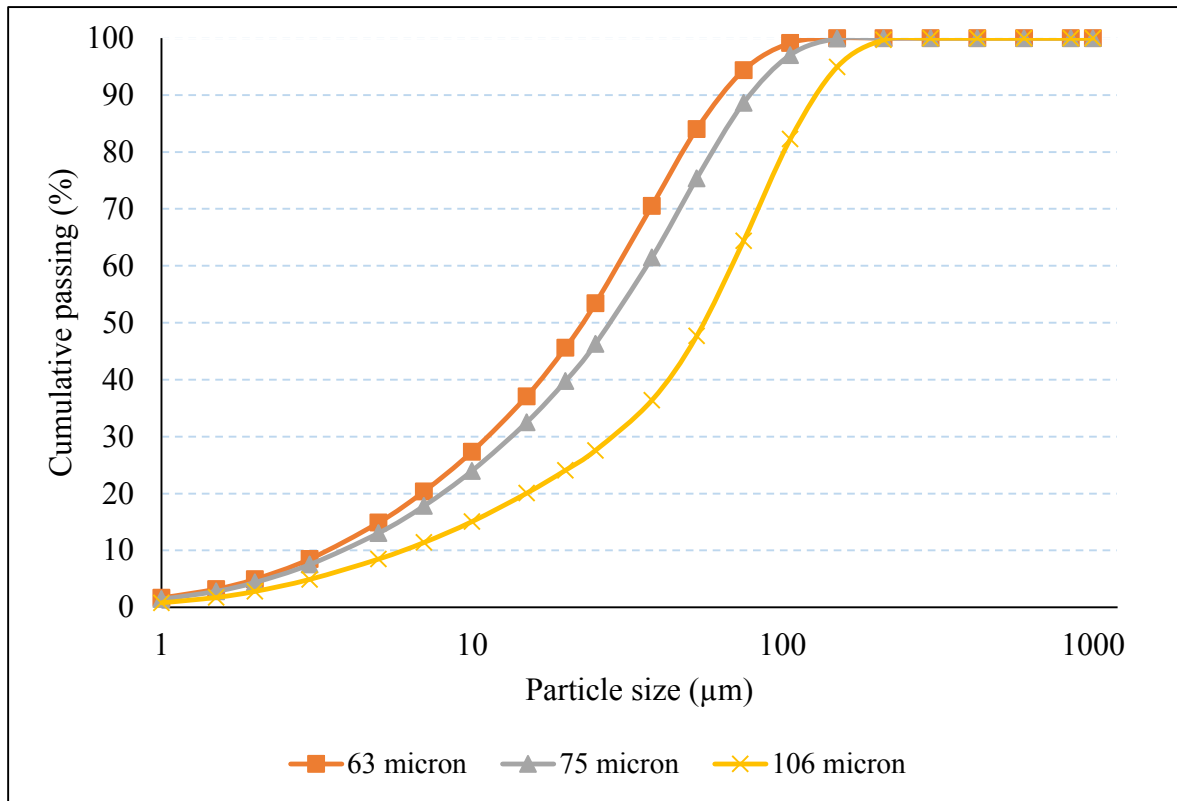


**Figure 3-1:** Cumulative particle size distribution

**Table 3-1:** D<sub>50</sub> values of coal particles as determined by Malvern Mastersizer size analysis

Particle size (µm)	D <sub>50</sub>
-63	22.76
-75	27.97
-106	55.92

### 3.1.1.2 Proximate and Ultimate Analysis

The proximate and ultimate analysis were performed to characterize the coal sample; the bulk of this analysis was done by ALS (WITLAB) laboratories in South Africa according to the SANAS ISO 17025 accredited standards and the ASTM standards. Table 3-2 shows the proximate and ultimate analysis of the coal sample.

Proximate and ultimate analysis test work were done on coal samples to characterize the different percentages of ash, total sulphur, volatile matter, inherent moisture content, carbon, hydrogen, oxygen and nitrogen as well as the calorific value of the coal. Recognised on the

ASTM accredited standards (American Society for Testing and Standards), coal can be classed as medium-volatile bituminous coal with carbon and volatile matter content of around 67.15 % and 22.50 % by weight respectively. The coal sample with a calorific value of 23.07 MJ/kg indicates that coal can be burned efficiently.

**Table 3-2:** Proximate and ultimate analysis of coal samples on dry basis

Component	Coal type	
	Witbank Coal	
Proximate analysis	Ash (%)	24.30
	Total sulphur (%)	0.60
	Volatile matter (%)	22.50
	Fixed carbon (%)	50.40
	Inherent moisture (%)	2.80
Ultimate analysis	C (%)	67.15
	H (%)	2.98
	O (%)	0.68
	N (%)	1.49
Other analysis	Calorific value (MJ/Kg)	23.07
	True relative density	1.58

<sup>a</sup> Proximate analysis was determined using SANAS ISO 17025 accredited standards

<sup>b</sup> Ultimate analysis was determined using an ASTM standard

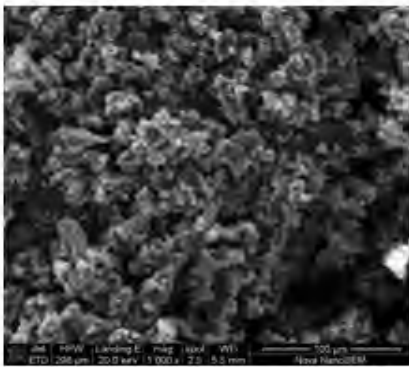
### 3.1.1.3 Morphological characteristics

The UCT (Centre for Images and Analysis) unit using the scanning electron microscope (SEM) and energy dispersive spectroscopy techniques (EDS) conducted the detailed topographical images and elemental analysis of the coal particle size. The SEM operates by producing images on the coal surfaces by scanning it with a focused beam of electrons. The electrons interact with the particles in the samples to create images, which contain information about the samples structure. The SEM/EDS analysis of the different particle sizes, is shown in Figure 3-2 and Table 3-3 respectively. The main elemental ash constituents of the coal are mostly silica and alumina. According to the elements as shown in Table 3-3, the relative elemental composition was found to be in the order of Si > Al > Ca > S. The elements shown in Table 3-3 resemble the order in which these metals are found in the coal sample. Silicon was found the most

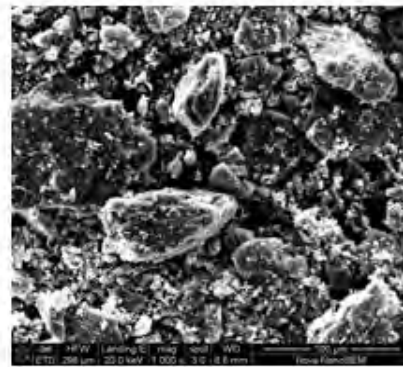
abundant element followed by alumina approximately 3.29 % (by weight). The elements are represented in compound form as SiO<sub>2</sub> and Al<sub>2</sub>O<sub>3</sub> with sulphur (S) and calcium (Ca) been present in trace amounts. It is worth noting that comparing the energy dispersive spectrometer results with proximate and ultimate analysis; there exist some correlation between both analyses. Examination of both tables shows that carbon content was within the same range.

**Table 3-3:** Elemental composition spectrums for Witbank coal

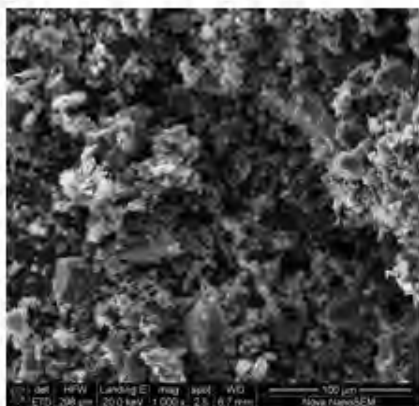
Elements	C	Al	Si	S	Ca	Total
Mean (weight %)	64.18	3.29	3.78	0.32	1.78	100
Std. deviation	2.53	0.26	0.06	0.12	0.47	



**Scanning electron microscopy (SEM) image of 63 micron particle**



**Scanning electron microscopy (SEM) image of 106 micron particle**



**Scanning electron microscopy (SEM) image of 75 micron particle**



**Portion selected for EDS (75 micron particle)**

**Figure 3-2:** Diagram showing SEM images of the different particles sizes and portion selected for EDS

### 3.1.2 Dispersants

Three newly developed anionic chemical agents were used as dispersing agents for both rheology and stability analysis, namely Sendep 30D, Sendep 30F, and N8058. The research was carried out with less than 1% chemical agent by weight. These reagents are variations of CMC, a cellulose derivative with carboxymethyl groups (-CH<sub>2</sub>COOH) bonded to some hydroxyl groups of the glucopyranose monomers. The chemical structure of the dispersing agent is shown in Figure 3-3.

The physical properties of the chemical agents are shown in Table 3-4. The sendep 30D has the lowest molecular weight, with the molecular weights of Sendep 30F and Norilose 8058 being higher and within the same range.

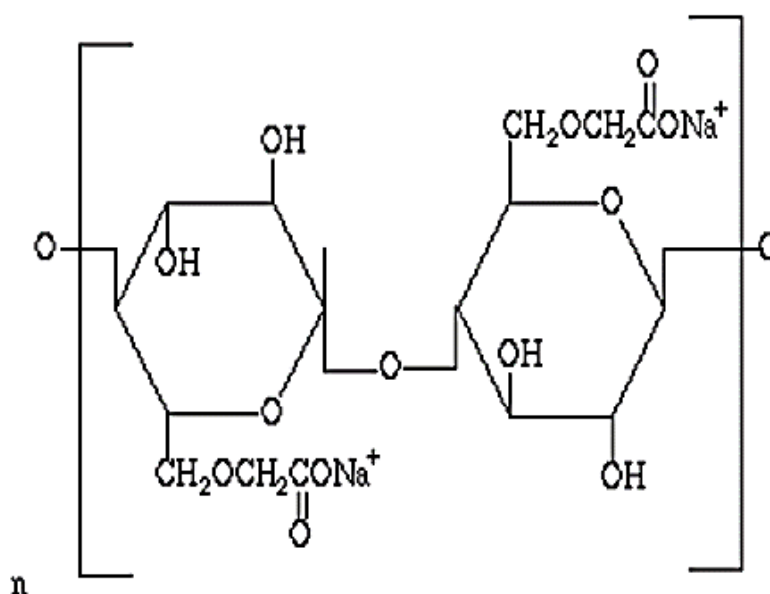


**Figure 3-3:** The chemical structure of carboxymethyl cellulose

**Table 3-4:** Physical properties of dispersants used for viscosity and stability experiments

Physical properties	Dispersant type		
	Sendep 30F	Sendep 30D	Norilose 8058
Moisture (%)	8.79	7.84	8.36
Purity (%)	59.5	66.14	58.89
Degree of subs.	0.78	0.62	0.73
pH	9.64	10.49	6.83
Mol. weight (g/mol)	325972	179502	343505

## 3.2 METHODS

### 3.2.1 Zeta potential

The zeta potential measurements were investigated using the Malvern zetasizer.

In all experiments, 0.1 g of 200 mesh size screen (-75  $\mu\text{m}$ ) coal sample was conditioned for 5 minutes at room temperature in a 50 ml of solution. Changing concentrations of dispersing agents ranging from 0.1-0.5 wt. % were weighed and added to 50 ml suspension containing distilled water. The experimental programme is described in Section 3.3.1.

Zeta potential measurements were determined using the Helmholtz Smoluchowski equation shown below. Each sample was repeated three times and the value reported was the mean value.

$$\zeta = \frac{4\pi V_t}{D_t} XEM \quad (3.1)$$

Where  $V_t$  is the viscosity of the aqueous medium at the electrokinetic shear layer,  $EM$  is the electrophoretic mobility of the particle at given temperature,  $D_t$  is dielectric constant,  $\pi$  is constant and  $\zeta$  is the zeta potential at the surface of the slipping plane.

### 3.2.2 Rheology

Rheology measurements were performed using an AR1500EA TA rheometer. The rheometer consists of a 60 ml pot compartment and a vane attachment, which is employed to add rotational stress to the coal slurry. The temperature of the rheometer is regulated by a constant flow of cooling water and was kept constant at 23 °C. Rheograms were generated in the shear rate range between 0 and 200s<sup>-1</sup>. The investigations were carried out at varying weights concentrations ranging from 10-60 % (by weight) with distilled water as the medium. The density of coal was obtained using the pycnometer.

In all experiments, an electronic balance was used for weighing each dispersing agent ranging from 0.1 to 0.5% by weight. The weighed reagents with distilled water and coal were mixed with a wooden spatula for 15 minutes. The mix was poured into the rheometer pot, and the rotating vane attachment applied torque. The experimental plan is identified in Section 3.3.2.

### 3.2.3 Static stability

The static stability test prescribed by Usui *et al.*, (1999) was carried out to assess the stability of the coal-water slurries. This was achieved by measuring the hard pack layer at the bottom of the measuring cylinder, as demonstrated in Figure 3-4 and Figure 3-5 respectively.

The set-up was allowed to stand in 250 ml graduated glass measuring cylinder, 100 mm in diameter for 240 hours (10 days). The hard layer deposited at the bottom of the measuring cylinder were measured by a steel rod (4mm in diameter, 195 mm in length, and 30 g in weight) which was dipped vertically to the bottom of the glass measuring cylinder.

The initial maximum distance ( $d_t$ ) was recorded just after mixing by penetrating the rod. Then after several regular days of storage, the rod distance ( $d_p$ ) was recorded. Penetration percent was calculated using the Equation (3.2) shown below;

$$\% \text{ penetration} = \frac{d_p}{d_t} \times 100 \quad (3.2)$$

Where  $d_p$  is the distance of the rod travel (mm) and  $d_t$  is the maximum length of rod travel (mm). The experimental programme is described in Section 3.3.3.

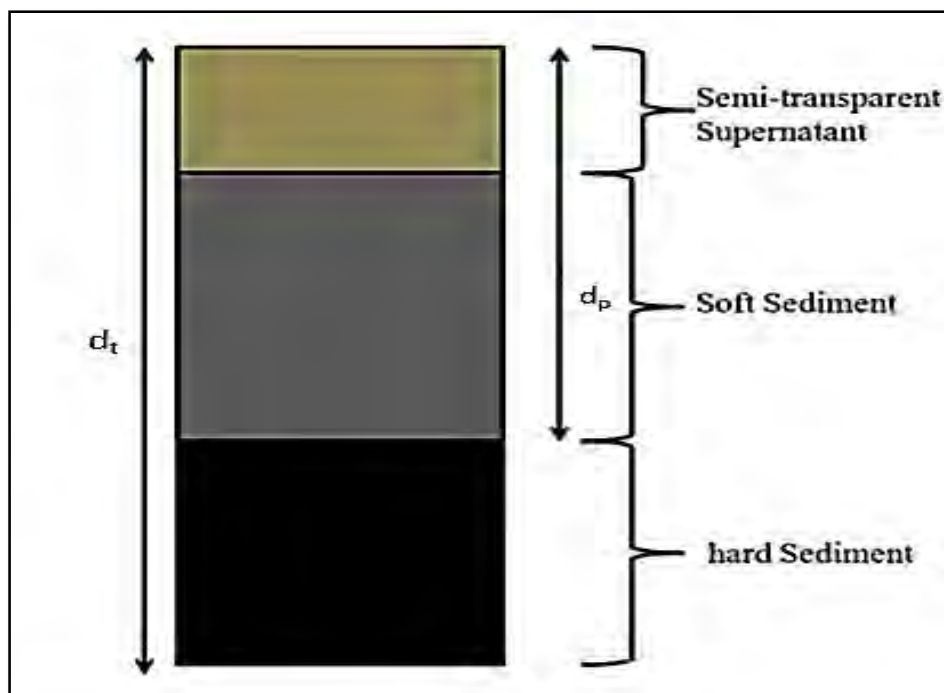


**Figure 3-4:** Diagram showing the separation of coal water slurry in cylinder after several days of storage



**Figure 3-5:** Static stability measuring cylinders with measuring rod

### **3.3 PROGRAMME**

The overall experimental design for this study was categorised into three stages. The first phase investigated the particle surface charge of the coal sample. With an understanding of the coal surface charge, the rheology of coal in suspension was considered in the second stage. Having seen the coal surface charge in response to chemical additives, pH and electrolyte addition about rheological properties, the third phase of the experiment investigated the issue of surface charge within the context of static stability in the presence of chemical additives. The summary of the experimental programme used for this study is shown in Figure 3-6.

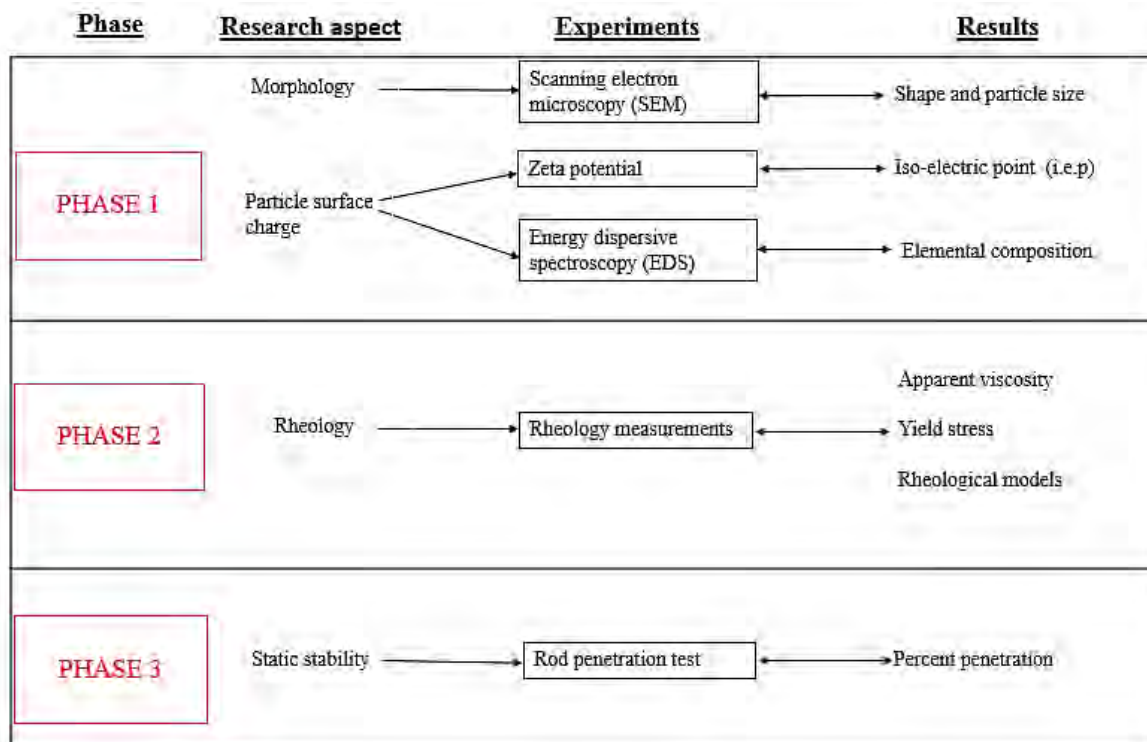


**Figure 3-6:** Schematic diagram showing experimental programme

### 3.3.1 Zeta potential

In all the experiments, zeta potential measurements were done at a pH range of 2 to 10. Nevertheless, most tests were investigated at the natural pH of coal samples (pH of 8). To maintain the pHs at the desired level, diluted HCl or NaOH was used to maintain the pH at the desired point in all experiments. Table 3-5 provides a summary of the zeta potential test.

**Table 3-5:** Summary of zeta potential test

Parameter	Value
pH	2, 4, 6, 8, 10,
Dispersants dosage (%)	0.1, 0.2, 0.3, 0.4, 0.5
Temperature (°C)	23
Volume (ml)	50

### 3.3.2 Rheology

In all the experiments, rheology measurements were performed at pH of 8, which was the natural pH of coal sample. Again, to maintain the pHs at the desired level, diluted HCl or NaOH

was used to maintain the pH at the desired level. Table 3-6 provides a summary of the rheology measurements.

**Table 3-6:** Summary of rheological tests

<b>Parameter</b>	<b>Value</b>
pH	8
Dispersants dosage (%)	0.1, 0.2, 0.3, 0.4, 0.5
Temperature (°C)	23
Shear rate (s <sup>-1</sup> )	0-200
Concentration (wt. %)	10, 20, 30, 40, 50, 60
Density of coal (g/cm <sup>3</sup> )	1.6
Volume of mixture (ml)	50

### 3.3.3 Static stability

Stability measurements were performed at pH of 8, which was the natural pH of coal sample. Table 3-7 provides a summary of the stability measurements.

**Table 3-7:** Summary of stability tests

<b>Parameter</b>	<b>Value</b>
pH	8
Dispersants dosage (%)	0.1, 0.2, 0.3, 0.4, 0.5
Temperature (°C)	25
Concentration (wt. %)	54
Density of coal (g/cm <sup>3</sup> )	1.6
Volume of mixture (ml)	150
Storage period (hours)	240

## 3.4 EXPERIMENTAL ERROR

All tests in this section were done in either double or triplicate. To measure the coefficient of variation, the standard error equation defined below was used.

$$S_y = \frac{s}{\sqrt{n}} \quad (3.3)$$

Where  $s$  is the standard deviation and  $n$  represents the number of replicates conducted

Table 3-8 shows the range for the coefficient of variation of zeta potential and rheology tests. As can be seen, there were slight deviations. Nevertheless, the coefficient of variations falls within the tolerance error limit.

**Table 3-8:** Showing coefficient of variation of measured variables

Measurements	Number of repeats (n)	Coefficient of variation (%)
Zeta potential	3	0.98-5.06
Rheology	3	0.1-5

## CHAPTER FOUR: RESULTS AND DISCUSSION

This chapter presents the results on zeta potential, rheology, and static stability of Witbank CWMs that were carried out in this research. Section 4.1 shows the zeta potential results on surface charge evaluated as a function of pH, electrolyte concentration, and dispersant addition. Section 4.2 shows the results on rheology of coal suspension assessed as a function of solids concentration, particle size, pH and dispersant addition. Lastly, Section 4.3 shows the results on static stability evaluated as a function of particle size and dispersant addition.

### 4.1 SURFACE CHARGE

The results presented in Section 4.1.1 and 4.1.2 show the effect of zeta potential on coal surface with pH in demineralised water and 1 M KCl electrolyte solution.

#### 4.1.1 Effect of pH

Figure 4-1 shows the zeta potential of coal samples as a function of pH in demineralised water and 1 M KCl solution.

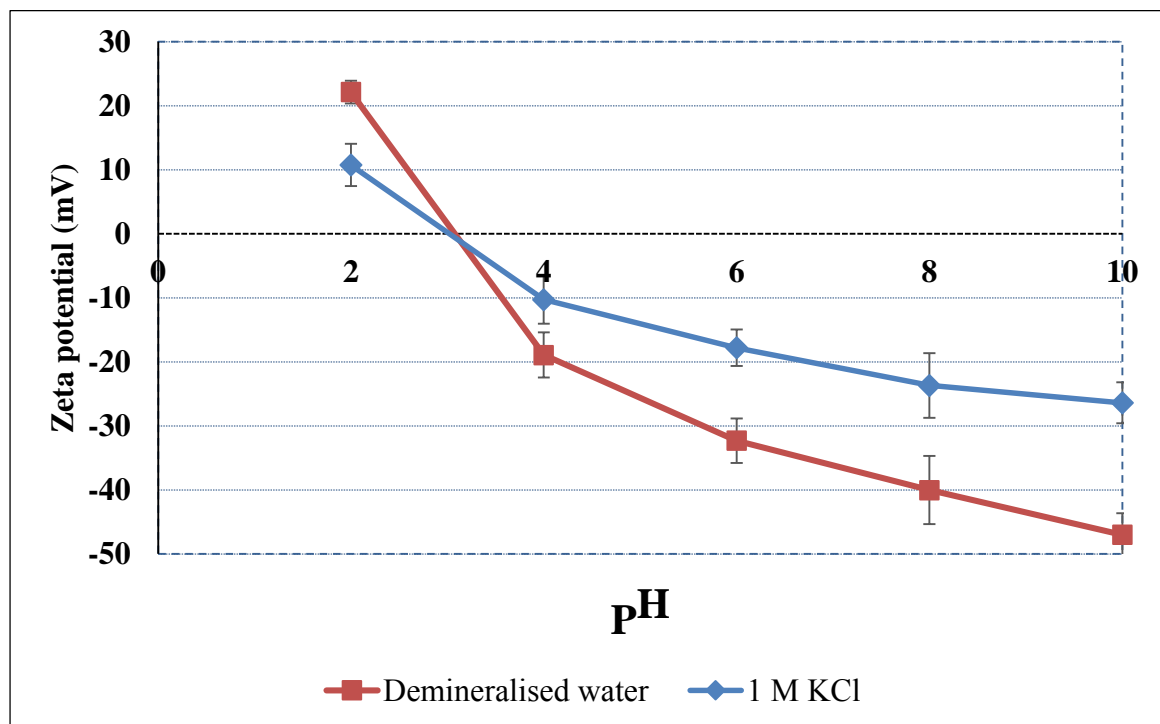


**Figure 4-1:** Graph of zeta potential (mV) versus pH of demineralised water and 1 M KCl

From Figure 4-1, in demineralised water, it is evident that increasing the pH of the demineralised water resulted in an increase in zeta potential. The results showed a positive zeta potential at pH 2. However the zeta potential became negative as pH is increased from acidic pH to basic pH. An isoelectric point (i.e.p) for the coal particles was observed at pH 3. Moreover, the highest absolute zeta potential in demineralised water at the natural pH of coal (pH 8) was observed at -38.86 mV.

The same trends were observed on the coal sample in 1 M KCl solution. This was shown on the same scale as in the case of demineralised water to emphasize the result of ion concentration on coal surface. However, the zeta potential values were seen to be slightly affected by the presence of electrolytes in solution. The outcomes show a positive zeta potential at pH 2, after that the zeta potential became negative as the pH increased from pH 3 to pH 10. An isoelectric point for the coal sample in 1 M KCl was observed at pH 3. As was noted in 1 M KCl solution, a slightly less positive and negative result was noticed in the acidic and basic pH conditions respectively.

Two significant factors can influence the interactions occurring on coal surfaces in the presence of demineralised water. Firstly, the surface characteristics of the coal sample. According to Pawlik *et al.*, (2007), the surface properties of low-rank coals (sub-bituminous and lignite) contains acidic groups and may dissolve in the presence of alkaline solutions. The coal surface is identified by the presence of polar groups, such as carboxyl ( $\text{COOH}_2^+$ ) and hydroxyl ( $\text{OH}_2^+$ ), attached to the hydrocarbon skeleton connected by cross-links (Mishra *et al.*, 2002). Hence, the mechanism occurring on the coal surface can be attributed to the pH dependent dissociation or protonation of these groups (Das *et al.*, 2009).

At low pH conditions, the positive zeta potential observed is due to the protonation of hydroxyl (OH) and carboxyl ( $\text{COOH}_2^+$ ) ions that are adsorbed on the coal surface contributing to the partial neutralization of surface charge. Likewise, in alkaline pH conditions, the negative zeta potential can be attributed to dissociation of hydroxyl ( $\text{OH}^-$ ) and carboxyl ( $\text{COOH}_2^+$ ) ions contributing to the increase in coal surface repulsion. According to Boger *et al.*, (1987), the functional groups present on coal surfaces play a significant role in influencing the apparent viscosity and yield stress of coal suspension.

On the other hand, the mineral matter present such as ash also plays a vital part. According to Mishra and Kanungo, (2000), an increase in the ash content shifted the isoelectric point towards a more alkaline pH. The presence of many inorganic oxides/hydroxides mostly  $\text{Fe}_2\text{O}_3$ ,  $\text{FeOOH}$ ,

clays, sulphide minerals ( $\text{FeS}_2$ ) can significantly contribute to the surface charge on coal surface with an aqueous medium (Mishra *et al.*, 2002).

The effects of electrolyte addition can be attributed to the fact that with an addition of electrolyte, the electrical double layer repulsion is strongly compressed towards zero due to the masking effect of ions in solutions. Although the compression of the electrical double layer seems to be the primary mechanism for the difference in zeta potential results observed. According to other researchers like Doymus, (2007) and Kaji *et al.*, (1987), the electrolyte concentration may have changed the surface charge due to the dissociation of ionogenic groups on the coal surface. It is, therefore, important that the charge distribution on the coal surface be considered when analysing both pure coal particles (completely liberated) and particles with minerals (partially liberated) because each coal particle may behave significantly different during electrokinetic measurement.

#### 4.1.2 Effect of dispersants

Figure 4-2 shows the variation of zeta potential on a coal sample with the addition of dispersants in demineralised water at the natural pH of 8.

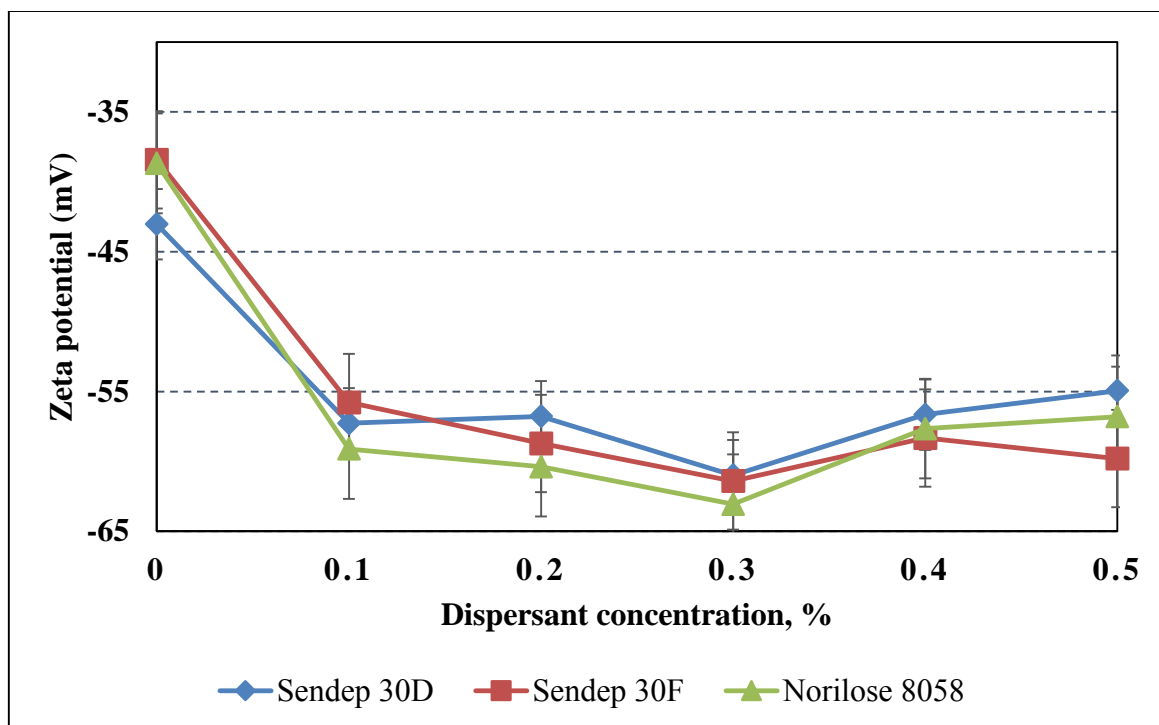


**Figure 4-2:** Graph of zeta potential at pH 8 in demineralised water with the addition of dispersants

As illustrated in Figure 4-2, the results indicate that in demineralised water at the natural pH of coal, the zeta potential was observed to be negative reaching a value of -38.86 mV. With the addition of dispersants into a mixture of coal and demineralised water, the zeta potential increased and remained relatively constant as the dispersant dosage was increased from 0.1 to 0.5 %. The most significant change in zeta potential was observed for Norilose 8058 at -63.06 mV at 0.3 %. Similar trends were observed for Sendep 30F and Sendep 30D at -61.4 mV and -60.99 mV respectively. Previous studies conducted on the effect of dispersants on a coal surface by Aktas, (2000) have indicated that the zeta potential of coal in the presence of dispersants is negative, and thus in conformity with the results of the Witbank coal sample. Also, the electrokinetic behaviour of the coal sample in the presence of dispersants agrees well with previous studies by Pawlic (2005), who studied the effect of dispersant adsorption on coal.

Figure 4-3 shows the variation of zeta potential on a coal sample with the addition of dispersants in 1 M KCl solution at the natural pH of 8.

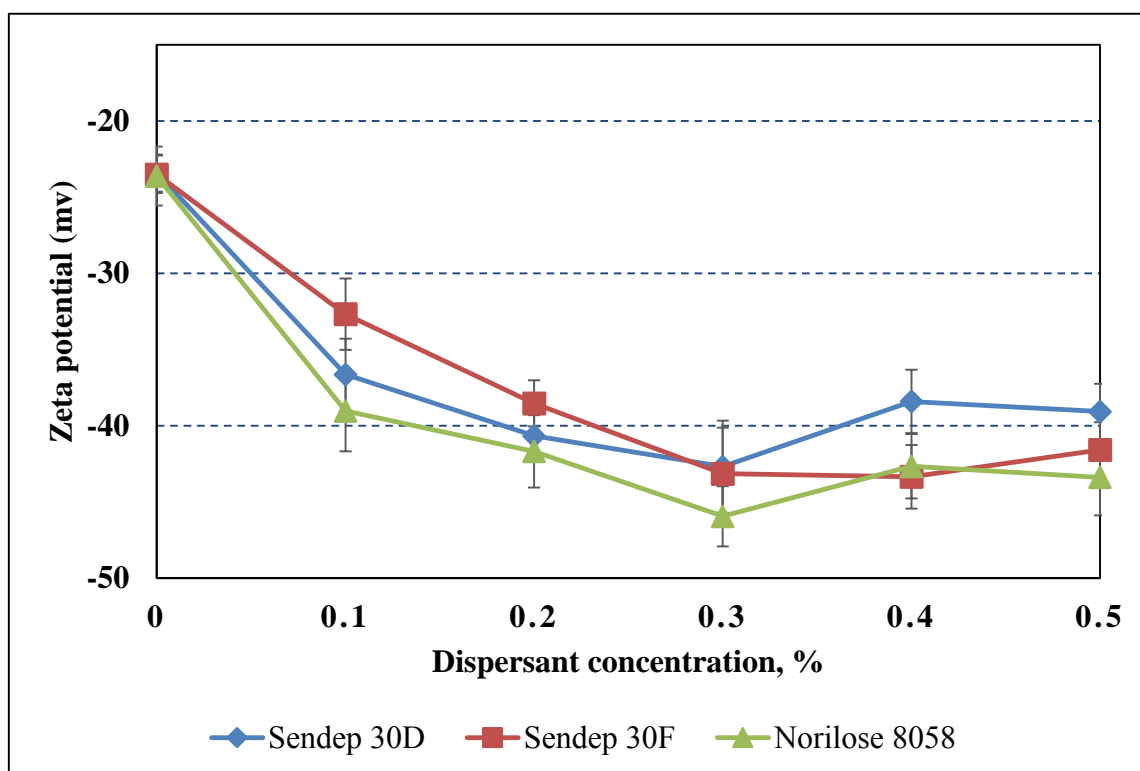


**Figure 4-3:** Graph of zeta potential of coal at natural pH 8 in 1 M KCl with the addition of dispersants in solution

From Figure 4-3, the zeta potential of the coal sample in 1 M KCl is negative reaching a value of -23.68 mV at the natural pH of coal. With the addition of a dispersant, the zeta potential

became more negative as the dispersant dosage is increased from 0.1 to 0.5 %. The highest absolute zeta potential value was observed for Norilose 8058 at -45.90 mV at 0.3 %. However, the zeta potential seen in the presence of 1 M KCl was less than that in the demineralised water alone. Others have reported the decrease in zeta potential on coal surface in the presence of electrolyte concentration (Dincer *et al.* 2003; Doymus, 2007 and Mishra and Kanungo, 2000).

When compared to existing literature, the experimental results were acceptable as seen in Figure 4-2 and Figure 4-3 in comparison to the results obtained from Dincer *et al.* (2003). Although experimental values were obtained using new dispersants, there seems to be a good correlation between the tested dispersants and commercial additives. This phenomenon observed, can be attributed to the adsorption of dispersants by the hydrophobic organic surface of coal (Doymus, 2007). Hence, the thicker the adsorption layer, the more the prevention of coal particles from mutual interactions.

This conclusion is in accord with the investigations of Atesok *et al.*, (2002), who also observed similar results on three different Turkish coals using dispersant and concluded that dispersant increased the zeta potential of the coal surface. Also, other researchers, e.g. Aktas (2000) and Harvey *et al.*, (2002) obtained similar negative shifts with the addition of CMC on coal surface in solution. Mishra and Kanungo, (2000) showed that generally the electrical double of coal particles in solution becomes thicker in the presence of dispersants; hence, the electrophoretic mobility of the coal particle changes consequently. According to Rao (2004), at high concentration of dispersants in solution, the electrical double layer eventually increases, and surface charge of the mineral may be altered.

## **4.2 RHEOLOGY**

This section presents the results on the rheology of CWMs. Section 4.2.1 shows the results on rheograms of CWMs at varying solids concentration ranging from 10 – 60 wt.%. Section 4.2.2 shows the results on the empirical non-Newtonian data model fitted at a solid concentration of 54 wt.%. The results on the effect of solids concentration and particle size on rheology are shown in Section 4.2.3 and 4.2.4 respectively. Section 4.2.5 shows the outcomes on the effect of pH on rheology. Lastly, the result indicating the effect of dispersant addition on rheology is shown in Section 4.2.6.

### 4.2.1 Rheograms

Figure 4-4 and Figure 4-5 show the rheograms of fine particle (PSD,  $-75\ \mu\text{m}$ ) tested at different solids concentrations showing the general rheological behaviour of CWMs.

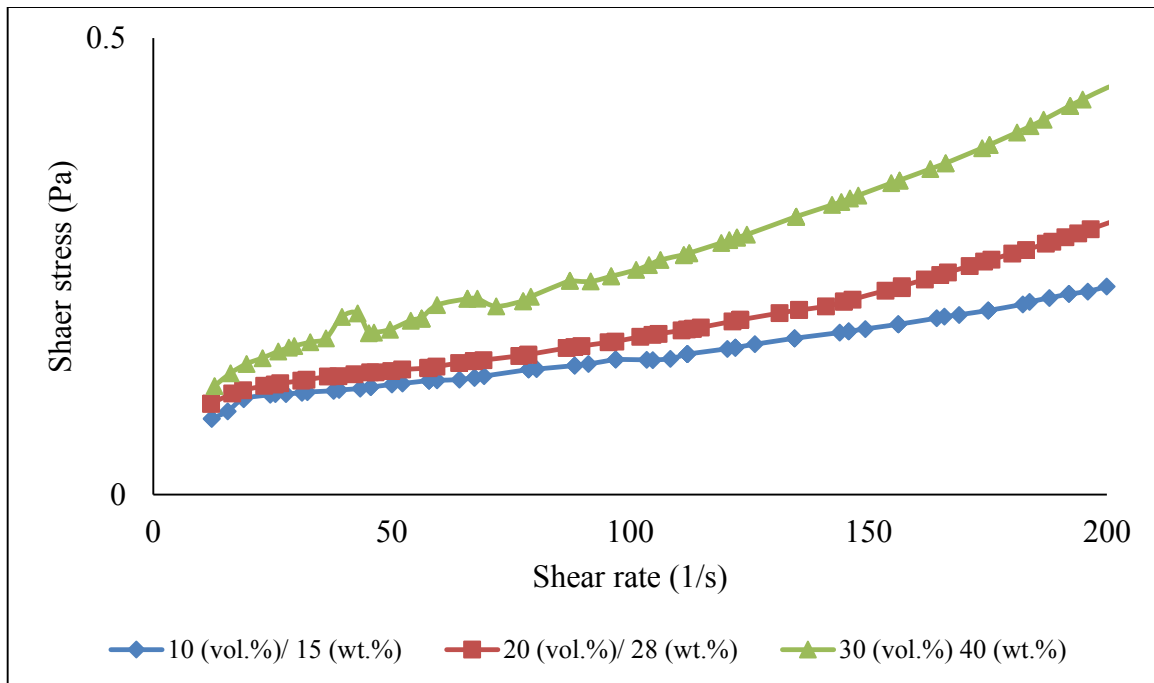


**Figure 4-4:** Graph showing shear stress as a function of shear rate

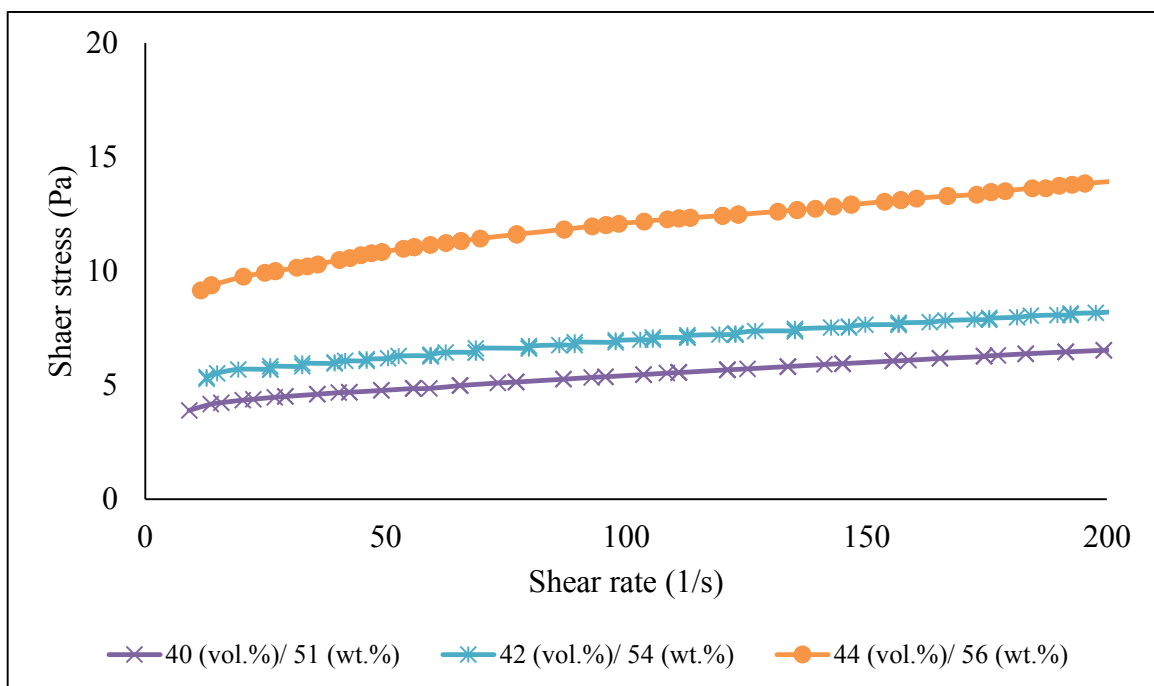


**Figure 4-5:** Graph showing shear stress as a function of shear rate

As can be seen from Figure 4-5 and Figure 4-5 , it is clear from the graph that rheograms cover a considerable range in shear rate of  $0 \text{ s}^{-1}$  to  $200 \text{ s}^{-1}$ . Clearly two major trends are presented in the plot: the suspensions are strongly Newtonian at a low solids concentration below 51 wt.% as shown in Figure 4-4. However, as the concentration increases above 51 wt.%, the curves seem to tend toward non-Newtonian behaviour. It is clear that the relationship between shear rate and shear stress is not linear and exhibit high yield stresses. The yield stress increased with an increase in the solids concentrations in all cases.

The increase in yield stress described in this work is in good agreement with the investigations by Turian *et al.*, (2002) who observed similar phenomena on the rheology of concentrated fine particulate mineral slurries. Figure 4-6 shows viscosity as a function of shear rate for CWMs.

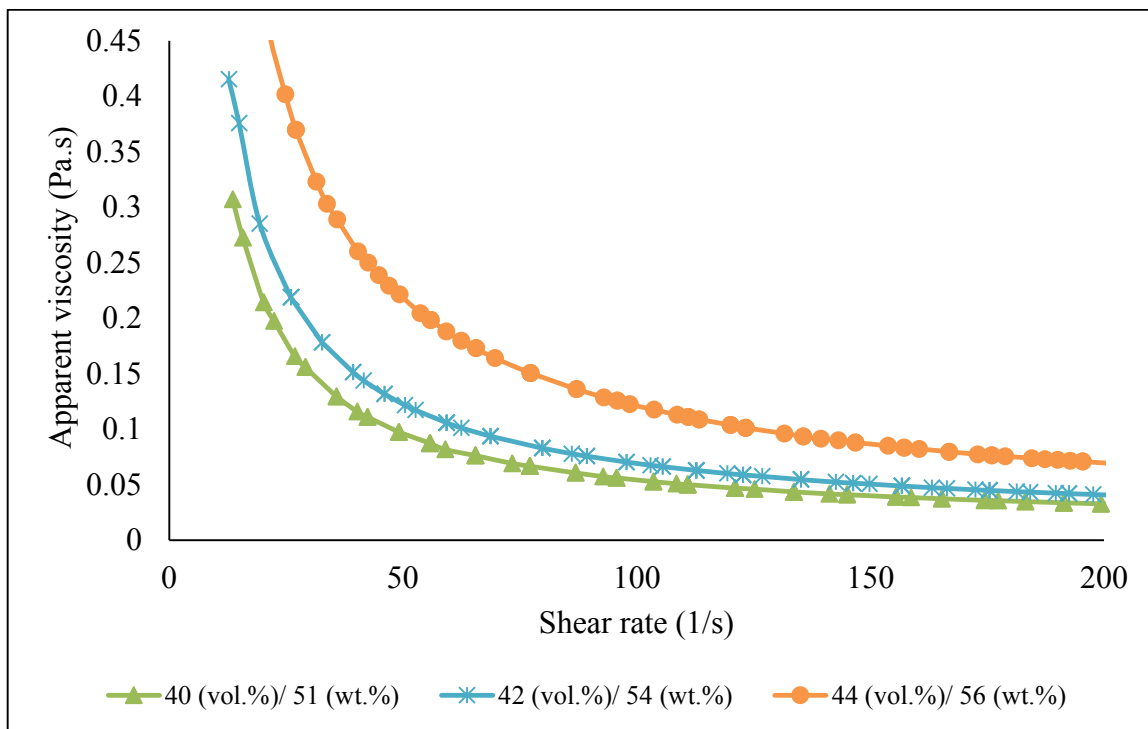


**Figure 4-6:** Graph showing viscosity versus shear rate for the shear thinning system

As seen from Figure 4-6, with an increase in solids content above 51 wt.%, the viscosity rapidly increases and exhibits progressively more non-Newtonian behaviour. The viscosity of the suspension, decreased with increasing shear rate showing the characteristics of shear thinning (pseudoplastic) fluids. The decrease in apparent viscosity with increasing shear rate is probably due to the breakdown of the flocculated structure as the shear rate increases. The non-

Newtonian behaviour observed shows that, there is an increase in inter-particle interactions as the coal concentration increases.

The shear thinning (pseudoplastic), non-Newtonian behaviour is similar as mentioned by Shukla *et al.*, (2008). In their investigation, increasing the coal concentration above 20 wt.%, suspensions showed pseudoplastic behaviour with increasing Bingham yield stress. Roh *et al.* (1995) observed similar phenomena with coal loading between 50-63 wt.%, and they attributed the rise in viscosity to inter-particle interactions and formation of complex flocculated structures in the suspension. According to Laskowski, (2011), in a highly loaded coal concentrated suspension, an increase in apparent viscosity could probably cause by the interaction between particles becoming significantly with an increase in the number of particles per unit volume.

#### 4.2.2 Rheological models

The shear rate – shear stress data shown in Figure 4-5 was fitted with the Herschel-Bulkley empirical non-Newtonian models described in Equations (2.6) at a coal concentration of 54 wt.% using excel solver functions. Figure 4-7 shows the flow curves for the coal suspension obtained at a solid concentration of 54 wt.%.

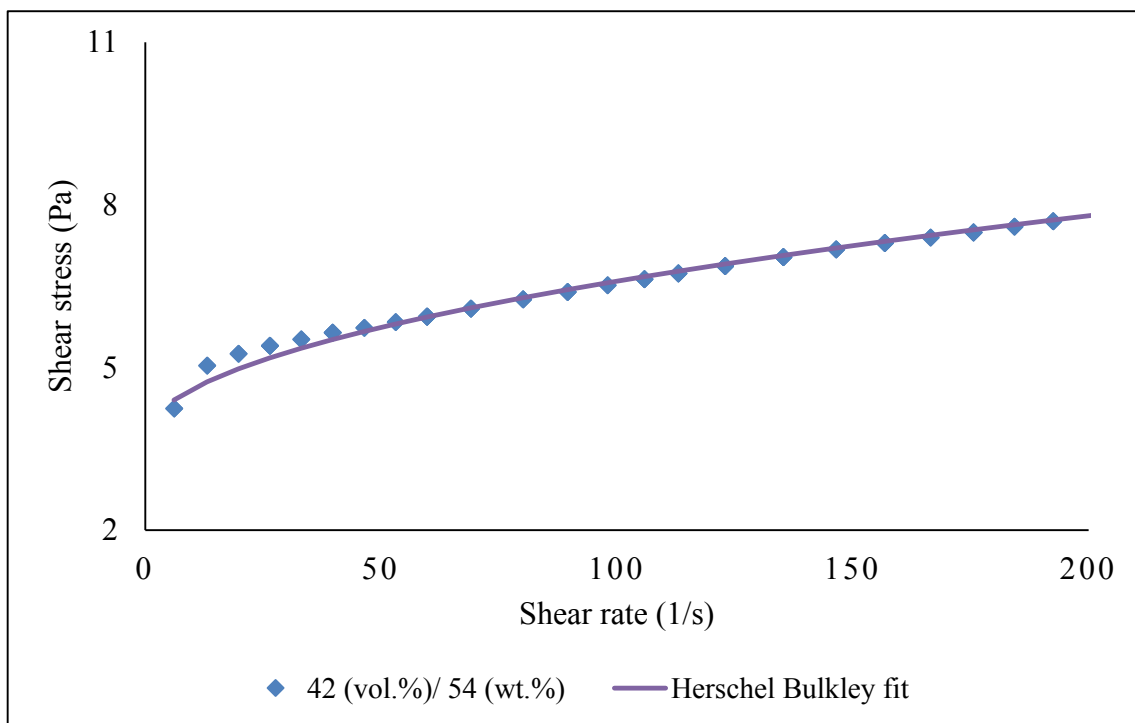


**Figure 4-7:** Graph showing the comparison of the predicted model fit with coal at 54 wt. %

From Figure 4-7, it can be seen that the three-parameter Herschel-Bulkley model did the overall job of describing the experimental data over the whole shear range of the suspension. The Herschel-Bulkley model covered the entirely possible shear rate.

Table 4-1 compares the rheological models and evaluates different fluids adjustable parameters by making a comparison between consistency indexes (K), flow behaviour index ( $\eta$ ), yield stress, and viscosity. These adjustable fluid parameters will be explained in the subsequent sections.

**Table 4-1:** Rheological model with -75- $\mu\text{m}$  particle size with different coal concentration

Model	Coal conc. (Wt. %)	Parameters			Standard error
Bingham law		$\tau_0$	$\mu_p$		
	10	0.22	2.48E-03		98.68
	20	0.42	1.17E-04		98.34
	30	0.59	3.24E-04		91.4
	52	3.64	8.01E-03		58.69
	54	5.52	9.88E-03		46.53
	56	11.52	0.16		26.18
Power law		K	$\eta$		
	10	0.22	1		98.68
	20	0.72	0.93		91.38
	30	0.74	0.90		90.34
	52	1.24	0.28		51.16
	54	2.16	0.24		40.75
	56	5.23	0.2		32.21
Herschel-Bulkley		$\tau_0$	K	$\eta$	
	10	0.22	0	1	98.68
	20	1.56	0.14	0.92	97.01
	30	1.76	0.18	0.95	91.38
	52	2.06	0.26	0.48	47.97
	54	3.68	0.29	0.47	34.98
	56	8.18	0.55	0.45	26.18

The result shown in Table 4-1 depicts that the yield stress ( $\tau_0$ ) and the consistency index (K) increases with increasing solids concentration. On the other hand, the consistency index (K) increases with increasing solids concentration, whereas the flow behaviour index ( $\eta$ ) was

observed to decrease with increasing solids concentration. The observed differences in the response of the consistency index (K) and the flow behaviour index ( $\eta$ ) are likely to be attributed to the shear thinning behaviour of the fluid.

The model described in this work are in good accord with the investigations by Guibaud *et al.*, (2004) and Turin *et al.*, (2002) who observed similar phenomena on mineral slurries. They concluded that the Herschel-Bulkley is useful for describing the rheology of a suspension at high concentrations in comparison to the Bingham model and Power-law models. Haser *et al.*, (2004) and Pollice *et al.*, (2007), showed that the Power law model was best for describing the rheology of suspensions in a low shear rate range.

The values obtained by Garakani *et al.*, (2011) studying a whole range of rheological parameters of different mixed liquor suspended solids of activated sludge are in good agreement with the experimental data shown in Table 4-1. Previous studies by Pawlic, (2005), observed similar effects on increasing solids concentration with adjustable fluid parameters. According to Tiwari *et al.*, (2003), physical and chemical properties of coal as well play an important role on colloidal particles in solution.

### **4.2.3 Effect of solids concentration**

The following results demonstrate the effects of solids concentration of coal-water slurries. The purpose of this section is primarily to investigate how solids concentration affects rheology. Therefore, in the following sub-sections yield stress and apparent viscosity will be investigated to determine how these parameters influence the rheology of coal suspensions.

#### **4.2.3.1 Yield stress**

Figure 4-8 shows the effect of yield stress as a function of coal solids concentration.

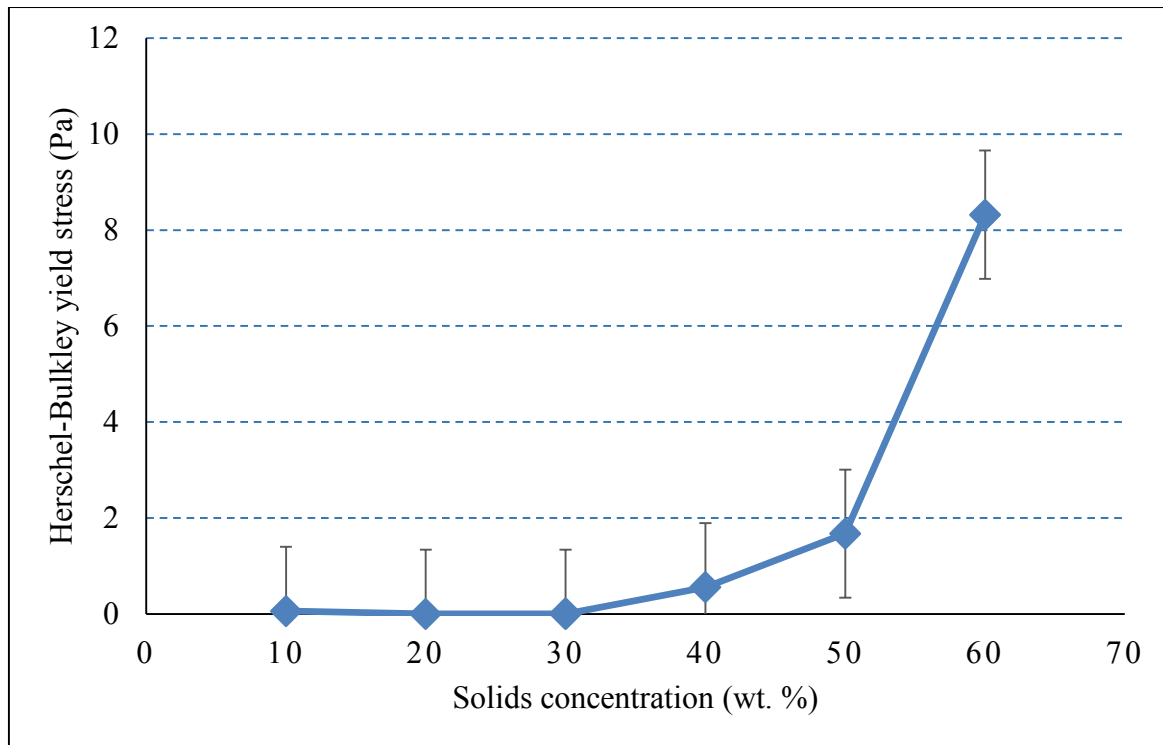


**Figure 4-8:** Graph of Herschel-Bulkley yields stress versus solids concentration for  $-75 \mu\text{m}$  particle size

From Figure 4-8, it can be seen that coal suspension below 30 % (by weight) has low yield stresses ( $< 0.1 \text{ Pa}$ ). The yield stress, increased exponentially with increasing solids concentration above 40 % (by weight). This indicates that below 30 % (by weight) there is little interaction between coal particles in suspension. However, coal suspension above 40 wt.% was characterized by high yield stresses ( $> 0.5 \text{ Pa}$ ). The increase in yield stress with an increase in solids concentration is in conformity with previous studies by Klimpel (1984), who observed similar effects at solids concentrations greater than 45 wt.%. Although the objective of CWMs is to maximise its solids concentration, the effect of high yield stresses can be observed as the coal concentration increases.

#### 4.2.3.2 Apparent viscosity

The results presented in Figure 4-9 shows the outcome of increasing solids concentration on the apparent viscosity of CWMs.

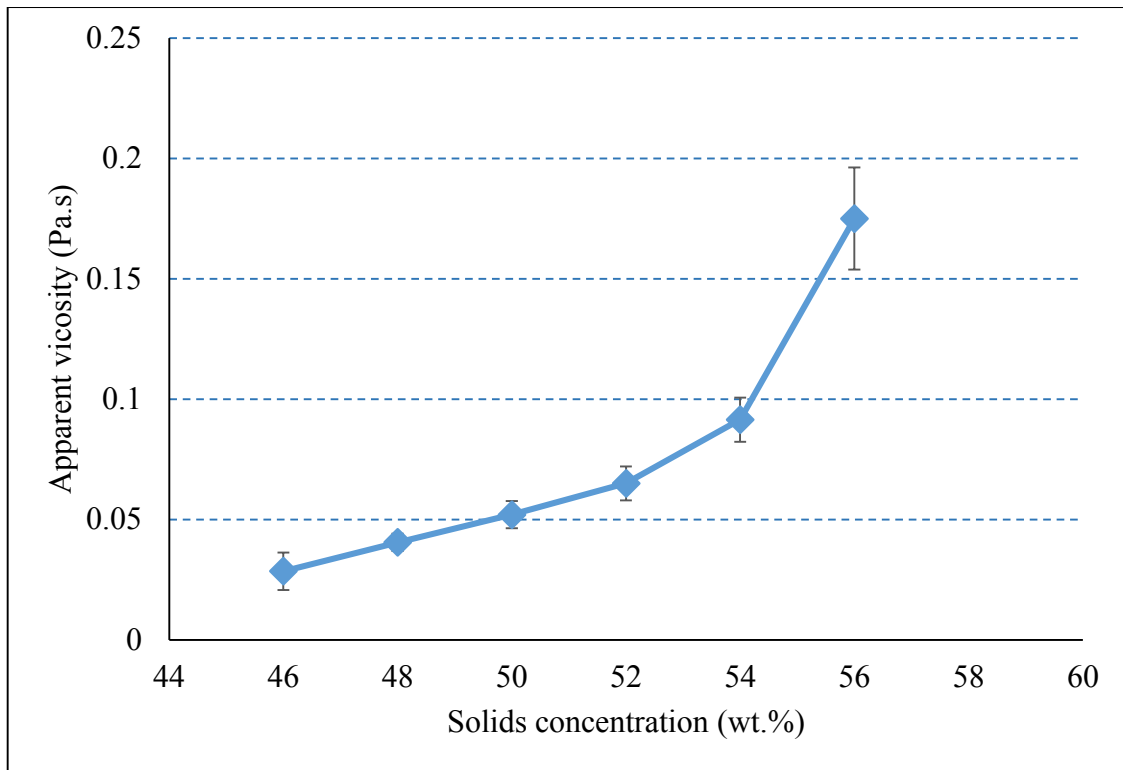


**Figure 4-9:** Graph of -75  $\mu\text{m}$  particle size showing the relationship between the apparent viscosity and solids coal concentration with 0 % dispersant at a shear rate of  $200 \text{ s}^{-1}$

From Figure 4-9, it can be determined that the viscosity of the coal suspension increased exponentially with increasing solids concentration. As the coal concentration is increased beyond 54 wt.%, a sharp increase is noticed. The point at which a drastic increase occurred is termed the critical solids concentration point. As the critical solids concentration is approached, the viscosity of the slurry increases sharply. The maximum critical solids concentration for the transportation of -75  $\mu\text{m}$  particle size without dispersant was obtained at 54 wt.%. This rheological behaviour of coal suspensions is similar to the findings obtained by Shukla *et al.*, (2008), studying the effect of solids concentration of Indian coal. A critical solids concentration point of 40 % (by weight) was obtained.

Figure 4-8 and Figure 4-9 show that both yield stress and apparent viscosity increased with increase in solids concentration as expected from a mixture containing the same type of material. Many researchers have carried out similar investigations on CWMs rheology. Roh *et al.*, (1995) and Turian *et al.*, (2002) in their study on increasing solids concentration noticed a yield stress on increasing solids concentration above 50 wt.%. The works of Leong *et al.*, (1987), studied the rheological behaviour of Victorian brown coal suspension for solids concentration between 25 wt.% and 65 wt.%. They found an interesting observation between

the equilibrium moisture content and solids concentration in CWM at a shear rate of  $5.2 \times 10^2 \text{ s}^{-1}$ . They found that decreasing the moisture content led to an increase in yield stress. Turian *et al.*, (1992), on the other hand, working on CWMs reported a solids concentration range between 47 wt.% and 65 wt.%. Cheng, (1980) and Uyar *et al.* (1994) suggested that the increase in apparent viscosity with an increase in solids concentration was probably due to particle-particle interactions in the fluid.

The mechanisms occurring within the fluid showing high yield stress and apparent viscosity as the coal concentration increases can be attributed to the fact that an increase in solids concentration will result in more particles interacting per unit volume. Hence, the increased in particle-particle interaction will lead to high yield stress and apparent viscosity. In most cases, high yield stress is identified by the formation of aggregates within the fluids.

#### 4.2.4 Particle size

The following results show the effect of particle size on coal-water slurries. The purpose is to investigate how particle sizes affect rheology.

##### 4.2.4.1 Yield stress

Figure 4-10 shows the variation of yield stress with particle size at a solids concentration of 54 wt.%.

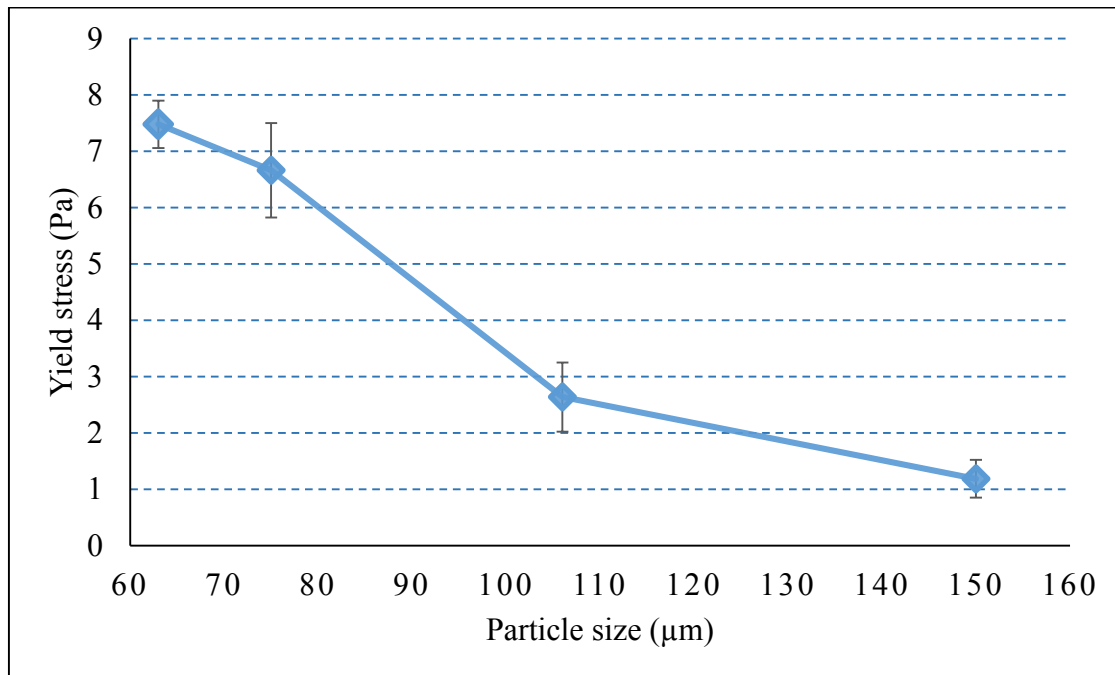


**Figure 4-10:** Graph of yield stress versus particle size on CWM at 54 wt.% coal concentration

From Figure 4-10, it can be seen that the yield stress of the coal concentration increases with a decrease in particle size. As can be seen, -63  $\mu\text{m}$  particles have a much higher yield stresses than -150  $\mu\text{m}$  particle size. The larger particle size showed the lowest yield stress values. Contrary, higher yield stress values were obtained as the particles become finer.

The increase in the yield stress of CWMs with decreasing particle size is in conformity with previous results obtained by Buranasrisak and Narasingha, (2012) and Kawatra, and Eisele (1998). Kawatra and Eisele (1998) reported that at a constant solids concentration, the reduction in particle size would result in an increase in yield stress of coal concentration.

#### 4.2.4.2 Apparent viscosity

Figure 4-11 shows the variation of apparent viscosity with particle size at a solids concentration of 54 wt.%.

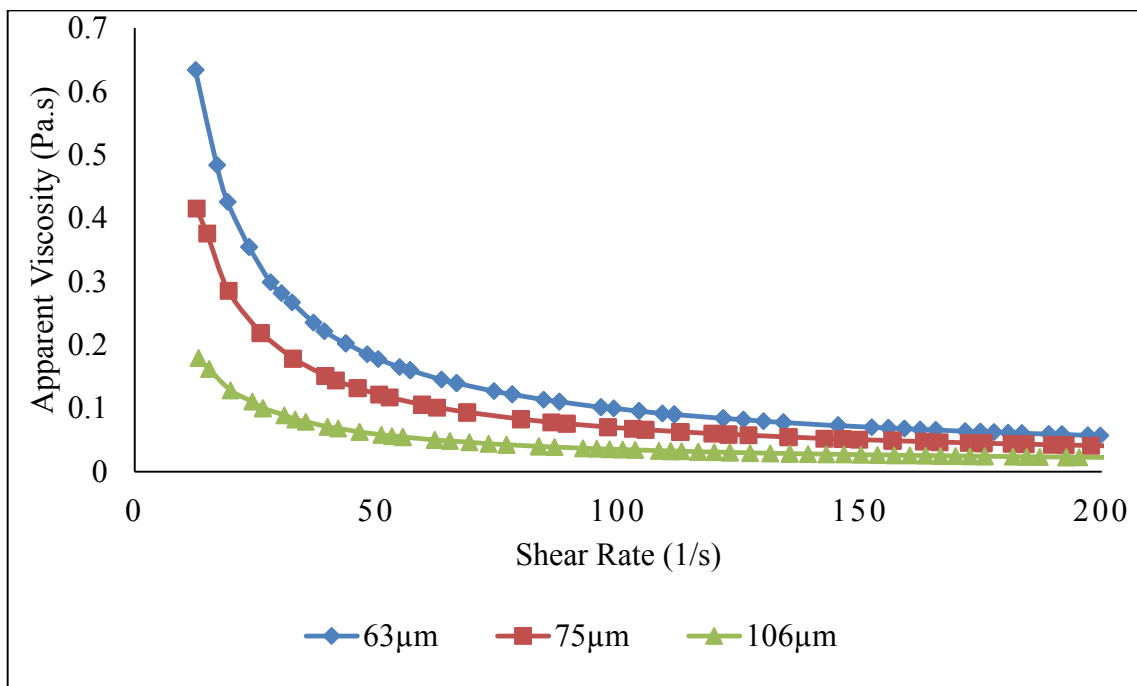


**Figure 4-11:** Graph showing the effect of particle size  $D_{50}$  on the apparent viscosity of CWS with 54 wt.% at shear rate of  $200 \text{ s}^{-1}$

As determined from Figure 4-11, it can be noticed that the apparent viscosities of all CWMs with different particle size decreased when increasing the shear rate applied. From the figure, it can be seen that the smaller particle size ranges exhibited higher apparent viscosities than those of, the larger particle size. The results obtained above is in agreement with Roh *et al.*,

(1995) who observed similar conclusions on the effect of particle size on the preparation of highly loaded CWMs.

From both graphs yield stress and apparent viscosity increases with a reduction in particle size as expected from a mixture containing similar particle size and coal concentration. Hence, the reason affecting yield stress is the same as those affecting apparent viscosity. The primary mechanism occurring within the fluid showing high yield stress and apparent viscosity with a decrease in particle size can be inferred from the fact that smaller particles contain more particles per unit volume and, as a result, more particle interactions. In addition to this reason, smaller particles have a high surface area and are affected by inter-particle forces.

Although, particle size seems to be the main factor affecting yield stress and apparent viscosity. According to other researchers like Barnes *et al.*, (1986) and Farries (1968), the yield stress and apparent viscosity of CWMs can be improved by mixing different ratios of fines and coarser coal particles. Buranasrisak and Narasingha (2012), results clearly demonstrate that a highly CWMs can be obtained only by adjusting the coal particle size and distribution. They proposed that by mixing different fractions of fines and coarse particle size distribution, the apparent viscosity of CWMs can be enhanced and optimised. According to studies by Roh *et al.*, (1995), they observed a decrease in yield stress and attributed that the decrease was probably due to the fine particle filling the voids of the coarser particles, therefore, increasing the fluidity of the suspension at fixed volume solids.

#### **4.2.5 Effect of pH**

The following result shows the effect of pH on coal-water slurries. The purpose of this section is to investigate the effect of pH on rheology.

##### **4.2.5.1 Yield Stress**

Figure 4-12 shows the variation of yield stress with pH at a varying solids concentration by weight.

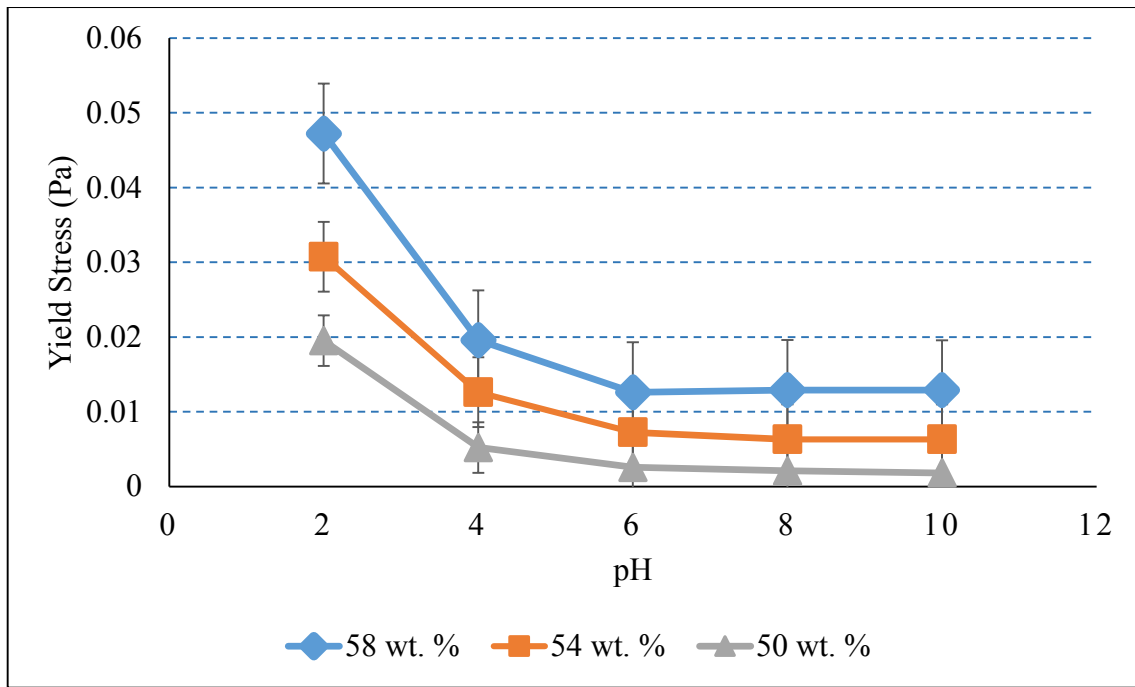


**Figure 4-12:** Graph showing yield stress as a function of pH at a shear rate of  $200 \text{ s}^{-1}$

It can be seen from Figure 4-12 that, yield stress value increases with a decrease in pH. The lowest yield stress value was obtained in the basic pH range. On the contrary, the yield stress values increased as the pH decreases (i.e. acidic pH). Kaji *et al.*, (1987), reported that the yield stress properties of coal suspension could be altered by changing the charge density, i.e. by adjusting the pH of the solution, which is in conformity with this finding.

#### 4.2.5.2 Apparent viscosity

Figure 4-13 shows the variation of apparent viscosity with pH at a varying solids concentration by weight.

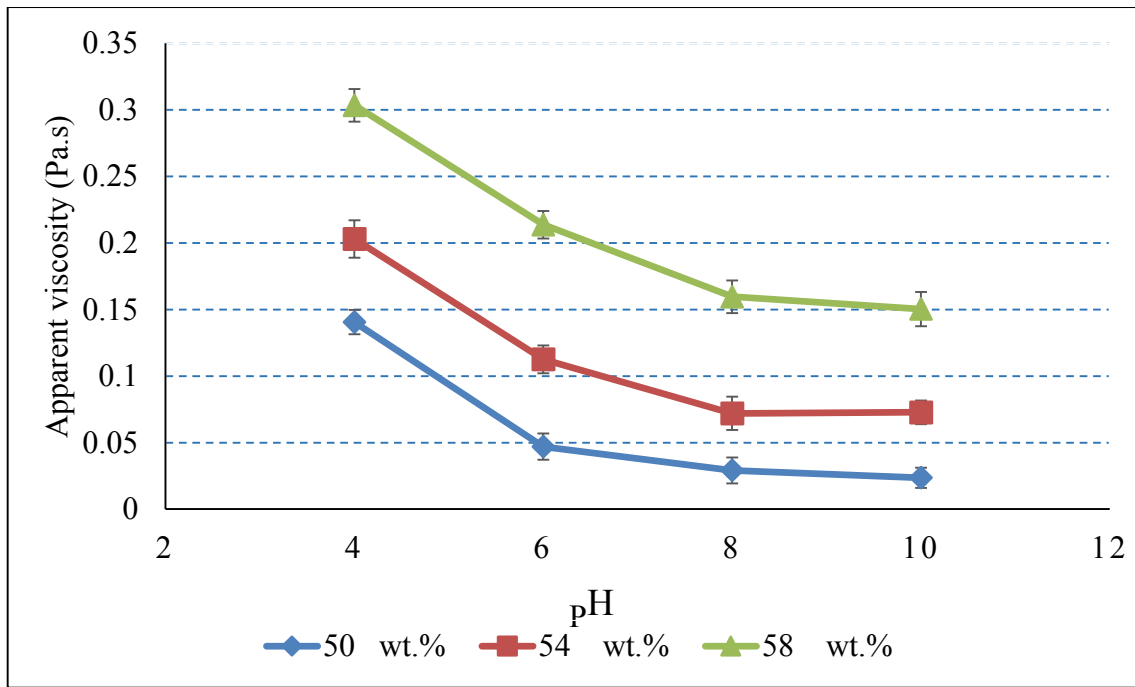


**Figure 4-13:** Graph showing the effect of pH on the apparent viscosity of CWM ( $d_{50} = 27.97 \mu\text{m}$ )

As can be seen, values of apparent viscosity plotted against pH are shown in Figure 4-13. For all the solids concentrations, the viscosity increases with a decrease in pH. CWMs containing the same solids concentration seemed to follow the same pattern for both yield stress as well as apparent viscosity graph.

The increase in yield stress and apparent viscosity with a decrease in pH of CWMs is in conformity with previous results from Boger *et al.*, (1987); Kaji *et al.* (1987); Mishra *et al.*, (2002) and Tiwari *et al.*, (2002). Recent work by Benyounes and Benmounah (2012), on the effects of cations on solid particle concentration is also in agreement with the findings of this study. In support of this observation, it is worth recalling Figure 4-1, which shows the effect of the zeta potential of coal particles versus pH. The increase in pH from acidic to basic pH range increased the zeta potential from -10 mV to -38.86 mV, higher zeta potential at a basic pH range means there are more electrostatic repulsion forces which are shown in lowering the yield stress as well as apparent viscosity curves at the basic pH range.

#### 4.2.6 Effect of dispersants

The following results demonstrate the effects of dispersants on coal-water slurries. The purpose of this section is to investigate how dispersants affect rheology.

##### 4.2.6.1 Yield Stress

Figure 4-14 shows the relationship between dispersant concentrations as a function of yield stress at 54 wt.% coal.

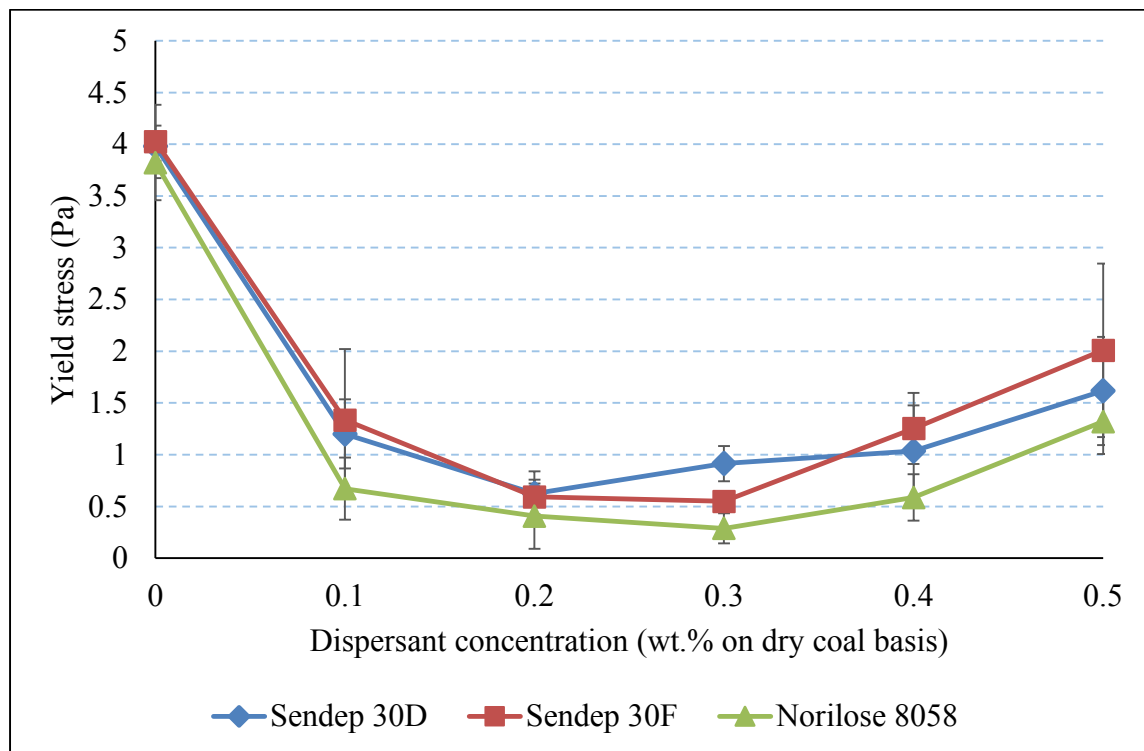


**Figure 4-14:** Graph showing Bingham yield stress as a function of dispersant concentration at 54 wt.%

It can be seen from Figure 4-14 that at solids concentrations of 54 wt.%, which has no chemical in it, the yield stress was observed reaching a value of about 4 Pa. Upon the addition of dispersants, the yield stress was noted to be decreasing suggesting a modification in the surface chemistry of coal due to interactions of dispersants on mineral surface. A remarkable decrease in yield stress up to 0.5 Pa was obtained in the presence of the dispersant. The decline in yield stress seen in this finding is in agreement with the previous studies by He *et al.*, (2009). In addition, the decrease in yield stress with an increase in dispersant of CWMs is in conformity with previous results from Pawlic, (2005).

#### 4.2.6.2 Apparent Viscosity

Figure 4-15 shows the relationship between dispersant concentrations as a function of apparent viscosity at 54 wt.%.

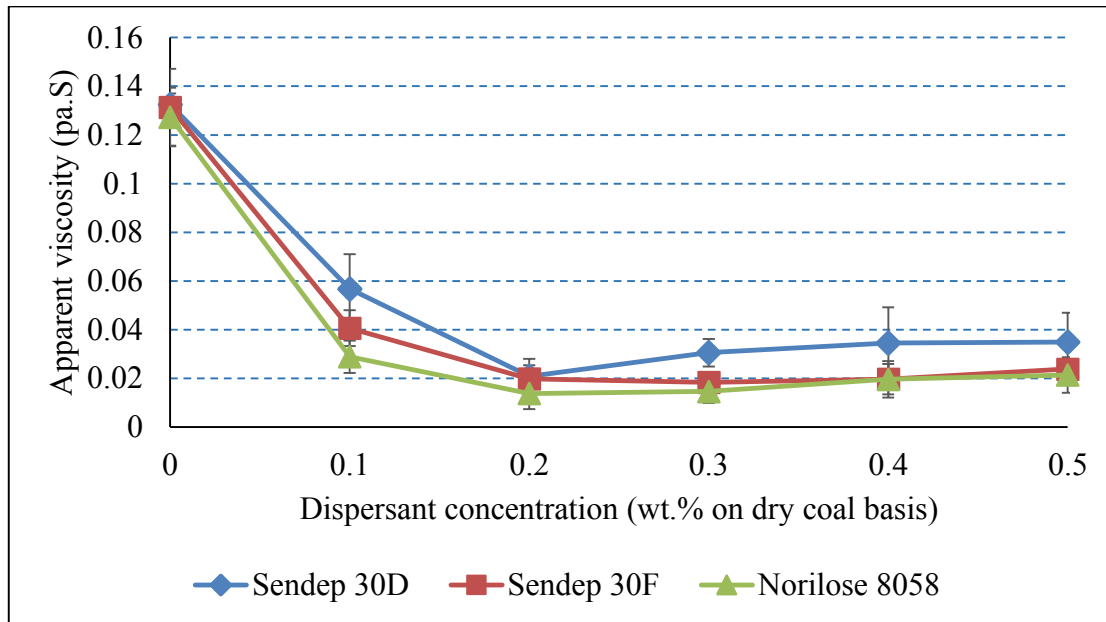


**Figure 4-15:** Graph showing apparent viscosity of CWMs at  $200 \text{ s}^{-1}$  with a varying dispersing dosage at solid concentration 54 wt.%

As shown in Figure 4-15, at the solids concentration of 54 wt.%, which has no dispersant in it, the apparent viscosity was observed reaching a value of about 0.13 Pa.s. However, the apparent viscosities decrease sharply with an increase in dispersant dosages from 0.1 to 0.5 with.%. A significant decrease in apparent viscosity up to 0.02 Pa.s was obtained in the presence of the dispersant. In light of this, 0.2 wt.% was chosen as the ‘optimum’ dispersant dosage.

In this context, Trochet-Mignard *et al.*, (1995) reported a similar observation, and it was concluded that a densely adsorbing chemical additive is not necessarily a better coal dispersant. The ability of these polymers to depress the natural floatability of Witbank bituminous coal is also quite evident. According to Pawlic (2005), suitable dispersants are also good flotation depressants. In reinforcement of this observation, it is worth recalling Figure 4-2, which shows the effect of dispersant dosage on zeta potential, and, as discussed in Section 4.2.6. Increasing dispersants dosage resulted in an increase in the zeta potential. The low yield stress and viscosity values observed correlates well with the zeta potential results. Comparing the tested dispersants is it desirable that the dispersant used in coal- water slurries are as low as possible

with low apparent viscosities. Hence, Norilose 8058 looks more promising dispersant for the preparation of Witbank coal-water slurries in the industrial application.

### 4.3 STATIC STABILITY

The following results investigate the effects of dispersants as an anti-settling additive on coal-water slurries. Section 4.3.1 and 4.3.2 seek to investigate the stability of CWMs and assessed by rod penetration tests as described by Usui *et al.*, (1999).

#### 4.3.1 Effect of particle size

Figure 4-16 shows the graphs of percent penetration ratio of coal storage at 54 wt.% of storage time with different particle size.

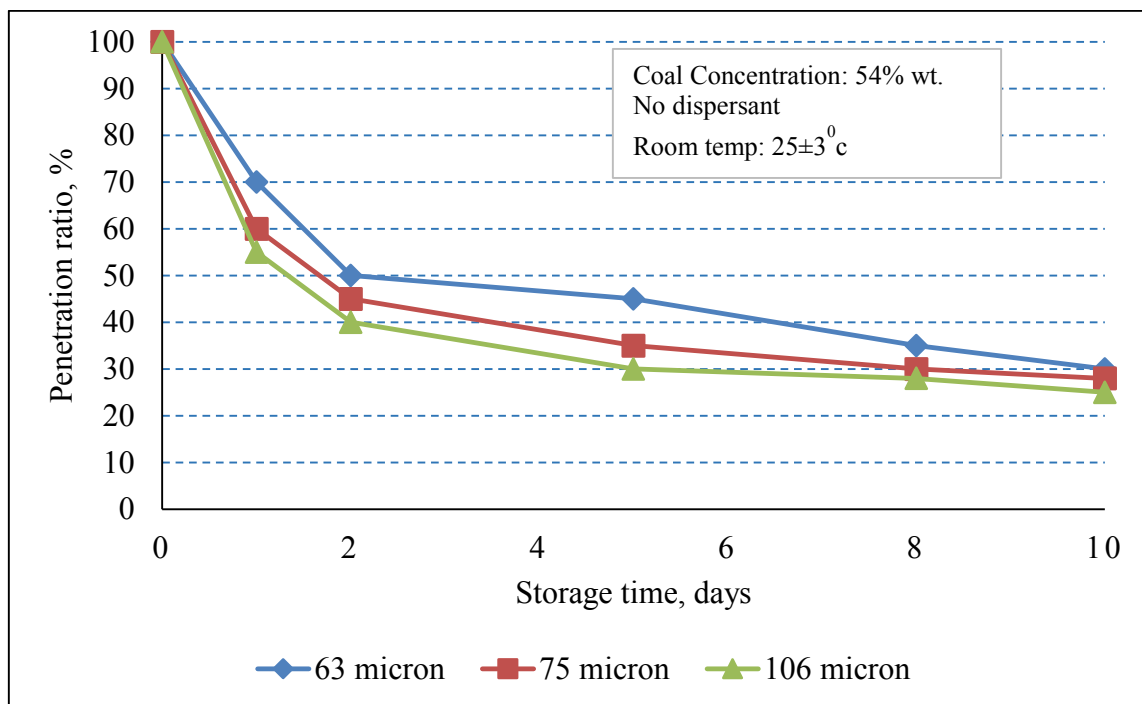


**Figure 4-16:** Graph showing stability of a coal sample prepared using different particle size

As examined in Figure 4-16, the penetration ratio of the coal-water slurries prepared with various particle sizes was observed reaching an initial penetration of 100%. However, the penetration rate kept decreasing with the increase of storage time within 48 hours. It was noted that by increasing the storage period to 120 hours the penetration of coal was unacceptable with a compacted hard-packed layer detected at the bottom of the measuring cylinder. The penetration ratio reached a maximum of about 35% after 240 hours. This shows that coal suspension is susceptible to settling if allowed to be stored for specific days.

The decrease in penetration ratio with an increase in storage time of coal suspension is in conformity with previous results from Dincer *et al.*, (2005) and Usui *et al.* (1999). From this perspective, Usui *et al.*, (1999) suggested that an aggregation of coal particles is likely to exist in a concentrated coal suspension with no chemicals.

### 4.3.2 Effects of dispersants

Figure 4-17 shows the effect of stability on coal suspension in the presence of dispersant additives.

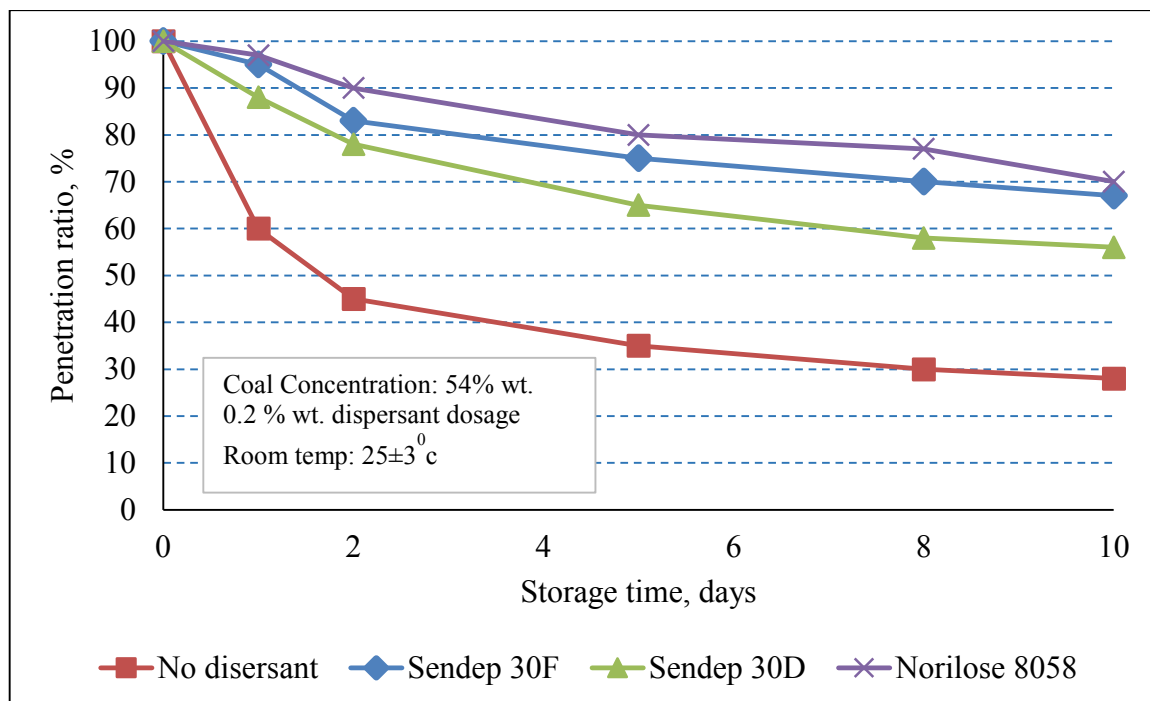


**Figure 4-17:** Graph showing the stability of a coal sample prepared using at 0.2 % wt. dosages of Sendep 30F, Sendep 30D and Norilose 8058 (coal content: at 54 wt.%)

As seen in Figure 4-17, the penetration ratios of coal suspension prepared with no dispersant kept decreasing with the increase of the storage time, mainly decreasing sharply within 48 hours. In contrast, coal suspensions prepared with dispersants showed higher penetration ratios, indicating complete destabilization of CWMs. The trends show that more than 70% penetration was obtained after 120 hours (5 days) with Norilose 8058 at 0.2 % wt. The rod penetration through the glass was observed to be very gentle and not compacted. However, the penetration ratio with dispersants kept decreasing with increasing storage time, mainly decreasing sharply after 240 hours.

The settling of coal particles in suspension can be interpreted by the fact that CWMs contains solid particles in water, and the possibility of sedimentation or aggregation is possible without the presence of dispersants. According to Morrison *et al.*, (1993), coal concentrations with less than 80 % penetration after 504 hours (21 days), the stabilization of such coal is not recommended for industrial application.

In support of this observation, it is worth recalling Figure 4-2, which shows the effect of dispersant dosage on zeta potential, increasing dispersant dosage resulted in an increase in zeta potential. Higher zeta potential in the presence of dispersants means there are more electrostatic repulsion forces that have been shown in improving the stability of the coal suspension.

Based on this result, the coal water slurries prepared from Norilose 8058 show better stability than Sendep 30D and Sendep 30F respectively. Comparing the three dispersants used Sendep 30D show inferior results for Witbank CWMs formulation.

## CHAPTER FIVE: CONCLUSION AND RECOMMENDATION

### 5.1 CONCLUSIONS

The purpose of this subject area as stated in the introduction was to investigate the effect of dispersant addition on CWM rheology and stability. From this study, the following conclusions can be obtained.

#### Surface charge

- The zeta potential as determined in demineralised water and 1 M KCl solutions obtained an absolute zeta potential value of -38.68 mV and -23.68 mV at the natural pH of coal samples respectively.
- The zeta potential in both solutions was enhanced with the addition of dispersants. By adsorbing on the coal surface, dispersants increased the surface charge towards more negative values, thus increasing surface electrostatic repulsion between particles. The most significant change in zeta potential was observed for Norilose 8058 at -63.03 mV and -45.94 mV in demineralised and 1 M KCl solutions respectively.

#### Rheology

- The rheological test indicates that CWM were strongly non-Newtonian and showed shear thinning (pseudoplastic) behaviour as the coal concentration increased above 51 wt.%. The attractive hydrophobic interactions resulted in particle aggregation that led to high yield stresses and increased viscosity.
- The empirical non-Newtonian model (Herschel-Bulkley) described showed a reasonable approximation of the experimental data. The Herschel-Bulkley model provided the best fit for the flow curves.
- The rheological tests on solids concentration indicate that an increase in solids concentration led to high yield stresses and increased viscosity due a rise in the number of particles per unit volume.
- The rheological experiments on the effect of particle size indicate that yield stresses and apparent viscosity increased with a decrease in particle size.
- The rheological test for pH indicates that yield stress and apparent viscosity of CWMs increased with a decrease in pH.
- Rheological behaviour of CWMs employing dispersants strongly affected the surface charge of coal. With an initial apparent viscosity of 0.13 Pa.s at coal concentration of

54 wt.%. By adding a dispersant on the coal surface, the apparent viscosity decreased to 0.02 Pa.s, thus increasing electrostatic repulsion between coal particles.

### Stability

- The static stability behaviour of CWMs with different particle size indicates that the penetration ratio (%) decreased with increasing storage time. CWMs showed poor stability with a hard packed layer determined at the bottom of the cylinder without a dispersant.
- Static stability of CWMs employing dispersants strongly affected the surface charge of coal. CWMs prepared without dispersants showed poor stability after 48 hours with penetration ratio of about 35 %. By adding dispersants on coal, the stability was improved after 120 hours with a penetration ratio of more than 75 % for Norilose 8058, thus increasing electrostatic repulsion between particles. However, the penetration ratio (%) was observed below 80 % after 240 hours. According to Morrison *et al.*, (1993), the stabilization of such a suspension is not good for industrial application.

## 5.2 RECOMMENDATIONS

From this investigation, several questions remain unanswered at the completion of this study. Therefore, based on the previous conclusions, the following areas will require a more detailed study.

1. On viscosity and stability analysis, a great deal of work should be carried out to optimize the particle size. It could be possible to control the particle size by mixing different fractions of fines and coarse coal particles to predict the maximum solids concentration. It is recommended that the well-known Rosin-Rammler mathematical model is applied to investigate the size distributions of the coal samples.
2. In that respect is also a need to improve the stability and viscosity solutions. It is recommended that a wider range of dispersant and stabilizer types be investigated. Hence, a more in-depth comparison of the selected dispersants with commercial additives needs to be researched.
3. More study should be carried out to optimize the slurry properties, i.e. low viscosity and high stability in a wide scope of temperature conditions. In this regards, investigating different temperatures will be useful in optimising the slurry properties.

4. It is also recommended that studies of the flow properties of various types of South African coal samples be conducted. Although the present study offers insight into the Witbank coals rheological behaviour, understanding the interaction between dispersants and other South Africa coal samples needs to be explored.

## CHAPTER SIX: REFERENCES

- Addai-Mensah, J. and Ralston, J. 2005, "Investigation of the role of interfacial chemistry on particle interactions, sedimentation and electro-osmotic dewatering of model kaolinite dispersions", *Powder Technology*, vol. 160, pp. 35-39.
- Aktas, Z. 2000. "Effect of non-ionic reagent adsorption on the zeta potential of fine coal particles", *Turkish Journal of Chemistry*, vol. 24, no. 2, pp. 117-130.
- Aktaş, Z. & Woodburn, E.T. 2000. "Effect of addition of surface active agent on the viscosity of a high concentration slurry of a low-rank British coal in the water", *Fuel Processing Technology*, vol. 62, no. 1, pp. 1-15.
- Atesok, G., Boylu, F., Sirkeci, A.A. & Dincer, H. 2002. "The effect of coal properties on the viscosity of coal–water slurries", *Fuel*, vol. 81, no. 14, pp. 1855-1858.
- Atesok, G., Ozer, M., Boylu, F. & Dincer, H. 2005. "The effect of anionic dispersants on grindability of different rank coals", *International Journal of Mineral Processing*, vol. 77, no. 4, pp. 199-207.
- Atlas, H., Casassa, E., Parfitt, G., Rao, A. & Toor, E. 1985. "The stability and rheology of coal/water slurries", *10th Ann. Powder & Bulk Solids Conf. Proc., Rosemont, ill., University of Microfilm International, Ann Arbor, Michigan*, pp. 771.
- Barba, C., Montané, D., Rinaudo, M. & Farriol, X. 2002. "Synthesis and characterization of carboxymethylcelluloses (CMC) from non-wood fibers I. Accessibility of cellulose fibers and CMC synthesis", *Cellulose*, vol. 9, no. 3-4, pp. 319-326.
- Barnes, H. 1989. "Shear-Thickening ('Dilatancy') in Suspensions of Non aggregating Solid Particles Dispersed in Newtonian Liquids", *Journal of Rheology (1978-present)*, vol. 33, no. 2, pp. 329-366.
- Barnes, H.A. 1999. The yield stress - a review or 'παντα ρει' - everything flows?  
*Journal of Non-Newtonian Fluid Mechanics*, 81:133-178.
- Benyounes, K. & Benmounah, A. 2012, "Rheological and electrokinetic properties of carboxymethylcellulose-water dispersions in the presence of salts"

- Bingham, E.C. 1922. *Fluidity and plasticity*. New York. McGraw-Hill Book Company Incorporated.
- Bingham, E.C., and Green, H. 1920. Paint, a plastic material and not a viscous liquid; the measurement of its mobility and yield value. *Proceedings - American Society for Testing Materials*. 20:640-675.
- Boger, D., Leong, Y., Mainwaring, D. & Christie, G. 1987. "Victorian brown coal water suspensions as liquid fuels", *I Chem E Symp Ser*, pp. 1.
- Boylu, F., Ateşok, G. & Dinçer, H. 2005. "The effect of carboxymethyl cellulose (CMC) on the stability of coal-water slurries", *Fuel*, vol. 84, no. 2–3, pp. 315-319.
- Camesano, T.A. & Wilkinson, K.J. 2001. "Single molecule study of xanthan conformation using atomic force microscopy", *Biomacromolecules*, vol. 2, no. 4, pp. 1184-1191.
- Cheng, D. C-H. 1980. Viscosity-concentration equations and flow curves for suspensions. *Chemistry and Industry*, vol. 17. pp. 403–406.
- Chhabra, R.P. & Richardson, J.F. 2011. *Non-Newtonian flow and applied rheology: engineering applications*. Butterworth-Heinemann. Burlington-USA.
- Das, D., Panigrahi, S., Senapati, P.K. & Misra, P.K. 2009, "Effect of Organized Assemblies. Part 5: Study on the Rheology and Stabilization of a Concentrated Coal– Water Slurry Using Saponin of the *Acacia concinna* Plant", *Energy & Fuels*, vol. 23, no. 6, pp. 3217-3226
- Derjaguin, B.V. and Landau, L. 1941, "Theory of stability of strongly charged lyophobic sols and the adhesion of strongly charged particles in a solution of electrolytes", *Acta Physicochem* 14, pp. 633-662
- Dincer, H., Boylu, F., Sirkeci, A. & Ateşok, G. 2003. "The effect of chemicals on the viscosity and stability of coal-water slurries", *International Journal of Mineral Processing*, vol. 70, no. 1, pp. 41-51.
- Doymuş, K. 2007, "The effect of ionic electrolytes and pH on the zeta potential of fine coal particles", *Turkish Journal of Chemistry*, vol. 31, no. 6, pp. 589-597.

- Eberhard, A. 2011. The future of South African coal: Market, investment, and policy challenges. Working Paper No. 100. Programme on Energy and Sustainable Development,
- Farris, R. 1968. "Prediction of the viscosity of multimodal suspensions from unimodal viscosity data", *Transactions of the Society of Rheology (1957-1977)*, vol. 12, no. 2, pp. 281-301.
- Fuerstenau, D. 2005. "Zeta potentials in the flotation of oxide and silicate minerals", *Advances in Colloid and Interface Science*, vol. 114, pp. 9-26.
- Fuerstenau, D.W., Rosenbaum, J.M. & Laskowski, J. 1983, "Effect of surface functional groups on the flotation of coal", *Colloids and Surfaces*, vol. 8, no. 2, pp. 153-173.
- Garakani, A.K., Mostoufi, N., Sadeghi, F., Fatourechi, H., Sarrafzadeh, M. & Mehrnia, M. 2011, "Comparison between different models for rheological characterization of activated sludge", *Iranian journal of environmental health science & engineering*, vol. 8, no. 3, pp. 255-264.
- Goudoulas, T.B., Kastrinakis, E.G. & Nychas, S.G. 2003, "Rheological aspects of dense lignite-water suspensions; time dependence, preshear and solids loading effects", *Rheologica acta*, vol. 42, no. 1-2, pp. 73-85.
- Guibaud, G., Dollet, P., Tixier, N., Dagot, C. & Baudu, M. 2004, "Characterisation of the evolution of activated sludges using rheological measurements", *Process Biochemistry*, vol. 39, no. 11, pp. 1803-1810.
- Hamaker, H. C., "The-Van der Waals attraction between spherical particles, physical 4, pp. 1058-1072
- Hasar, H., Kinaci, C., Ünlü, A., Toğrul, H. & Ipek, U. 2004, "Rheological properties of activated sludge in a SMBR", *Biochemical engineering journal*, vol. 20, no. 1, pp. 1-6.
- He, M., Wang, Y., and Forssberg, E. 2004. Slurry rheology in wet ultrafine grinding of industrial minerals: a review. *Powder Technology*, 147:94-112.
- Herschel, W.H. & Bulkley, R. 1926. "Konsistenzmessungen von gummi-benzollösungen", *Kolloid-Zeitschrift*, vol. 39, no. 4, pp. 291-300.

- Horsfall, D. 1990. "The properties and uses of mixtures of coal, and water or oil", *Journal of The South African Institute of Mining and Metallurgy*, vol. 90, no. 8, pp. 199-204.
- Hunter, R.J. 1987. "Polymeric stabilization and flocculation", *Foundations of Colloid Science*, vol. 1, pp. 71-141.
- Israelachvili, J.N. 1992, "Adhesion forces between surfaces in liquids and condensable vapours", *Surface Science Reports*, vol. 14, no. 3, pp. 109-159.
- Johnson, S.B., Franks, G.V., Scales P.J., Boger, D.V. & Healy, T.W. 2000. Surface chemistry–Rheology relationships in concentrated mineral suspensions. *International Journal of Mineral Processing*, vol. 58, pp 267–304.
- Kaji, R., Muranaka, Y., Miyadera, H. & Hishinuma, Y. 1987. "Effect of electrolyte on the rheological properties of coal-water mixtures", *AIChE Journal*, vol. 33, no. 1, pp. 11-18.
- Kawatra, S. & Eisele, T. 1988. "Rheological effects in grinding circuits", *International Journal of Mineral Processing*, vol. 22, no. 1, pp. 251-259.
- Klimpel, R.R. 1864, "Influence of material breakage properties and associated slurry rheology on breakage rates in wet grinding of coal/ores in tumbling media mills".
- Kulicke, W., Kull, A.H., Kull, W., Thielking, H., Engelhardt, J. & Pannek, J. 1996. "Characterization of aqueous carboxymethyl cellulose solutions in terms of their molecular structure and its influence on rheological behaviour", *Polymer*, vol. 37, no. 13, pp. 2723-2731.
- Laskowski, J.S. 2001. "Chapter 10 Fine-coal utilization", *Developments in Mineral Processing*, vol. 14, no. 0, pp. 307-351.
- Laskowski, J. & Parfitt, G. 1989. "Electrokinetics of coal-water suspensions", *Interfacial Phenomena in Coal Technology*, pp. 279-327.
- Leong, Y. K. 2005, "Yield stress and zeta potential of nanoparticulate silica dispersions under the influence of adsorbed hydrolysis products of metal ions –Cu(II), Al(III) and Th(IV)", *Journal of Colloid and Interface Science*, vol. 292, pp. 557-566.

- Liu, Q., Zhang, Y. & Laskowski, J. 2000. "The adsorption of polysaccharides onto mineral surfaces: an acid/base interaction", *International Journal of Mineral Processing*, vol. 60, no. 3, pp. 229-245.
- Logos, C. & Nguyen, Q. 1996. "Effect of particle size on the flow properties of a South Australian coal-water slurry", *Powder Technology*, vol. 88, no. 1, pp. 55-58.
- Mishra, S. & Kanungo, S. 2000, "Factor Affecting the Preparation of Highly Concentrated Coal-Water Slurry (Hccws)", *Journal of Scientific and Industrial Research*, vol. 59, no. 10, pp. 765-790.
- Meikap, B., Purohit, N. & Mahadevan, V. 2005. "Effect of microwave pretreatment of coal for improvement of rheological characteristics of coal-water slurries", *Journal of colloid and interface science*, vol. 281, no. 1, pp. 225-235.
- Mezger, T.G. 2006. *The Rheology Handbook: For users of rotational and oscillatory rheometers*, Vincentz Network GmbH & Co KG.
- Mishra, S. & Kanungo, S. 2000, "Factor Affecting the Preparation of Highly Concentrated Coal-Water Slurry (Hccws)", *Journal of Scientific and Industrial Research*, vol. 59, no. 10, pp. 765-790.
- Mishra, S., Senapati, P. & Panda, D. 2002. "Rheological behavior of coal-water slurry", *Energy Sources*, vol. 24, no. 2, pp. 159-167.
- Morrison, J.L., Bruce M., & Scaroni A.W. 1993. "Preparing and handling coal water slurry fuels: potential problems and solutions". *18th International Technical Conference On Coal Utilization and Fuel Systems*, Florida, USA, p. 361-8
- Narasingha, M. H and Buranasrisak, P. 2012. "Effects of Particle Size Distribution and Packing Characteristics on the Preparation of Highly-Loaded Coal-Water Slurry", *International Journal of Chemical Engineering and Applications*, vol. 3, no. 5.
- Nguyen, A and Schulze H.J. 2004. *Colloidal Science of Flotation*. 1st Edition, Marcel Dekker, New York.

- Ongsirimongkol, N., & Narasingha, M.H. 2012. "Effects of Stabilizing Agents on Stability and Rheological Characteristics of the Highly-Loaded Coal-Water Slurry". *International Journal of Chemical Engineering and Applications*, 3(1), 49.
- Osborne, D.G. & Fonseca, A.G. 1992. "Coal preparation – The past ten years", *Coal Preparation*, vol. 11, no. 3-4, pp. 115-143.
- Overbeek, J.T.G. 1966. "Colloid stability in aqueous and non-aqueous media". Introductory paper, *Discussions of the Faraday Society*, vol. 42, pp. 7-13.
- Pawlik, M. 2005. "Polymeric dispersants for coal–water slurries", *Colloids and Surfaces A: Physicochemical and Engineering Aspects*, vol. 266, no. 1, pp. 82-90.
- Pollice, A., Giordano, C., Laera, G., Saturno, D. & Mininni, G. 2007, "Physical characteristics of the sludge in a complete retention membrane bioreactor", *Water research*, vol. 41, no. 8, pp. 1832-1840.
- Prutton, M. 1994. *Introduction to Surface Physics*, Oxford University Press.
- Reddick, J., Blottnitz, H.v. & Kothuis, B. 2007. "A cleaner production assessment of the ultra-fine coal waste generated in South Africa", *Journal of the South African Institute of Mining & Metallurgy*, vol. 107, no. 12, pp. 811.
- Reiner, M. 1926. "Ueber die Strömung einer elastischen Flüssigkeit durch eine Kapillare", *Kolloid-Zeitschrift*, vol. 39, no. 1, pp. 80-87.
- Roh, N., Shin, D., Kim, D. & Kim, J. 1995, "Rheological behaviour of coal-water mixtures. Effects of coal type, loading and particle size", *Fuel*, vol. 74, no. 8, pp. 1220-1225.
- Sadler, L.Y. & Sim, K. 1991. "Minimize solid-liquid mixture viscosity by optimizing particle-size distribution", *Chemical Engineering Progress*, vol. 87, no. 3, pp. 68-71.
- Saeki, T., Usui, H. & Kawamoto, T. 1993. "Coagulation and dispersion characteristics of coal water mixtures in higher temperature range.", *Journal of Chemical Engineering of Japan*, vol. 26, no. 1, pp. 59-63.

- Shukla, S.C., Kukade, S., Mandal, S.K. & Kundu, G. 2008. "Coal–oil–water multiphase fuel: Rheological behavior and prediction of optimum particle size", *Fuel*, vol. 87, no. 15, pp. 3428-3432.
- TA Instruments. Operator's manual – AR 1500EX rheometer. March 2010.
- Thompson, T.L. and Aude, T.C., 1981. Slurry Pipelines. Design, Research and Experience. *Journal of Pipelines*, **1**(1), pp. 25-44.
- Tiwari, K.K., Basu, S.K., Bit, K.C., Banerjee, S. & Mishra, K.K. 2004, "High-concentration coal–water slurry from Indian coals using newly developed additives", *Fuel Processing Technology*, vol. 85, no. 1, pp. 31-42.
- Trochet-Mignard, L., Taylor, P., Bognolo, G. & Tadros, T.F. 1995. "Concentrated coal-water suspensions containing nonionic surfactants and polyelectrolytes 2. Adsorption of nonyl phenyl propylene oxide-ethylene oxide on coal and the rheology of the resulting suspension", *Colloids and Surfaces A: Physicochemical and Engineering Aspects*, vol. 95, no. 1, pp. 37-42.
- Truesdell, C. & Noll, W. 1992. *The Nonlinear Field Theories of Mechanics*. Berlin: Springer-Verlag,
- Turian, R.M., Attal, J.F., Sung, D. & Wedgewood, L.E. 2002. "Properties and rheology of coal–water mixtures using different coals", *Fuel*, vol. 81, no. 16, pp. 2019-2033.
- Umar, D.F., Usui, H. & Komoda, Y. 2009. "Effect of dispersing and stabilizing additives on rheological characteristics of the upgraded brown coal water mixture", *Fuel Processing Technology*, vol. 90, no. 4, pp. 611-615.
- Usui, H., Tatsukawa, T., Saeki, T. & Katagiri, K. 1999. "Upgrading of low-rank coal by a combined process of vacuum drying and tar coating", *Coal Preparation*, vol. 21, no. 1, pp. 71-81.
- Uyar, T. S., Ö. Özil, & G. Erdönmez. "Preparation of low-rank coal-water mixtures." 1994: 271-278.

- Verwey, E. 1947. "Theory of the stability of lyophobic colloids.", *The Journal of Physical Chemistry*, vol. 51, no. 3, pp. 631-636.
- Verwey, E.J.W. and Overbeek, J.T.G. 1948, *Theory Stability of Lyophobic Solids*, Amsterdam, Elsevier.
- Warchol, J. J., & Vecci, S. J. (1985). *Coal-water-slurry evaluation. Volume 1. Revised laboratory test standards*. Babcock and Wilcox Co., Alliance, OH (USA). Research and Development Division.
- Yavuz, R. & Küçükbayrak, S. 1998, "Effect of particle-size distribution on the rheology of lignite-water slurry", *Energy Sources*, vol. 20, no. 9, pp. 787-794.
- Zhu, J., Zhang, G., Liu, G., Qu, Q. & Li, Y. 2014, "Investigation of the rheological and stability characteristics of coal–water slurry with long side-chain polycarboxylate dispersant", *Fuel Processing Technology*, vol. 118, pp. 187-191.

## CHAPTER SEVEN: APPENDICES

### SECTION 4.1

#### APPENDIX A: ZETA POTENTIAL ANALYSIS

**Table A-1:** Zeta potential of coal in demineralised water

pH	Zeta potential (mV)				
	Run 1	Run 2	Run 3	Mean	Std. dev.
2	26.12	30.9	25.42	27.47	2.99
4	-17.13	-16.66	-22.98	-18.91	3.53
6	-28.6	-28.45	-32.87	-29.97	2.51
8	-37.81	-42.13	-36.15	-38.68	3.07
10	-50.89	-44.98	-45.14	-46.99	3.38
12	-60.87	-66.15	-59.78	-62.25	3.38

**Table A-2:** Zeta potential of coal in KCl ( $1 \times 10^{-1}$  mol/dm<sup>-3</sup>)

pH	Zeta potential (mV)					
	Run 1	Run 2	Run 3	Mean	Std. dev.	Std. error
2	7.12	8.13	6.98	7.12	0.62	0.36
4	-8.35	-7.89	-8.59	-8.35	0.35	0.20
6	-16.23	-17.1	-16.1	-16.23	0.54	0.31
8	-20.5	-21.1	-20.43	-20.5	0.36	0.21
10	-24.7	-23.1	-24.43	-24.43	0.85	0.49
12	-32.32	-33.1	-32.18	-32.32	0.49	0.28

**Table A-3:** Zeta potential with Sendep 30D at natural pH of 8 in KCl ( $1 \times 10^{-1} \text{ mol dm}^{-3}$ )

Dispersant agent (wt.%)	Sendep 30D				
	Zeta potential (mV)				
	Run 1	Run 2	Run 3	Mean	Std. dev.
0	-21.5	-24.81	-23.94	-23.42	1.72
0.1	-36.7	-35.67	-37.54	-36.64	0.94
0.2	-39.8	-42.1	-40.1	-40.67	1.25
0.3	-45.2	-41.2	-41.67	-42.69	2.19
0.4	-40.8	-33.3	-41.12	-38.41	4.43
0.5	-39.56	-37.1	-40.56	-39.07	1.78

**Table A-4:** Zeta potential with Sendep 30F at natural pH in KCl ( $1 \times 10^{-1} \text{ mol dm}^{-3}$ )

Dispersant agent (wt.%)	Sendep 30F				
	Zeta potential (mV)				
	Run 1	Run 2	Run 3	Mean	Std. dev.
0	-23.81	-22.15	-24.53	-23.50	1.22
0.1	-34.7	-30.1	-33.23	-32.68	2.35
0.2	-37.1	-38.4	-40.1	-38.53	1.50
0.3	-40.1	-43.2	-46.16	-43.35	3.03
0.4	-43.1	-45.55	-41.4	-43.15	2.09
0.5	-39.56	-42.1	-43.1	-41.59	1.82

**Table A-5:** Zeta potential with Norilose 8058 at natural pH in KCl ( $1 \times 10^{-1} \text{ mol dm}^{-3}$ )

Dispersant agent (wt.%)	Norilose 8058				
	Zeta potential (mV)				
	Run 1	Run 2	Run 3	Mean	Std. dev.
0	-25.75	-22	-23.1	-23.62	1.93
0.1	-37.4	-42.1	-37.6	-39.03	2.66
0.2	-44.3	-39.67	-41.1	-41.69	2.37
0.3	-45.5	-44.23	-48.1	-45.94	1.97
0.4	-44.5	-40.35	-43.15	-42.67	2.12
0.5	-40.56	-44.45	-45.18	-43.40	2.48

**Table A-6:** Zeta potential with Sendep 30D at natural pH in demineralised water

Dispersant agent (wt.%)	Sendep 30D				
	Zeta potential (mV)				
	Run 1	Run 2	Run 3	Mean	Std. dev.
0	-37.68	-52.67	-38.78	-43.04	8.36
0.1	-56.6	-55.1	-60.1	-57.27	2.57
0.2	-57.9	-54.31	-58.12	-56.78	2.14
0.3	-61.2	-62.2	-59.56	-60.99	1.33
0.4	-59.17	-53.23	-57.56	-56.65	3.07
0.5	-57.25	-49.14	-58.45	-54.95	5.06

**Table A-7:** Zeta potential with Sendep 30F at natural pH in demineralised water

Dispersant agent (wt.%)	Sendep 30F				
	Zeta potential (mV)				
	Run 1	Run 2	Run 3	Mean	Std. dev.
0	-39.34	-35.78	-40.16	-38.43	2.33
0.1	-59.8	-49.1	-58.45	-55.78	5.83
0.2	-57.34	-58.9	-59.9	-58.71	1.29
0.3	-61.4	-63.12	-59.67	-61.40	1.73
0.4	-59.12	-58.65	-57.19	-58.32	1.01
0.5	-58.38	-60.56	-60.45	-59.80	1.23

**Table A-8:** Zeta potential with Norilose 8058 at natural pH in demineralised water

Dispersant agent (wt.%)	Norilose 8058				
	Zeta potential (mV)				
	Run 1	Run 2	Run 3	Mean	Std. dev.
0	-37.12	-38.78	-40.16	-38.69	1.52
0.1	-59.8	-60.1	-57.45	-59.12	1.45
0.2	-58.34	-59.9	-62.9	-60.38	2.32
0.3	-62.4	-66.12	-60.67	-63.06	2.78
0.4	-59.12	-54.65	-59.19	-57.65	2.60
0.5	-53.38	-57.56	-59.45	-56.80	3.11

## SECTION 4.2

### APPENDIX B: RHEOLOGICAL ANALYSIS

**Table B-1:** CWM formulation formulas

V <sub>w</sub>	Volume of water (ml)
M <sub>s</sub>	Mass of sample (g)
$\rho_s$	Density of slurry (kg/m <sup>3</sup> )
V <sub>sl</sub>	Volume of slurry (ml)
$\Phi_s$	Fraction by volume (C <sub>v</sub> )
M <sub>w</sub>	Mass of solids by weight (C <sub>w</sub> )
M <sub>s</sub>	$(V_{sl}/100) * \rho_s * V_{sl}$
V <sub>w</sub>	$(\rho_s * V_{sl} - M_s) / \rho_s$
C <sub>w</sub>	$M_s / (V_{sl} + M_s) * 100$

**Table B-2:** Witbank coal mixture preparation for viscosity tests without dispersant agents

<b>RHEOMETER ANALYSIS</b>			
Density of coal	1.6		
Volume of mixture (ml)	50		
Fraction by volume (C <sub>v</sub> )	Mass of sample (M <sub>s</sub> )	Volume of water (V <sub>w</sub> )	Mass of solids by weight (C <sub>w</sub> )
10	8.00	45	15.09
20	16.00	40	28.57
30	24.00	35	40.68
40	32.00	30	51.61
42	33.60	29	53.67
44	35.20	28	55.70
46	36.80	27	57.68
48	38.40	26	59.63
50	40.00	25	61.54

## SECTION 4.2.5: SOLIDS CONCENTRATION

**Table B-3:** Variation of coal and water with dispersants at 56 wt.% (PSD: -75  $\mu\text{m}$ ,  $d_{50}$ -27.97 $\mu\text{m}$ )

Coal concentration (Cw.%)	Dispersant agent (% by weight)	Dispersant addition (g)	Amount of water (ml)	Amount of coal (g)
54	0.1	0.03	29	33.60
56	0.2	0.07	29	33.60
56	0.3	0.10	29	33.60
56	0.4	0.13	29	33.60
56	0.5	0.17	29	33.60

**Table B-4:** Variation of coal and water with dispersants at 58 % (PSD: -75  $\mu\text{m}$ ,  $d_{50}$ -27.97 $\mu\text{m}$ )

Coal concentration (Cw.%)	Dispersant agent (% by weight)	Dispersant addition (g)	Amount of water (ml)	Amount of coal (g)
58	0.1	0.04	27	36.80
58	0.2	0.07	27	36.80
58	0.3	0.11	27	36.80
58	0.4	0.15	27	36.80
58	0.5	0.18	27	36.80

**Table B- 5:** Variation of coal and water with dispersants at 60 wt.% (PSD: -75  $\mu\text{m}$ ,  $d_{50}$ -27.97  $\mu\text{m}$ )

Coal concentration (Cw.%)	Dispersant agent (% by weight)	Dispersant addition (g)	Amount of water (ml)	Amount of coal (g)
60	0.1	0.04	26	38.40
60	0.2	0.08	26	38.40
60	0.3	0.12	26	38.40
60	0.4	0.16	26	38.40
60	0.5	0.19	26	38.40

#### SECTION 4.2.4: PARTICLE SIZE

**Table B-6:** Yield stress with 54 wt.% solids concentration on different particle sizes

Particle size ( $\mu\text{m}$ )	Yield stress (Pa)				
	Test 1	Test 2	Test 3	Mean	Std. dev
63	6.95	7.97	7.52	7.48	0.42
75	6.94	5.52	7.52	6.66	0.84
106	3.49	2.38	2.04	2.64	0.62
150	1.45	0.64	1.47	1.19	0.34

## RHEOLOGICAL MODEL FIT ANALYSIS

**Table B-7:** Rheological model rheograms at 54 wt.% without chemical agents

42 (vol.%)/ 54 (wt.%)				
shear stress	shear rate	Bingham fit	Power law fit	Herschel-Bulkley fit
[Pa]	[1/s]			
4.25	6.10	5.68	3.39	4.40
5.25	19.75	5.81	4.52	4.98
5.40	26.41	5.87	4.86	5.18
5.52	33.08	5.94	5.13	5.36
5.94	59.75	6.19	5.94	5.93
6.09	69.07	6.28	6.16	6.10
6.40	89.57	6.48	6.56	6.44
6.52	98.04	6.56	6.71	6.57
6.52	98.04	6.56	6.71	6.57
7.04	135.30	6.92	7.26	7.07
7.04	135.30	6.92	7.26	7.07
7.30	156.80	7.13	7.53	7.33
7.40	166.50	7.22	7.65	7.44
7.91	208.00	7.62	8.08	7.88
7.91	208.00	7.62	8.08	7.88
8.08	222.30	7.76	8.21	8.02
8.16	229.10	7.83	8.27	8.09
8.37	251.70	8.04	8.47	8.30
8.37	263.80	8.16	8.56	8.41
8.60	275.30	8.27	8.65	8.51
8.73	286.30	8.38	8.74	8.61
8.87	296.90	8.48	8.82	8.70
9.15	326.60	8.77	9.03	8.95
9.15	326.60	8.77	9.03	8.95
9.23	335.90	8.86	9.09	9.02
9.48	378.90	9.27	9.36	9.35
9.48	378.90	9.27	9.36	9.35
9.57	394.80	9.42	9.46	9.47
9.69	424.80	9.71	9.63	9.69
9.76	438.90	9.85	9.71	9.78
9.80	445.90	9.92	9.75	9.83
9.82	452.70	9.98	9.78	9.88
10.00	480.60	10.25	9.93	10.07
10.10	498.50	10.42	10.02	10.19
10.04	500.00	10.44	10.03	10.20

## APPENDIX C: STATIC STABILITY ANALYSIS

<b>ROD PENETRATION ANALYSIS</b>			
<b>Density of slurry</b>	<b>1.6</b>		
<b>Volume of slurry</b>	<b>150</b>		
% Solids by volume	Mass of sample in (g)	Volume of water (ml)	% solids by mass
40	96.00	90	51.61
42	100.80	87	53.67
44	105.60	84	55.70
46	110.40	81	57.68
48	115.20	78	59.63
50	120.00	75	61.54
52	124.80	72	63.41
54	129.60	69	65.26
56	134.40	66	67.07

### SECTION 4.3: ROD PENETRATION TEST.

**Table C-1:** The stability of CWM prepared using different particle sizes at 54 wt.% without dispersant addition

<b>Days</b>	<b>Penetration ratio, %</b>			
	<b>Coal concentration (54 wt.%)</b>	<b>-63 (µm)</b>	<b>-75 (µm)</b>	<b>-106 (µm)</b>
0	54	100	100	28
2	54	50	45	40
5	54	45	35	30
8	54	35	30	28
10	54	30	28	25

**Table C-2:** The static stability of CWM prepared using 200 mesh sieve size (-75  $\mu\text{m}$ ) particles at 54 wt.% using 0.2 % wt. dosage of Sendep 30D, Sendep 30F and Norilose 8058 after 240 hours

Days	Penetration ratio, %				
	Coal concentration (54 wt. %)	No dispersant	Sendep 30D	Sendep 30F	Norilose 8058
0	54	100	100	100	100
2	54	45	78	83	90
5	54	35	65	75	80
8	54	30	58	70	77
10	54	28	56	67	70

## APPENDIX D: EBE ETHICS FORM

### EBE Faculty: Assessment of Ethics in Research Projects

Any person planning to undertake research in the Faculty of Engineering and the Built Environment at the University of Cape Town is required to complete this form before collecting or analysing data. When completed it should be submitted to the supervisor (where applicable) and from there to the Head of Department. If any of the questions below have been answered YES, and the applicant is NOT a fourth-year student, the Head should forward this form for approval by the Faculty EIR committee, e-mail to Ms Zakiya Chikwe ([Zakiyachikwe@uct.ac.za](mailto:Zakiyachikwe@uct.ac.za)), New TDE Building, PB 021, 650 5-336. Students must include a copy of the completed form with the dissertation/thesis when it is submitted for examination.

Name of Principal Researcher/Student: Prince Owusu Gyebi Department: Chemical Engineering Dept.

If a Student: Degree: MSc Supervisor: Prof. David Degon

If a Research Contract indicate source of funding/sponsorship: Minerals to Minerals (MIM)/ NRF

Research Project Title: Investigating the rheological behavior of Witbank coal water mixtures (CWMs)

#### Overview of ethics issues in your research project:

Question 1: Is there a possibility that your research could cause harm to a third party (i.e. a person not involved in your project)?	YES	<input checked="" type="checkbox"/>
Question 2: Is your research making use of human subjects as sources of data? If your answer is YES, please complete Addendum 2.	YES	<input checked="" type="checkbox"/>
Question 3: Does your research involve the participation of or provision of services to communities? If your answer is YES, please complete Addendum 3.	YES	<input checked="" type="checkbox"/>
Question 4: If your research is sponsored, is there any potential for conflicts of interest? If your answer is YES, please complete Addendum 4.	YES	<input checked="" type="checkbox"/>

If you have answered YES to any of the above questions, please append a copy of your research proposal, as well as any interview schedules or questionnaires (Addendum 1) and please complete further addenda as appropriate.

#### I hereby undertake to carry out my research in such a way that:

- there is no apparent legal objection to the nature or the method of research; and
- the research will not compromise staff or students or the other responsibilities of the University;
- the stated objective will be achieved, and the findings will have a high degree of validity;
- limitations and alternative interpretations will be considered;
- the findings could be subject to peer review and publicly available; and
- I will comply with the conventions of copyright and avoid any practice that would constitute plagiarism.

Signed by:

	Full name and signature	Date
Principal Researcher/Student:	Prince Owusu Gyebi	12-02-2016

This application is approved by:  
Supervisor (if applicable):

Prof. David Degon 12-02-2016

HOD (or delegated nominee):  
Final authority for all assessments with NO to all questions and for all undergraduate research.

Prof. Eric van Steyn 12-02-2016

Chair: Faculty EIR Committee  
For applicants other than undergraduate students who have answered YES to any of the above questions